Remote sensing tools for the large-scale monitoring of vegetation dynamics in wetland ecosystems

By

Sophie Taddeo

A dissertation submitted in partial satisfaction of the

requirements for the degree of

Doctor of Philosophy

in

Landscape Architecture and Environmental Planning

in the

Graduate Division

of the

University of California, Berkeley

Committee in charge:

Professor Iryna Dronova, Chair
Professor Gregory S. Biging
Professor John D. Radke

Spring 2019

Remote sensing tools for the large-scale monitoring of vegetation dynamics in wetland ecosystems

by Sophie Taddeo

Abstract

Remote sensing tools for the large-scale monitoring of vegetation dynamics in wetland ecosystems

by

Sophie Taddeo

Doctor of Philosophy in Landscape Architecture and Environmental Planning

University of California, Berkeley

Professor Iryna Dronova, Chair

Continued worldwide urban and agricultural expansion has triggered a loss and degradation of wetland resources. The United States alone seen a 50% decline in its wetland extent, with this percentage reaching a staggering 70% in certain states. With this widespread fragmentation and degradation of habitats, fewer sites are left with the important role of providing ecosystem services critical to the well-being of human populations. A thorough monitoring of wetland resources is necessary for rapidly identifying areas that require adaptive management and for best allocating limited conservation resources. This dissertation explores different methodological approaches for the large-scale monitoring of wetland ecosystems at low cost using open source remote sensing data. The first chapter provides a review of current monitoring practices in restored wetlands of the San Francisco estuary, California, USA. It identifies opportunities to leverage geospatial tools and datasets, including remote sensing products, to measure the contribution of individual restoration efforts towards regional wetland conservation goals. The second chapter examines the response of landscape metrics characterizing the distribution, size, and shape of vegetated patches to vegetation dynamics in a subset of restored wetlands and reference sites in the Sacramento-San Joaquin Delta of California. To portray vegetation response to restoration treatments, this chapter leverages high resolution aerial images from the National Agriculture Inventory Program and a collection of bi-monthly satellite images from the Landsat archives. The third chapter studies changes in the phenology of wetland sites throughout a 17-year period to identify phenological metrics most responsive to restoration interventions. This chapter outlines the impact of site characteristics and vegetation dynamics on landscape phenology. Finally, the fourth chapter uses a broader scale of analysis to examine how vegetation structure, composition, and spatial distribution modulate wetland greenness as measured by spectral vegetation indices derived from satellite data. By examining the relationships between field properties and spectral greenness across 1,138 wetlands of the conterminous United States, this chapter identifies the spectral vegetation indices most suited for wetland monitoring across different wetland types, vegetation densities, and disturbance levels.

Acknowledgements

I am forever indebted to phenomenal people, both within and outside Berkeley's campus, who have supported me along the way. This dissertation would not be what it is without their help.

First and foremost, I would like to thank my committee members for their continued intellectual input and encouragement. I have been incredibly lucky to count Iryna Dronova as an advisor and mentor. It has been a true privilege and joy working alongside her. Her intelligence, passion for science and ecology, and kindness are inspiring. Despite a very busy schedule, she always had time to provide advice, guide me through road blocks, and celebrate my accomplishments, and for all of that I will forever be grateful. There are many reasons to be thankful for the help of Greg Biging as well. Perhaps most important of all, because he saved my qualification exam by stepping in at the last minute! I also appreciated his insightful comments and suggestions along the way, which significantly improved my dissertation. Last but not least, I am grateful for the guidance of John Radke. His altruism, intelligence, and commitment to his students is remarkable. Above all, his many stories helped make my years at Berkeley infinitely more enjoyable.

I am appreciative for the financial support of this research by the California Sea Grant Delta Science program (Award R/SF-71) and the Farrand Fund. Berkeley's Student Mentor and Research Teams (SMART) program has helped shape the researcher and educator I have become and for that, I am grateful for all that Sabrina Soracco and Linda M. Von Hoene taught me. Thank you to a wonderful group of hard-working and extremely capable undergraduate assistants: Julia Painter Evered, Suwon Noh, Madison McKee, Metta Nicholson, Kelsey Foster, Annemarie Peacock, Shehnaz Mannan, Isabel Johnson, and Erin Voss. I have thoroughly enjoyed working with Kyle, Elke, Alex, Kuno, and Sara of Dr. Baldocchi's Biomet lab.

I am thankful for all my colleagues and friends in the LAEP program. I was incredibly lucky to be surrounded by such a talented, thoughtful, and creative group. Thank you to Scott, Sarah, Mam, Daniella, Yang, Tessa, Beki, and Janet for all your help. I am looking forward to following your upcoming professional accomplishments. Jen, Anneliese, Sooyeon and Celina – thank you for encouraging me to write.

I would not be here without my family. Thank you to my dad for his strength and love and to my mum for her encouragements and empathy. Thank you Christiane and Michel for being so caring and generous – you are truly like a second set of parents to me. My eternal gratitude to my grandmother: I hope to one day be as wise and loving as you are. Thank you to Liliane and Nathan for the love, support, and laughter. I am lucky to be surrounded by wonderful friends who continuously make me feel loved and welcomed even when I am far away. Thank you Alex, Isabelle, Alexis, Sophie, Geneviève, Krittika and so many others. Your friendship means the world to me.

Finally, I am forever grateful for the loving support of my partner Jeff. He encouraged me through difficult times, celebrated my successes, and spent countless hours reading and commenting on these chapters. Most importantly, he made these years in California both adventurous and joyful. I could not have made it without him.

Table of Contents

List of Acronyms and Abbreviations

ANOVA: Analysis of variance

DOY: Day of the Year

EH: Estuarine Herbaceous wetlands

EPA: Environmental Protection Agency

EVI: Enhanced Vegetation Index

EW: Estuarine Woody wetlands

GCC: Green Chromatic Coordinate

GNDVI: Green Normalized Difference Vegetation Index

IEVI: Integrated Enhanced Vegetation Index

LSWI: Land Surface Water Index

MODIS: Moderate Resolution Imaging Spectroradiometer

NAIP: National Agriculture Inventory Program

NIR: Near-infrared

NDVI: Normalized Difference Vegetation Index

NWCA: National Wetland Condition Assessment

OBIA: Object-Based Image Analysis

PCA: Principal Component Analysis

PDSI: Palmer Drought Severity Index

ROI: Region of Interest

SAVI: Soil-Adjusted Vegetation Index

SVI: Spectral Vegetation Indices

SVM: Support Vector Machine

SWIR: Shortwave infrared

USDA: United States Department of Agriculture

Introduction

This dissertation focuses on the use of remote sensing data to monitor vegetation dynamics in restored wetlands. Free, open source remote sensing data is used to track vegetation changes across restored wetlands in the Sacramento-San Joaquin Delta of California and wetlands of the conterminous United States monitored by the U.S. EPA's National Wetland Condition Assessment. This effort is motivated by a critical need to develop tools supporting the large-scale monitoring of wetland ecosystems at low cost. By studying vegetation dynamics through regional and national samples this dissertation aims to enhance our understanding of how wetland vegetation — and the ecosystem functions it supports — responds to stressors and restoration treatments for a better planning of restoration and conservation efforts.

Background

A continued urban and agricultural expansion over the last few centuries has triggered a worldwide loss and degradation of wetland resources. The United States alone seen a 50% decline in its wetland extent since the industrial revolution, with this percentage reaching a staggering 70% in certain states (Bedford 1999; Dahl 2000). Remaining wetlands are subject to increasing pressure from biological invasions, agricultural and urban runoff, and habitat fragmentation among other stressors (Zedler 2003; Allan et al. 2013; US EPA 2016a). According to the latest National Wetland Condition Assessment Report (here after NWCA), 32% of wetlands in the conterminous United States are in a "poor" biological condition (US EPA 2016a). This percentage rises to 61% in the western part of the country as a result of vegetation removal, soil hardening, and ditching (US EPA 2016a). Climate change further threatens the ecological integrity of wetland ecosystems by increasing their salinity, impacting their vegetation productivity, and altering their species composition towards more disturbance-tolerant species (Parker et al. 2011; Allan et al. 2013; Chapple et al. 2017). With this widespread loss and degradation of habitats, fewer sites are left with the important role of providing ecosystem services critical to the well-being of local human populations (Simenstad et al. 2006). These include water storage and filtration, carbon sequestration, and habitat provisioning (Zedler 2003; Kayranli et al. 2010). The loss of wetland regulation threatens to increase the vulnerability of human populations to land subsidence, flooding, and coastal erosion (Barbier et al. 2013; Almeida et al. 2016; Jankowski et al. 2017).

Ecological restoration has emerged in the early 20th century as a solution to the ongoing degradation of ecosystems and resulting loss of ecosystem services. Ecological restoration can be defined as the assisted recovery of an ecosystem towards a desired state or ecological condition (SER, 2014). Interventions to "assist" ecosystem recovery range from active (i.e., significant modifications to ecosystem conditions) to passive (i.e., removal of ecosystem stressors) (Zhao et al. 2016). Active interventions include excavation and gradation, planting, and site breeching to enhance tidal flow and connectivity. Project managers often use nearby, historical, and undisturbed sites as a reference point to establish restoration targets (or the ideal final composition of the ecosystem).

While the first American restoration projects date from the late 19th century, the body of scientific literature focusing on wetland restoration is relatively recent (Wortley et al. 2013).

Aesthetic and utilitarian aims predominantly motivated early wetland restoration efforts, with little consideration for natural processes or the need for ecosystems to self-perpetuate (Higgs 2003). Restoration efforts remained sporadic during the first half of the 20th century until 1989 when the U.S. government established a federal policy of "no-net loss of wetlands". This led to a substantial increase in the funding allocated to wetland restoration projects by the Environmental Protection Agency. Coincidentally, the scientific community's collective interest in restoration ecology grew during the 1980s and led to the foundation of the Society for Ecological Restoration in 1983. During that time, restoration projects were placed under increasing scientific scrutiny which revealed several project shortcomings. For example, Zedler (1999) questioned the assumption that ecosystems follow predictable trajectories and Kentula (2000) discussed the lack of clear metrics to define restoration success.

Despite the substantial increase in wetland restoration projects, recent empirical studies (e.g., Matthews & Endress 2008; Van den Bosch & Matthews 2017) and meta-analyses (e.g., Moreno-Mateos et al. 2015) have reported a wide variability in wetland response to restoration treatments, with projects sometimes falling short of restoration targets (Matthews 2015; Brudvig et al. 2017). In the literature, vegetation response has ranged from immediate and linear (e.g., Staszak & Armitage 2013) to slow and chaotic (Moreno-Mateos et al. 2012). With this significant variability, it becomes difficult to predict a site's capacity to support long-term restoration objectives or identify the site design best suited to local conditions and ecological goals (Suding 2011). Brudvig et al. (2017) urged the scientific community to study the causes of this variation to improve our capacity to predict both short-term and long-term restoration outcomes. Developing low-cost monitoring tools is critical to gaining a better understanding of factors causing this variability, considering the intensification of the wetland restoration effort throughout the country. Between 2004 and 2009, the country experienced the greatest rate of wetland re-establishment (i.e., human manipulation of site characteristics to recover wetland functions) in three decades (Dahl 2011).

The ecological literature counts several efforts comparing long-term vegetation dynamics across a site sample. For example, Matthews (2015) associated variability in vegetation coverage and composition to site age and landscape context. Moreno-Mateos et al. (2015) revealed the slow recovery of wetlands' biological resources, with some wetlands remaining below restoration targets even after 100 years. However, most studies published to date have focused on plot-level indicators of restoration progress (i.e., indicators directly measured in the field). These indicators include species composition, vegetation height, or functional diversity among many others. While these plot-level indicators can provide a robust measure of post-restoration recovery, they are resource intensive in large sites or where long-term monitoring is needed to account for fluctuations. Previous studies have noted that restoration monitoring tends to be limited in space and time, which can lead to an overestimation of success or fail to detect unexpected fluctuations (Van den Bosch and Matthews 2017).

Remote sensing could address these shortcomings by complementing field surveys at low cost to expand the scale of monitoring efforts. When applied at a large scale, remote sensing favors data upscaling through well-calibrated equations (Byrd et al. 2016; Knox et al. 2017) or training samples used to produce land cover classifications and map suitable habitats (Fleskes and Gregory 2010; Stralberg et al. 2010; Nagendra et al. 2013). It also provides a basis for the landscape-scale comparison of multiple sites. Such large-scale ecological data can help measure ecosystem services including habitat provisioning (Kelly et al. 2011), carbon sequestration

(Kulawardhana et al. 2015), and subsidence reversal (Rosso et al. 2006; Kulawardhana et al. 2015). Remote sensing also provides a key opportunity to detect ecosystem stressors or unexpected site changes (Chapple and Dronova 2017). However, remote sensing remains underutilized in wetland restoration monitoring and few studies have used this technology to produce regional syntheses of restoration progress.

Scope

This dissertation uses the Sacramento San-Joaquin Delta (here after termed the Delta) as a case study to explore the potential of free remote sensing datasets for post-restoration wetland monitoring. The Delta is confined between the cities of Tracy (37.7397° N, 121.4252° W) and Sacramento (38.5816° N, 121.4944° W) and located at the confluence of the Sacramento and San Joaquin rivers. It shelters freshwater marshes dominated by *Schoenoplectus acutus* and *Typha spp.* as well as tidal wetlands dominated by *Sarcocornia pacifica* and *Spartina spp*. (Parker et al. 2011). The Suisun Marsh, adjacent to the Delta, is the largest remaining brackish wetland in the Western United States and includes sites dominated by *Salicornia virginica* and *Distchilis spicata*.

In the Delta, a large-scale reclamation of wetlands during the 1850s and the subsequent agricultural and urban development have degraded wetland habitats and their capacity to fulfill critical ecosystem functions (SFEI-ASC, 2014; Whipple et al., 2012). These transformations have resulted in the loss of 98% of freshwater wetlands and 95% of tidal marshes historically found in the region (Whipple et al. 2012). This large-scale land conversion has triggered a phenomenon of land subsidence, with some islands subsiding at an average rate of 0.3 to 1m per year (Lund et al. 2010). Furthermore, the sediment supply critical to wetland expansion and build-up has been altered by the construction of dams in the early 20th century. Yearly removal of depositional sediments for the maintenance of transportation canals further decreases the amount of sediment available for soil accretion, which in turn hampers wetlands from increasing their elevation and resisting sea level rise (Krone and Hu 2001; Wright and Schoellhamer 2005). Large-scale fragmentation has also impacted fish species historically using tidal wetlands (SFEI-ASC 2014) and the dispersal capacity of certain plant species (Grewell et al. 2013).

Today, the Delta remains under considerable pressure as a provider of freshwater for 25 million Californians and 4.5 million acres of cropland. The expected increase in the frequency and magnitude of droughts in California (Diffenbaugh et al. 2015) will further impact the region's wetlands and the species it shelters (Parker et al. 2011). Substantial effort has been deployed in the last twenty years to restore wetlands in the Delta. Over 25,000 acres of wetland habitat have already been restored while 2,000 additional acres are underway (CWMW,2018). The acreage of wetland habitat will increase considerably with the recent adoption of measure AA, a California parcel tax funding wetland restoration projects in the estuary. This expansion of restoration effort presents both a critical need and unique opportunity to learn from past projects to improve future planning and design.

Research objectives

Most studies published to date have focused on plot-level vegetation indicators to characterize the post restoration trajectories of sites (i.e., temporal dynamics from time of restoration to

present day) while fewer studies have measured vegetation progress at the site scale. My dissertation seeks to address this gap by developing a methodological framework leveraging open source remote sensing data to characterize site trajectories and compare vegetation dynamics across multiple sites. I apply this methodological framework to a sample of restored and reference sites in the Sacramento-San Joaquin Delta to assess how site design, management characteristics, and landscape context affect vegetation dynamics following restoration treatments with an emphasis on emergent vegetation. In the last chapter, I expand the scope of my analysis by studying the relationships between wetland vegetation properties, abiotic factors, and spectral indices throughout different wetland types of the conterminous United States. Expanding the scale of analysis in the last chapter enables me to explore relationships based on remote sensing data that could be used to monitor spatiotemporal changes in properties of wetland vegetation in the Delta and elsewhere. The specific objectives of the dissertation are listed below.

1. **Provide the first landscape-scale synthesis of wetland restoration efforts in the Delta** (chapters 1, 2, and 3)**.** While the region has been the object of an extensive body of literature, no study published to date has provided a comprehensive assessment of the ongoing restoration effort in the Delta. Published studies have focused on a single site or presented a "snapshot" of a site sample. I aim to fulfill this gap by examining the vegetation dynamics of 21 restored and 5 reference wetlands across 20 years of remote sensing data. By comparing long-term changes in this sample of sites, I seek to identify landscape factors (e.g., adjacent land uses, connectivity to other wetland habitats) that promote vegetation growth and resistance to stressors. Such an effort can help improve the planning and design of future projects, by highlighting the most successful restoration practices and landscape contexts most likely to produce enduring ecological benefits. It provides a much-needed landscape perspectives on past and future restoration projects in the Delta (Kimmerer et al. 2005).

2. **Improve our understanding of post-restoration wetland dynamics** (chapters 2 and 3)**.** The current monitoring of restoration projects tends to be limited in both spatial and temporal scope. Most scientific publications describing the post-restoration trajectory of wetlands have focused on plot-level indicators of recovery. This study is one of the first to use remotely-sensed data to describe changes in the spatial structure and diversity of plant communities in restored wetlands. In addition, this dissertation advances our current understanding of site and landscape-level factors affecting the trajectory of wetlands.

3. **Identify cost-effective metrics of vegetation dynamics that show a rapid and consistent response to site changes** (chapters 1, 2, 3, 4). Previous studies have pointed to a lack of consistent monitoring as a possible cause for the substantial variability in restoration outcomes reported in the literature (Brudvig 2011; Suding 2011). This dissertation addresses the issue by reviewing current methods for post-restoration appraisal (chapter 1). Chapter 1 discusses how novel and well-established geospatial tools and methods could complement field monitoring effort in the Delta and elsewhere. Then, chapter 2 identifies landscape metrics (i.e., metrics characterizing the form, distribution, and diversity of land cover patches) most responsive to restoration treatments, time, and vegetation dynamics. Chapter 3 tests the potential of phenology metrics (i.e., metrics derived from seasonal growing vegetation curves) to track vegetation dynamics in restored wetlands. Chapter 4 tests the impacts of land surface properties (i.e., vegetation cover and composition, proportion of open water, bare soil coverage) on spectral

vegetation indices typically used to monitor wetlands. These analyses will hopefully provide cost-effective tools to promote long-term and large-scale monitoring of wetlands.

Thesis structure

Chapter 1 reviews methods and metrics currently used to monitor wetland restoration progress in the Bay-Delta region. Using recent literature focusing on the Bay-Delta and elsewhere, it discusses how geospatial tools and datasets could be used to complement field surveys and expand the current spatiotemporal scope of wetland monitoring at low cost.

Chapters 2 and 3 seek to address some of the gaps identified in chapter 1 by developing remote sensing-based strategies to track wetland restoration progress at a landscape-scale. These monitoring strategies are applied to a sample of restoration projects in the Delta to gain insights on factors modulating the responses of local vegetation to restoration treatments.

Chapter 2 seeks to identify a set of landscape metrics (i.e., metrics describing the geometry, distribution, and diversity of land cover patches) most responsive to restoration treatments and vegetation dynamics. Specifically, this chapter leverages breakpoint analysis - a time series segmentation method frequently used to measure ecosystem response to disturbances– to identify phases in the development of wetland vegetation following restoration treatments across 21 restored sites. High resolution data from USDA's National Agriculture Inventory Program (NAIP) is then used to relate these phases in vegetation development to a set of landscape metrics describing changes in the distribution and shape of vegetated patches. Lastly, sites showing similar phases are grouped to assess the incidence of site design and landscape context on vegetation dynamics. Results demonstrate that several landscape metrics, including patch density, mean patch area, and distance to nearest neighbor, show significant responses to restoration treatments and vegetation processes including colonization. This chapter shows that landscape metric analyses and public remote sensing data can be combined to compare site trajectories at low cost and to identify landscape and site factors modulating wetland recovery.

Chapter 3 studies phenological changes within 20 restored wetlands and 5 reference sites. Using spectral vegetation indices derived from Landsat 7 ETM + and 8 OLI data, growing season curves are generated for each site from 2000 to 2017. Phenological metrics are derived from these growing season curves to reveal temporal changes in vegetation extent, productivity, and site feedbacks impacting the timing of key phenological events. Results reveal a significant phenological response of wetland sites to restoration treatments and climatic fluctuations. These phenological variations can impact the provisioning of key ecosystem functions provided by wetlands of the Delta, indicating that phenological analyses could be utilized to both characterize wetland recovery and help measure key ecosystem functions.

Chapter 4 expands the scale of analysis by leveraging the National Wetland Condition Assessment dataset to study relationships between wetland surface properties and a suite of spectral vegetation indices (i.e., NDVI, EVI, GCC, GNDVI, SAVI and LSWI) typically used as a proxy for vegetation coverage and productivity. Specifically, this chapter leverages field data collected by the National Wetland Condition Assessment in 1,138 sites of the conterminous United States. Applying both single and multivariate linear models, the chapter assesses how spectral vegetation indices respond to vegetation structure and composition, abiotic factors, and climatic and edaphic conditions. Results show substantial variability among wetland types in the

performance of vegetation indices, likely due to differences in vegetation density, dominant growth forms, and water levels. This suggests that the selection of vegetation indices and incorporation of attenuation factors (e.g., water levels, litter) should be tailored to the wetland type of interest.

References

Allan, J. D., P. B. McIntyre, S. D. P. Smith, B. S. Halpern, G. L. Boyer, A. Buchsbaum, G. A. Burton, L. M. Campbell, W. L. Chadderton, J. J. H. Ciborowski, P. J. Doran, T. Eder, D. M. Infante, L. B. Johnson, C. A. Joseph, A. L. Marino, A. Prusevich, J. G. Read, J. B. Rose, E. S. Rutherford, S. P. Sowa, and A. D. Steinman. 2013. Joint analysis of stressors and ecosystem services to enhance restoration effectiveness. Proceedings of the National Academy of Sciences of the United States of America 110:372–377.

Almeida, D., J. Rocha, C. Neto, and P. Arsénio. 2016. Landscape metrics applied to formerly reclaimed saltmarshes: A tool to evaluate ecosystem services? Estuarine, Coastal and Shelf Science 181:100–113.

Barbier, E. B., I. Y. Georgiou, B. Enchelmeyer, and D. J. Reed. 2013. The Value of Wetlands in Protecting Southeast Louisiana from Hurricane Storm Surges. PLoS ONE 8:1–6.

Bedford, B. L. 1999. Cumulative Effects on Wetland Landscapes: Links to Wetland Restoration in the United States and Southern Canada. Wetlands 19:775–788.

Van den Bosch, K., and J. W. Matthews. 2017. An Assessment of Long-Term Compliance with Performance Standards in Compensatory Mitigation Wetlands. Environmental Management 59:546–556.

Brudvig, L. A. 2011. The restoration of biodiversity: where has research been and where does it need to go? American journal of botany 98:549–58.

Brudvig, L. A., R. S. Barak, J. T. Bauer, T. T. Caughlin, D. C. Laughlin, L. Larios, J. W. Matthews, K. L. Stuble, N. E. Turley, and C. R. Zirbel. 2017. Interpreting variation to advance predictive restoration science. Journal of Applied Ecology:1018–1027.

Byrd, K. B., L. Windham-Myers, T. Leeuw, B. Downing, J. T. Morris, and M. C. Ferner. 2016. Forecasting tidal marsh elevation and habitat change through fusion of Earth observations and a process model. Ecosphere 7:1–27.

California Wetlands Monitoring Workgroup (CWMW). 2018. EcoAtlas. Accessed April 3, 2018. https://www.ecoatlas.org.

Chapple, D., and I. Dronova. 2017. Vegetation Development in a Tidal Marsh Restoration Project during a Historic Drought: A Remote Sensing Approach. Frontiers in Marine Science 4.

Chapple, D. E., P. Faber, K. N. Suding, and A. M. Merenlender. 2017. Climate Variability Structures Plant Community Dynamics in Mediterranean Restored and Reference Tidal

Wetlands. Water 9:209–226.

Dahl, T. E. 2000. Status and Trends of Wetlands in the Conterminous United States 1986 to 1997. Washington, DC.

Dahl, T. E. 2011. Status and Trends of Wetlands in the Contermious United States 2004 to 2009. Washington, DC.

Diffenbaugh, N. S., D. L. Swain, and D. Touma. 2015. Anthropogenic warming has increased drought risk in California. Proceedings of the National Academy of Sciences 112:201422385.

Fleskes, J. P., and C. J. Gregory. 2010. Distribution and Dynamics of Waterbird Habitat During Spring in Southern Oregon—Northeastern California. Western North American Naturalist 70:26–38.

Grewell, B. J., E. K. Espeland, and P. L. Fiedler. 2013. Sea change under climate change : case studies in rare plant conservation from the dynamic San Francisco Estuary. Botany 91:309–318.

Higgs, E. 2003. Nature by design: people, natural process, and ecological restoration. MIT Press, Cambridge, Mass.

Jankowski, K. L., T. E. Törnqvist, and A. M. Fernandes. 2017. Vulnerability of Louisiana's coastal wetlands to present-day rates of relative sea-level rise. Nature Communications 8:1–7.

Kayranli, B., M. Scholz, A. Mustafa, and Å. Hedmark. 2010. Carbon storage and fluxes within freshwater wetlands: A critical review. Wetlands 30:111–124.

Kelly, M., K. a. Tuxen, and D. Stralberg. 2011. Mapping changes to vegetation pattern in a restoring wetland: Finding pattern metrics that are consistent across spatial scale and time. Ecological Indicators 11:263–273.

Kentula, M. E. 2000. Perspectives on setting success criteria for wetland restoration. Ecological Engineering 15:199–209.

Kimmerer, W. J., D. D. Murphy, and P. J. Angermeier. 2005. A Landscape-level Model for Ecosystem Restoration in the San Francisco Estuary and its Watershed. San Francisco Estuary & Watershed 3.

Knox, S. H., I. Dronova, C. Sturtevant, P. Y. Oikawa, J. H. Matthes, J. Verfaillie, and D. Baldocchi. 2017. Using digital camera and Landsat imagery with eddy covariance data to model gross primary production in restored wetlands. Agricultural and Forest Meteorology 237–238:233–245.

Krone, R., and G. Hu. 2001. Restoration of subsided sites and calculation of historic marsh elevations. Journal of Coastal Research SI:162–169.

Kulawardhana, R. W., R. A. Feagin, S. C. Popescu, T. W. Boutton, K. M. Yeager, and T. S.

Bianchi. 2015. The role of elevation, relative sea-level history and vegetation transition in determining carbon distribution in Spartina alterniflora dominated salt marshes. Estuarine, Coastal and Shelf Science 154:48–57.

Lund, J., E. Hanak, W. Fleenor, W. Bennett, and R. Howitt. 2010. Comparing Futures for the Sacramento-San Joaquin Delta. University of California Press, Berkeley.

Matthews, J. W. 2015. Group-based modeling of ecological trajectories in restored wetlands. Ecological Applications 25:481–491.

Matthews, J. W., and A. G. Endress. 2008. Performance criteria, compliance success, and vegetation development in compensatory mitigation wetlands. Environmental Management 41:130–141.

Moreno-Mateos, D., P. Meli, M. I. Vara-Rodríguez, and J. Aronson. 2015. Ecosystem response to interventions: Lessons from restored and created wetland ecosystems. Journal of Applied Ecology 52:1528–1537.

Moreno-Mateos, D., M. E. Power, F. A. Comín, and R. Yockteng. 2012. Structural and functional loss in restored wetland ecosystems. PLoS Biology 10:e1001247.

Nagendra, H., R. Lucas, J. P. Honrado, R. H. G. Jongman, C. Tarantino, M. Adamo, and P. Mairota. 2013. Remote sensing for conservation monitoring: Assessing protected areas, habitat extent, habitat condition, species diversity, and threats. Ecological Indicators 33:45–59.

Parker, V. T., J. C. Callaway, L. M. Schile, M. C. Vasey, and E. R. Herbert. 2011. Climate Change and San Francisco Bay – Delta Tidal Wetlands. San Francisco Estuary and Watershed Science 9:1–15.

Rosso, P. H., S. L. Ustin, and a. Hastings. 2006. Use of lidar to study changes associated with Spartina invasion in San Francisco Bay marshes. Remote Sensing of Environment 100:295–306.

San Francisco Estuary Institute-Aquatic Science Center (SFEI-ASC). 2014. A Delta Transformed: Ecological Functions, Spatial Metrics, and Landscape Change in the Sacramento-San Joaquin Delta. SFEI Contribution No. 729. San Francisco Estuary Institute - Aquatic Science Center: Richmond, CA.

Simenstad, C., D. Reed, and M. Ford. 2006. When is restoration not? Incorporating landscape-scape processes to restore self-sustaining ecosystems in coastal wetland restoration. Ecological Engineering 26:27–39.

Staszak, L. a., and A. R. Armitage. 2013. Evaluating Salt Marsh Restoration Success with an Index of Ecosystem Integrity. Journal of Coastal Research 287:410–418.

Stralberg, D., M. P. Herzog, N. Nur, K. A. Tuxen, and M. Kelly. 2010. Predicting avian abundance within and across tidal marshes using fine-scale vegetation and geomorphic metrics. Wetlands 30:475–487.

Suding, K. N. 2011. Toward an Era of Restoration in Ecology: Successes, Failures, and Opportunities Ahead. Annual Review of Ecology, Evolution, and Systematics 42:465–487.

US Environmental Protection Agency (US EPA). 2016. National Wetland Condition Assessment 2011: A Collaborative Survey of the Nation's Wetlands. Washington, DC.

Whipple, A., A. Grossinger, D. Rankin, B. Stanford, and R. Askevold. 2012. Sacramento-San Joaquin Delta Historical Ecology Investigation : Exploring Pattern and Process.

Wortley, L., J.-M. Hero, and M. Howes. 2013. Evaluating Ecological Restoration Success: A Review of the Literature. Restoration Ecology 21:537–543.

Wright, S. a., and D. H. Schoellhamer. 2005. Estimating sediment budgets at the interface between rivers and estuaries with application to the Sacramento-San Joaquin River Delta. Water Resources Research 41:1–17.

Zedler, J. B. 2003. Wetlands at your service : reducing impacts of agriculture at the watershed scale. Frontiers in Ecology and the Environment 1:65–72.

Zedler, J. B. 2007. Success: An unclear, subjective descriptor of restoration outcomes. Ecological Restoration 25:162–168.

Zedler, J. B., J. C. Callaway, S. Diego, and S. M. Na-. 1999. Tracking Wetland Restoration : Do Mitigation Sites Follow Desired Trajectories ? Restoration Ecology 7:69–73.

Zhao, Q., J. Bai, L. Huang, B. Gu, Q. Lu, and Z. Gao. 2016. A review of methodologies and success indicators for coastal wetland restoration. Ecological Indicators 60:442–452.

Chapter 1

Geospatial tools for the large-scale monitoring of wetlands in the San Francisco Bay-Delta: opportunities and challenges

This chapter was co-authored with Iryna Dronova.

Abstract

Significant wetland losses and continuing threats to remnant habitats have motivated extensive restoration efforts in the San Francisco Bay-Delta estuary of California, the largest in the Western United States. Consistent monitoring of ecological outcomes from this restoration effort would help managers learn from past projects to improve the design of future endeavors. However, budget constraints and challenging field conditions can limit the scope of current monitoring programs. Geospatial tools and remote sensing datasets could help complement field efforts for a low cost, longer, and broader monitoring of wetland resources. To understand where geospatial tools could best complement current field monitoring practices, we reviewed the metrics and monitoring methods used by 42 wetland restoration projects implemented in the estuary. Monitoring strategies within our sample of monitoring plans relied predominantly on field surveys to assess key aspects of vegetation recovery while geospatial datasets were used sparingly. Drawing on recent publications that focus on the estuary and other wetland systems, we propose additional geospatial applications to help monitor the progress made towards site-specific and regional goals. These include the use of ecological niche models to target on-the-ground monitoring efforts, the upscaling of field measurements into regional estimates using remote sensing data, and the analysis of time series to detect ecosystem shifts. We discuss challenges and limitations to the broad scale application of remote sensing data in wetland monitoring. These notably include the need to find a venue to store and share computationally intensive datasets, the often cumbersome preprocessing effort needed for long-term analyses, and multiple confounding factors that can obscure the signal of remote sensing datasets.

1 Introduction

Ecological restoration is increasingly used to address the substantial worldwide loss of wetland ecosystems and their ecological benefits (Davidson 2014). In the United States, the *No Net Loss of Wetlands* policy mandates that federal agencies offset unavoidable wetland losses through the restoration, creation, or enhancement of a site of equal functional value. As a result, wetland restoration efforts have intensified across the country (Deland 1992; National Research Council 2001). The policy itself is implemented through different regulatory frameworks including Section 404 of the Clean Water Act enforced by the U.S. Army Corps of Engineers which regulates the discharge of dredged and fill material in most wetlands (National Research Council 2001). The growing societal awareness of wetlands' key role in supporting biodiversity and ecosystem services has further motivated non-profit and governmental organizations to fund restoration efforts throughout the United States (Dahl 2011). However, evidence from previous scientific studies shows a substantial variability in post-restoration outcomes, even under similar

approaches (Matthews and Spyreas 2010; Matthews 2015). Regional assessments and global meta-analyses have documented projects falling short of targets or failing to meet the richness or ecosystem functions of reference sites, sometimes even after more than 50 years (Matthews and Spyreas 2010; Moreno-Mateos et al. 2012). A current lack of consistent long-term monitoring, as reported in previous publications, limits the availability of robust ecological information to help identify the site characteristics, restoration interventions, and landscape planning strategies promoting site recovery (Simenstad et al. 2006; Matthews and Endress 2008; Suding 2011). There is an increasing recognition that monitoring is key to detecting ecosystem stressors and promoting adaptive management, particularly in sites exhibiting a high spatial and temporal complexity (Perring et al. 2015; Brudvig et al. 2017).

Nearly 80% of wetlands historically present in the San Francisco Bay and 95% of the wetlands in the Sacramento-San Joaquin Delta have been heavily modified or converted into urban and agricultural lands (Goals Project 1999; Whipple et al. 2012). In the Suisun Bay, most tidal wetlands were diked and are now managed as freshwater habitats used by duck clubs (Goals Project 1999; Moyle et al. 2013). Remaining wetlands are subject to increasing ecosystem stress due to rapid urbanization, urban and agricultural runoffs, and invasive species (Lund et al. 2010; Luoma et al. 2015). Global climate changes may further impact wetland processes by increasing droughts (Diffenbaugh et al. 2015), salinity, and sea level rise (Holmes 2012) which will affect plant growth and composition (Parker et al. 2011). Furthermore, these ecosystem stressors may increase the habitat extent needed to fulfill ecosystem services (Simenstad et al. 2006) and exacerbate the vulnerability of local human populations to extreme climatic events (Barbier et al. 2013; Jankowski et al. 2017).

In response to this continuing pressure on remaining wetland habitats, several restoration projects have been initiated in the San Francisco Bay-Delta estuary (here after “the estuary”). The first significant restoration efforts date from the early 1970s with the adoption of the Clean Water Act (Callaway et al. 2012). Wetland restoration intensified in the early 2000s with the formation of CALFED, a multi-agency effort to address both societal and environmental water needs in California. From 2002 to 2015, 6,300 acres were opened to the tides in the San Francisco Bay and 25,000 acres restored in the Sacramento-San Joaquin Delta (San Francisco Estuary Partnership 2015). Over the last two decades, projects have increased in size and topographic complexity (Callaway et al. 2011; Callaway and Parker 2012). Common restoration goals for the estuary include enhancing species diversity, reducing coastal erosion, and improving water quality among many other objectives (Table 1).

The current abundance and variety of restoration projects in the estuary present an outstanding opportunity for in-depth analyses of wetland monitoring practices and strategies to make this monitoring more cost-effective. Over 300 projects have been launched since the 1970s in different parts of the estuary (CWMW, 2018) which have been documented by impressive regional data collection efforts. The EcoAtlas database of restoration projects in California is a notable example which provides information on project scope and goals and thus significantly facilitates the understanding of project characteristics, time frames, and geographic representation (CWMW, 2018). However, the monitoring aspect of restoration has not yet been

extensively addressed by these efforts. There is an emergent need and opportunity to improve monitoring practices in the region given the recent approval of Measure AA, a California parcel tax funding wetland restoration projects in the region. This measure will fund the restoration of 24,000 acres of additional wetland habitats over the next 20-30 years.

Robust post-restoration data could inform the planning and design of future projects in the estuary and help measure the progress made towards regional goals (Table 1). Previous papers have called for a broadening of restoration planning (Kimmerer et al. 2005; Simenstad et al. 2006) and monitoring (Kentula 2000; Breaux et al. 2005), recognizing that the combined benefits of multiple restoration projects may be needed to fulfill regional wetland conservation objectives including increasing habitat quantity and connectivity or enhancing regional carbon sequestration potential (Table 1). These goals require data with a large spatial scope and high temporal frequency (Kentula 2000; Matthews and Spyreas 2010). Yet many field-focused approaches are resource intensive and need to be repeated in time and space (Noss 1990; Wilcox et al. 2002; Moorhead 2013). Geospatial tools (i.e., spatial or remote sensing-based analyses of changes in vegetation extent, structure, and composition) have been applied at both local and regional scales to measure the contribution of conservation efforts to ecosystem service provisioning (e.g., Botequilha Leitao and Ahern 2002; McGarigal et al. 2009; Nagendra et al. 2013) but remain somewhat underutilized in wetland restoration monitoring (Taddeo and Dronova 2018). The increasing availability of low-cost, frequent, and high-resolution remote sensing datasets (e.g., NAIP, Landsat, RapidEye) provides an opportunity to complement field surveys economically and at a larger scale to help project managers evaluate compliance with site-specific or region-wide wetland objectives. Recent papers focusing on the San Francisco Bay estuary have leveraged different geospatial time series to monitor fluctuations in vegetation productivity and composition (e.g., Tuxen et al. 2008; Chapple and Dronova 2017), upscale field measurements into regional estimates (e.g., Byrd et al. 2018), track invasive species (e.g., Hestir et al. 2008; Khanna et al. 2018), and map critical habitats for species of concern (e.g., Stralberg et al. 2010; Moffett et al. 2014).

To understand the extent to which geospatial tools are currently used in the estuary, this study reviewed 42 monitoring plans implemented in the region. Drawing on studies conducted in the estuary and elsewhere, we discuss how geospatial tools and datasets could be leveraged, in conjunction with field monitoring efforts, to track currently monitored vegetation metrics at a larger spatiotemporal scale. We also list indicators of vegetation recovery that remain more accurately monitored on the ground, due to limitations in the resolution and availability of geospatial datasets.

2 Methods

2.1 Study area

We focus on restored wetlands of the San Francisco Bay-Delta estuary in California, United States. The estuary is located between the cities of San Francisco at its western border and Stockton and Sacramento at its eastern border (Figure 1). The estuary also includes the cities of Santa Rosa, in the North, and Gilroy, in the South. It is characterized by a salinity gradient due to

the combined influence of the Pacific Ocean and freshwater from the Sacramento and San Joaquin rivers. The estuary supports a variety of wetland types including freshwater wetlands dominated by *Schoenoplectus acutus* and salt marshes dominated by *Salicornia pacifica* and *Spartina spp*. (Parker et al. 2011; Vasey et al. 2012). Brackish wetlands dominated by *Schoenoplectus americanus* and *Bolboschoenus maritimus* are found at the confluence between salt and freshwater in the Suisun Bay, the largest remaining brackish wetland in the Western United States (Vasey et al. 2012; Moyle et al. 2013).

2.2 Selection of projects/data collection

We used the EcoAtlas database of wetland restoration in California to find projects implemented within the estuary (Figure 1). Among the 332 projects listed for this region, we identified 35 restoration projects corresponding to our research criteria. Those criteria were: (1) wetland-based projects (or restoration projects including a wetland component); (2) located within the estuary, and for which (3) a monitoring plan or report was available. We also consulted the U.S. Army Corps of Engineers' RIBITS database to identify an additional seven sites with adequate documentation. Monitoring reports or plans had to include — at a minimum — the list of indicators used to evaluate their restoration progress.

For each monitoring plan and report, we recorded (1) the indicators used to monitor wetland restoration progress, (2) the sampling design used to measure these indicators; (3) the length and frequency of the monitoring effort, and (4) the success criteria used to assess whether restoration objectives had been met. We also noted information on initial restoration treatments and goals when such information was available. We noted whether spatial datasets, such as remote sensing data, were proposed or used as the basis to map and/or quantify some of the monitored indicators. Finally, we collected information on the "reference data" used to establish restoration targets including the number of reference sites considered, how these sites had been selected, and the sampling design used in these reference sites.

3 Results

3.1 General information about projects

We identified 42 wetland restoration projects with enough information to meet our filtering criteria. These projects were restored between 1976 and 2015, with 24 projects restored after 2000, and 14 restored after 2005. Our project sample included 24 tidal wetlands, three brackish sites, nine non-tidal or diked freshwater sites, four vernal pools, and two wet meadows (Table 2). Projects varied in size from 0.1 and 1,800 acres, with a mean area of 210.94 acres and a standard deviation of 366.33 acres.

Over half of the projects served as compensatory mitigation for the damage or destruction of existing wetlands due to levee maintenance and construction (e.g., Mare Island Navy Mitigation Marsh), freeway extension (e.g., Caldecott Tunnel), and infrastructure development (e.g., Muzzi Marsh, Madera del Presidio). The overall goals of compensatory mitigation were to replace lost ecosystem functions (e.g., habitat provisioning for wildlife and endangered species) via the restoration or enhancement of wetlands. Success criteria used to measure compliance with these

goals varied among projects but included maintaining a high diversity and coverage of native species and reaching a set acreage of wetland habitats (e.g., five acres of estuarine emergent wetlands). Restoration goals for non-compensatory projects included creating wildlife habitats, increasing species diversity, promoting recreational usage, or reversing land subsidence. For tidal wetlands, common restoration actions included breaching to restore flows and tidal prisms, creating a system of channels, excavating and grading to improve topographic heterogeneity, and using dredged material to increase elevation. Common restoration treatments for freshwater wetlands included planting native or desirable species (e.g., *Schoenoplectus acutus* or *Salicornia pacifica*) and removing non-native species.

3.2 Length and frequency of monitoring

Most of the reviewed projects included a monitoring plan to collect information on post-restoration dynamics. Twenty sites were monitored for five years or less, while 34 sites were monitored for 10 years or less. Three sites had planned for 15-25 years of monitoring, while two sites planned to monitor in perpetuity. Lastly, three sites established a monitoring protocol but did not specify the intended length of post-restoration monitoring. In terms of monitoring frequency, 34 sites planned to sample wetland conditions every year, three monitored every other year. Five sites adopted an incremental monitoring schedule, with yearly monitoring during the first five years and every other year after that. Another project planned to monitor every year from years 1 to 8, followed by monitoring every five years from years 10 to 20, and then every 10 years in perpetuity. Only one project used seasonal monitoring to account for the effect of plant phenological differences on composition.

3.3 Sampling design and references

Eighteen projects indicated using reference sites as a benchmark to set restoration targets and two of them utilized more than one reference site. One project described the statistical approach used to assess whether restored sites became statistically similar to reference sites. Fourteen projects had conducted a prior ecological assessment to establish baseline conditions (i.e., site condition before restoration). The length of baseline data monitoring was typically one year, although two sites conducted pre-restoration monitoring for two non-consecutive years. Most projects focused their baseline monitoring effort on the year prior to restoration, while three sites used monitoring data collected respectively two, seven, and eight years before restoration. No project specified the statistical test used to compare baseline and post-restoration conditions.

All projects included field observations to evaluate vegetation-based indicators of recovery while less than half of projects also used geospatial data to monitor progress at a broader site extent. The latter employed either high resolution satellite aerial imagery or ground level photography of vegetation coverage, but only two of these specified the sensor or image database used. In both cases, the images were obtained from a commercial satellite data provider (e.g., Ikonos, GeoEye). Remote sensing data were predominantly utilized to map annual changes in vegetation cover and patch extent. Seven sites used ground-level photography to compare annual changes in vegetation abundance by monitoring the proportion of a focal area covered by vegetation throughout a time series. Few of the restoration plans specified any methodology for the ground-

truthing of ecological data derived from aerial images. However, one site applied the framework developed for the *2009 Vegetation Map Update of the Suisun Marsh*, which infers restoration progress from true color imagery orthorectified using ground control points and a manual delineation of vegetation types (California DFG 2012).

All the reviewed projects leveraged vegetation indicators to evaluate restoration progress. All sites included structural indicators (i.e., indicators characterizing the distribution of plant biomass throughout the canopy) as part of their post-restoration assessments. Vegetation cover proxies were the most commonly used among all structural indicators, assessed either as the proportion of the surface covered by all green vegetation (total coverage) or the coverage of one single species or functional group (plant coverage). Fourteen projects specifically targeted the plant coverage of native or non-native species, while the remaining projects did not distinguish between species status. Three projects measured vegetation cover by functional types (i.e., classification of plants by their main physical, phylogenetic, or phenological characteristics) while four projects targeted a certain plant coverage for specific species (e.g., *Salicornia pacifica*, *Bolboschoenus maritimus*).

Twenty-six projects tracked indicators of plant composition (i.e., taxonomic identity, abundance, and diversity of species within the plant assemblage) to monitor site progress. Fifteen of these conducted a floristic inventory of sites through a visual identification of species presence within permanent monitoring plots. Floristic composition targets focused on the percentage of native species or wetland-specific species. Other projects concentrated on matching the species composition of reference sites. Three sites looked at species richness (i.e., number of species present in a plant community), while four sites examined species diversity (i.e., species richness and evenness). Two sites focused on target species: one considered rare species, and the other the coverage of Californian wetland-specific species.

Four project plans included spatial indicators of recovery. Three of them used habitat mapping (i.e., delineation and quantification of vegetated habitats) while the last one focused on the ratio of water to vegetation. Habitat mapping was achieved using both aerial and satellite images from commercial providers or delineation of the field boundary with a GPS. Finally, one site included an assessment of ecological function: in this case, seedling establishment and recruitment.

4 Discussion

Our analysis reveals a sustained effort in the estuary to track wetland response to restoration treatments. The spatiotemporal scope and performance metrics of this effort vary among projects, likely reflecting a diversity of goals and monitoring requirements as discussed in previous publications focusing on wetland restoration in California (e.g., Kimmerer et al. 2005) and elsewhere (e.g., Matthews and Endress 2008). Monitoring practices in our sample of projects focused on structural indices of vegetation recovery (e.g., plant coverage) and to a lesser extent on indicators of species composition. Only a subset of monitoring plans utilized geospatial tools, primarily to measure changes in vegetation cover or map habitats. While these are important objectives for wetland monitoring and restoration assessments, evidence from recent studies in the region and the growing accessibility of remote sensing data highlight other, still somewhat

underutilized, opportunities to cost-effectively expand the spatiotemporal scope at which we evaluate restoration progress (Table 3). With several conservation plans setting landscape-scale goals for the region (Table 1), there is now an opportunity to develop a more consistent monitoring framework to track the combined contribution of multiple projects towards regional objectives. Geospatial tools can also help project managers measure the progress made towards site-specific objectives.

Project managers now have access to a multitude of sensors providing repeated data (e.g., Ikonos, RapidEye, Landsat; Table 4) enabling vegetation tracking at a constant phenological stage, medium to high spatial resolution, and over large extents. Several of the sensors listed in Table 4 provide multispectral data in three to seven broad spectral bands sensitive to plant biomass and coverage (Pettorelli et al. 2005; Jensen 2007). Hyperspectral sensors can provide spectral information in thousands of narrow bands sensitive to plant chemical composition facilitating the identification of dominant species (Hestir et al. 2008; Andrew and Ustin 2009; Muller-Karger et al. 2018). While free medium-high resolution datasets (e.g., Landsat, SPOT; Table 3) can provide adequate spatial detail to detect general patterns of change in vegetation extent and productivity (e.g., Baker et al. 2007; Wang et al. 2015; Knox et al. 2017), higher resolution data is needed to track changes in plant composition and dominant species. The NAIP dataset provides the finest resolution (0.6 to 1m) of all free datasets (Table 4), but its low acquisition frequency (one image every 2-3 years) and variable timing of acquisition (some images captured at the beginning of the summer, others at the end) make change analysis difficult if relying on this dataset alone. However, combined with other products, the NAIP dataset can increase spatial detail and enhance vegetation mapping for a more robust quantification of wetland processes (e.g., Byrd et al. 2018). Some commercial datasets (Table 4) provide both high resolution and high frequency – but this can be costly for project managers overseeing large sites. Hyperspectral data can best differentiate species that would otherwise be too similar at a lower spectral resolution but is expensive for large sites or regional assessments.

4.1 Opportunities to complement field monitoring using geospatial tools

4.1.1 Habitat mapping

Increasing the extent and quality of ecological habitats is a key restoration objective in the estuary as reflected in the regional goals (Table 1) and objectives of both compensatory mitigation and non-compensatory projects. Habitat quality and extent can be characterized by several field-based vegetation metrics (Craft et al. 2003; Bradbury et al. 2005) or mapped from remote sensing data via well-established spatial analysis methods (Nagendra et al. 2013; Rocchini et al. 2018) to reduce the high cost associated with wildlife observations and stock assessments. Remote-sensing data can be utilized to map suitable habitats for species of interest based on prior knowledge of their occurrence and association with vegetation composition, height, structure, or phenology which translate into spectral contrasts among different habitat types (Nagendra et al. 2013; Andrew et al. 2014). For example, structural diversity (i.e., heterogeneity in growth forms or canopy height), which can be measured using LiDAR data, promotes avian and macroinvertebrate richness in wetlands (Zedler et al. 1999; St. Pierre and Kovalenko 2014). Pickleweed (*Salicornia pacifica*), a species used by the endangered Salt Marsh

Harvest Mouse (*Reithrodontomys raviventris*), can be identified by its late phenology and spectrally homogeneous stands (Tuxen and Kelly 2008). Recognition of different vegetation types can be further enhanced using multi-date imagery which accentuates phenological contrasts (e.g., Wang et al. 2012, Zhong et al. 2012) or narrowband hyperspectral datasets with greater sensitivity to biochemical differences among plant types based on leaf water or chlorophyll content (Andrew et al. 2014).

Analysts can combine different geospatial data sources or leverage ancillary data to improve habitat quantification. For example, using high-resolution topographic data improved the detection of suitable habitats for shorebirds in the Sacramento National Wildlife Refuge Complex (Schaffer-Smith et al. 2018). Stralberg et al. (2010) used LiDAR-derived elevation data, in addition to a remotely sensed survey of vegetation composition, to map suitable habitats for three endangered bird species in the Bay-Delta. Such analyses can also more effectively account for the impact of adjacent land uses and covers on the likelihood that species will adopt suitable habitats (Nagendra et al. 2013). For instance, Tuxen and Kelly (2008) leveraged high-resolution aerial photography and LiDAR data to map suitable habitats for the Salt Marsh Harvest Mouse (i.e., dense covers of pickleweed) and its preferred landscape context (i.e., proximity to elevated patches where it can find refuge during tides).

Landscape metrics (i.e., statistics describing the spatial structure, heterogeneity, and distribution of habitat patches) can help evaluate the quantity and quality of habitats as they reflect key processes and properties including species dispersal, water flows, and water quality (Moreno-Mateos et al. 2008; McGarigal et al. 2009; Sloey et al. 2015). As an example, three landscape metrics describing the size and shape of habitat patches were effective predictors of the Song Sparrow's (*Melospiza melodia pusillula*) distribution in the estuary (Moffett et al. 2014). Landscape metrics may also reveal patterns of fragmentation (Markle et al. 2018) or landscape homogenization (Costanza et al. 2011) which might reduce the capacity of sites to meet species diversity targets or maintain wildlife populations. Several conservation plans — including the BDCP and Delta Conservation Framework — are targeting an increase in the connectivity of wetland habitat patches, which can be similarly approximated by a suite of landscape metrics (Turner et al. 1998) but was not explicitly measured in the monitoring plans of our sample. Landscape connectivity promotes the movement of resources, genes, seeds, and individuals (Rudnick et al. 2012) critical to ecosystem resilience (Turner et al. 1998; Lindborg and Eriksson 2004). Using a consistent classification nomenclature and methodology to map suitable wetland habitats across the estuary could help measure the contribution of restoration efforts on regional habitat connectivity. To this effect, the *Tidal Monitoring Framework for the Upper San Francisco Estuary* (IEP TWM PWT 2017) recommends applying the CalVeg habitat classification system upon aerial images to maintain consistency among different monitoring efforts. Once such a consistent mapping of vegetated habitats is completed, different GIS-based methods, including network analyses and resistance kernels, can quantify habitat connectivity throughout the region (Minor and Urban 2008; Fortin et al. 2012; Rudnick et al. 2012).

Lastly, applying the aforementioned strategies to spatially contiguous remote sensing data may help detect the presence and coverage of target species, such as undesirable non-native species

or, in contrast, rare species as indicators of restoration progress. Both the Delta Plan (2013) and Delta Conservation Framework (2016) stress the importance of timely prevention and early detection of biological invasions, which are expected to intensify with climate change (Callaway and Parker 2012; Grewell et al. 2013). Furthermore, eradication is more cost-effective when populations are still small and isolated (Reaser et al. 2008; Kettenring and Adams 2011). Several studies conducted in the Bay-Delta highlight the promise of repeated remote sensing data to track the progression of non-native species (e.g., Hestir et al. 2008; Ta et al. 2017; Khanna et al. 2018) which were predominantly monitored in the field within our sample. Invasive species can be distinguished from co-existing native species when they present distinct spectral or phenological properties (Bradley 2014) such as unique flowering schedules (Andrew and Ustin 2008), or, in the case of aquatic weeds, a contrast to open water (Hestir et al. 2008; Bradley 2014). The characteristic spatial pattern, or "texture", of some invasive species can also facilitate their detection; for instance, Boers and Zedler (2008) identified areas of high *Typha x. glauca* dominance within aerial images by their dark homogeneous circular patches. Though more expensive, hyperspectral imagery facilitates the detection of invasive plant species based on more subtle spectral contrasts resulting from unique biochemical, anatomical, and structural plant properties (Hestir et al. 2008).

Ecological niche models may help target the monitoring of non-natives when sites are too large to use more costly high resolution or hyperspectral data or where populations are too small to be detected using remote sensing data alone (Andrew and Ustin 2009). Project managers could leverage existing datasets documenting non-native species occurrences to construct their habitat models (e.g., Calflora and Calflora's WeedMaper) and identify suitable habitats where monitoring efforts using high resolution, spectral, or field data should be targeted. Such a modelization approach could also be applied for a more targeted monitoring of rare species or species of particular interest because they provide habitat benefits and additional ecosystem services (Guisan and Thuiller 2005; Sousa-Silva et al. 2014).

4.2 Upscale field measurements into site or regional estimates

Some of the restoration goals set for the estuary will rely on the combined effect of multiple projects, which creates the need to develop region-wide estimates of the key ecosystem parameters and indicators assessed by individual projects. Well-calibrated relationships between ecosystem processes of interest and vegetation properties detectable from satellite images could enable such an upscaling of field measurements both within large spatial extents of individual projects and across the region. Several regional studies have demonstrated promise for upscaling wetland vegetation biomass (e.g., Byrd et al. 2014; Byrd et al. 2016; Byrd et al. 2018), leaf area index (e.g., Dronova and Taddeo 2016), primary productivity and greenhouse gas fluxes (e.g., Knox et al. 2017; McNicol et al. 2017) using spectral vegetation indices derived from open access and commercial remote sensing data. In general, these relationships, similar to previous successes from terrestrial ecosystems, are based on the effects of physiological, biochemical, and structural properties of vegetation on the absorption, transmission, and reflection of solar radiation shaping plant signatures in remote sensing data (Jensen 2007). Wetland environments, however, pose unique challenges to upscaling frameworks due to the patchiness of their

vegetation and the suppression of plant spectral signals by background effects of dead biomass (Rocha et al. 2008, Schile et al. 2013, Byrd et al. 2014) and water (Kearney et al. 2009; Byrd et al. 2014; Kulawardhana et al. 2014). Correcting for these effects may be possible using specialized image processing methods such as determining relative fractions of vegetation, water, and dead biomass inside minimum mapping units (Dronova and Taddeo 2016) or selecting data with spectral regions showing a high sensitivity to target properties (Byrd et al. 2014).

Other studies have tested the potential of light detection and ranging (LiDAR) instruments for the monitoring of vertical accretion in wetlands (e.g., Rosso et al. 2006; Kulawardhana et al. 2015). LiDAR systems are active sensors that emit and receive radiation signals. The time needed for a LiDAR pulse to reach land surfaces and return back provides information on the elevation and height of land features (Hudak et al. 2009), and, to some degree, on the vertical structure of plant canopies. Annual changes in the digital elevation model (DEM) derived from LiDAR data can be measured to characterize vertical accretion in wetlands (Rosso et al. 2006; Deverel et al. 2014). However, due to the high cost of LiDAR data acquisition and processing, it has not been used systemically across the Bay-Delta region to survey and make comparisons between sites.

4.3 Establish baseline and reference conditions for restoration targets

The monitoring of baseline and reference conditions in our project sample was typically limited to one year (or two years in rare cases). Current literature emphasizes the importance of tracking baseline and reference conditions for multiple years to account for the impact of climate, salinity, hydrology, and species succession on wetland conditions (White and Walker 1997; Zedler et al. 1999; Moorhead 2013; Johnson et al. 2017). Ecosystem variability is an important concern in the estuary where annual fluctuations in precipitation and salinity can impact the vegetation extent (Chapple and Dronova 2017), productivity (Parker et al. 2011), and composition (Chapple et al. 2017) of both restored and reference sites. Expanding the temporal scope and frequency at which reference or baseline data are collected is therefore critical in setting realistic restoration targets and accounting for the impact of landscape context and abiotic conditions on the capacity of a site to meet those targets. The dynamic reference concept proposes to set such flexible targets via a simultaneous monitoring of restored and reference sites to account for impacts of environmental fluctuations on restoration indicators and then adjusting restoration targets (Hiers et al. 2012). Repeatedly acquired remote sensing data can facilitate this task by tracking key environmental and vegetation parameters and comparing them among restored and reference sites. For example, Tuxen et al. (2011) used high resolution aerial photography to track changes in the extent and diversity of plant communities in a series of reference and restored tidal wetlands of the estuary. Their analyses revealed a higher variability and diversity of plant communities in more recently restored sites versus mature ones. Tracking environmental conditions in several reference sites could also help determine a range of acceptable post-restoration targets. Previous studies have even suggested using less successful restoration projects to set a lower limit of expectation and reference wetlands to set the upper range of acceptable wetland conditions (Kentula 2000; Matthews and Spyreas 2010). Understanding year-

to-year fluctuations in wetland vegetation properties could also help identify which specific characteristics should be measured with greater frequency. For example, Chapple and Dronova (2017) showed that droughts impact vegetation expansion, suggesting that monitoring may need to be intensified under such climatic conditions.

While there are still few examples of wetland studies using remote sensing to measure baseline and reference conditions, research conducted in other ecosystems shows interesting approaches that could be applied in wetlands. For example, a study in the Iberian Peninsula used a time series of vegetation indices spanning 20 years to describe the typical range of fluctuations in the spectral signature of different plant functional types in response to climatic conditions (Alcaraz-Segura et al. 2009). This allowed authors to identify a range of acceptable conditions accounting for natural fluctuations and consequently set thresholds under which large abnormal changes would require adaptive management. Adopting a similar method in wetlands could help establish a range of expected conditions while a departure from this expected range of values might indicate an ecosystem stress or a failure in recovery.

4.4 Resilience and detection of ecosystem stress and shifts

The ability to cost-effectively monitor wetland change with geospatial datasets is also crucial for assessing the resilience and adaptive capacity of both restored and reference systems. Some of the conservation frameworks for the region (Table 1) included resilience as a primary objective, although none of the reviewed plans explicitly tracked this or identified its specific indicators. Across our sample, monitoring efforts were limited to an average of one year before and six years after restoration, which may not be sufficient for assessing the effects of region-specific stressors such as droughts and fluctuations in salinity. Repeated efforts to map wetland cover or habitat types enable not only tracking of general dynamics, but also early signals of important shifts. For example, a change analysis conducted on an 85-yr dataset of manually classified aerial images revealed fluctuations in vegetation composition and habitat connectivity and their impact on the local herpetofauna of a Canadian wetland (Markle et al. 2018).

Resilience is notoriously hard to measure and predict, and several publications have called for the development of robust tools for its assessment (Carpenter et al. 2001; Standish et al. 2014). Recent publications leveraging long-term time series of remote sensing data show promising approaches to estimate resilience and detect early signs of ecosystem shifts (e.g., Díaz-Delgado et al. 2002; Sen et al. 2012; Alibakhshi et al. 2017). For example, Alibakhshi et al. (2017) showed that an increased temporal autocorrelation in a composite water-vegetation index could indicate an ecosystem shift triggered by repeated droughts. Similarly, Diaz-Delgado et al. (2002) used Landsat time series to measure the time needed for different forest patches to return to pre-disturbance biomass levels after a series of fires.

Maintaining a multimetric, site-wide monitoring effort to assess the progress made towards multiple objectives can increase the likelihood of detecting unexpected fluctuations, yet the required field effort may incur a high logistical and financial burden (Moreno-Mateos et al. 2015; Brudvig et al. 2017; Taddeo and Dronova 2018). Remote sensing provides a framework to detect ecosystem stressors that may warrant further on-the-ground monitoring and signal a

potential ecosystem shift. Shifts in the spectral properties or phenology of vegetation could expose environmental stress or reveal a decline in the quality of habitat patches (Nagendra et al. 2013). Project managers can detect early signs of ecosystem shifts (Moffett et al. 2015) by tracking spatial variations in vegetation extent and progression (Chapple and Dronova 2017) and habitat complexity (Moffett and Gorelick 2016). Monitoring programs can also focus on vegetation characteristics known to increase site resistance to ecological threats. For example, some monitoring plans are already tracking plant productivity, a key contributor to soil accretion, which increases wetlands' resistance to sea level rise and erosion (Miller et al. 2008; Parker et al. 2011), bird populations' resistance to droughts (Selwood et al. 2017), and could be measured using both large-scale remote sensing data and site-level phenocams (Shuman and Ambrose 2003; Kulawardhana et al. 2015; Knox et al. 2017). Response diversity (i.e., variability of plant responses to fluctuations in environmental conditions) has been shown in field observations and simulations to help ecosystems maintain key processes during and after disturbances. Response diversity can be measured as the range or degree of divergence within a set of traits (i.e., plant characteristics responding to resource availability, hydrology, disturbances) in a community (Mori et al. 2013), some of which can be measured using hyperspectral data (e.g., foliar nitrogen or chlorophyll content, height) or long-term time series of multispectral data (e.g., phenology) (Andrew et al. 2014).

4.5 Limitations and future directions

While different remote sensing datasets and tools are becoming increasingly available, their limitations in addressing the objectives of wetland restoration monitoring should be recognized and considered carefully. Despite an extended spatial and temporal observation scope compared to traditional ground surveys, most spatial instruments are not sufficiently sensitive to some of the critical characteristics of vegetation that can be assessed in the field, particularly indicators of floristic composition and diversity (Shuman and Ambrose 2003). Furthermore, field surveys are very important for the "ground-truthing" of remote sensing analyses to calibrate and validate the patterns observed from image datasets. Thus, future monitoring efforts should seek strategies to combine remote and ground observations in complementary ways. This section discusses some key monitoring needs and opportunities highlighting the importance of such complementary efforts.

4.5.1 Species composition and diversity

Increasing species diversity is a key goal of restoration efforts in the estuary (e.g., BDCP, CALFED I, Delta Conservation Framework; Table 1) due to its potential to promote productivity, resistance to biological invasions, and ecosystem stability (Yachi and Loreau 1999; Caldeira et al. 2005; Cardinale et al. 2012). Furthermore, Boyer and Thornton (2012) observed that restored sites in the estuary maintained fewer species than reference sites on average, further emphasizing the importance of monitoring species richness in the region. Incidentally, 26 of the monitoring plans we reviewed included indicators of species composition (e.g., richness, diversity). Monitoring species composition in the field is challenging because it requires frequent sampling to account for seasonal and annual variability in species composition and a large spatial extent to increase the likelihood of observing rare species (Noss 1990). Yet composition

assessments might be best completed using field observations, considering the limitations of remote sensing datasets. Remote sensing has been leveraged to map dominant species, but many wetland species can have similar spectral signatures at peak biomass (Schmidt and Skidmore 2003). It is much easier to distinguish plant functional types using remote sensing data than a single species unless it presents phenological characteristics or a spectral signature that is clearly distinct from its surroundings (Bradley 2014). Furthermore, to be detectable, this species must cover a significant portion of the pixel (Bradley 2014). LiDAR can help distinguish species by structural differences but has a limited effectiveness in short canopies where species have a similar structure or height (Kulawardhana et al. 2015). Hyperspectral images can help differentiate species by their chemical characteristics (e.g., chlorophyll and water content; Andrew et al. 2014) but remain more effective in ecosystems with a lower overall richness (Andrew and Ustin 2008).

4.5.2 Early stages of recovery

Some restoration plans in our sample included plant survival as a primary component of their monitoring program. It can be difficult to get a reliable signal of plant biomass or survival at the earliest stage of site development, when plant individuals are sparsely distributed, because the spectral signal of bare soil or water might obscure the spectral signature of green vegetation (Bradley 2014). Advances in the use of satellite images to map vegetation growth in arid environments nonetheless suggest potential methodological approaches to facilitate monitoring of sites at an early stage of vegetation development using remote sensing data. For example, Khanna et al. (2007) showed that indices based on the relationship, or angle, between the near and shortwave infrared bands could help distinguish green vegetation from background soil in arid environments. Alternatively, project managers could focus their effort on repeated field assessments in the very early stages of wetland recovery and transition into more remote-sensing based assessments for specific indicators when the vegetation is more established and perceivable using aerial or satellite images.

4.5.3 Tidal effects

In coastal wetlands, periodic tidal flooding attenuates the spectral reflectance of vegetation due to higher water levels and increased soil moisture (Kearney et al. 2009; Adam et al. 2010a). This introduces a lot of noise in data, particularly when studying wetland changes through a time series or trying to model the phenological cycle of tidal wetlands. Correction factors have been used to account for the attenuation of spectral signals by high water levels, but they must be tailored to the structural characteristics of dominant species (Kearney et al. 2009; Byrd et al. 2014) and their phenology (O'Connell et al. 2017) which both impact the proportion of water visible from aircrafts or sensors. Correction factors are typically established using field observations of plant biomass and structure including leaf area index and vegetation fraction (Mishra and Ghosh 2015). For example, O'Connell et al. (2016) developed a correction factor for tidal pixels based on plant phenology and spectral reflectance in the green and shortwave infrared bands. One of the projects we reviewed circumvented this challenge by restricting analyses to images acquired at low tide, which may be a tedious procedure for analysts focusing on large sites or extended time series.

4.5.4 Logistical challenges

As the quality and quantity of satellite data increases, so do data storage needs. The large scale and long-term monitoring of restored sites in the estuary, while critical to advancing our understanding of post-restoration dynamics, will generate heavy datasets that organizations with limited resources might have trouble maintaining. As such, there is a crucial need in the estuary to develop a platform enabling different organizations and managers to store and share their geospatial data. Developing such a repository could reduce redundancy in efforts but also provide large-scale, consistent datasets enabling regional analyses and syntheses.

In the meantime, advances in online application programming interface (API) platforms provide cost-effective opportunities for such analyses by allowing cloud-based access to some large remote sensing data repositories without manual download and pre-processing of the imagery. For instance, a cloud-based Google Earth Engine (GEE; https://earthengine.google.com/) API platform provides access to long-term datasets for several sensors and programs including Landsat, MODIS, and NAIP (Table 4). Users can utilize the GEE platform to perform a set of spatial analyses including change detection, land cover classification, and band arithmetic. A new data API by PlanetLabs (https://www.planet.com/) facilitates the access to and analysis of high-resolution (3-5m) imagery from Planet satellites. Several other remote sensing data repositories allow obtaining the raw satellite and aerial imagery and some of the derived products, for example, U.S. Geological Survey's Earth Explorer (https://earthexplorer.usgs.gov/), NASA's Land Process Distributed Active Archive Center (LPDAAC; https://lpdaac.usgs.gov/), NOAA Data Access Viewer (https://coast.noaa.gov/dataviewer/#/), and NAIP imagery collections at California Department of Fish and Wildlife libraries.

4.5.5 New tools and opportunities to reduce costs for multi-approach strategic monitoring

Several technological advances in remote sensors provide novel opportunities for customized monitoring of vegetation properties and seasonality at individual sites to circumvent the logistical challenges of ground surveys and reduce the risk of site disturbance. Unmanned aerial vehicles (UAVs), for example, allow collecting very high resolution imagery (<10-50cm) at a desired frequency (Anderson and Gaston 2013). The data can be mosaicked across site extent to map wetland surface and vegetation types or measure relevant indicators such as plant coverage (e.g., Zweig et al. 2015). Depending on the specifications of imaging instruments, it might be possible to detect individual species with such data, while greater ease of recognition by the human eye at such a scale may enable collection of reference samples of vegetation types directly from the images, thus reducing the scope of required field work. However, there are challenges with these techniques including the rigorous pre-processing of data to achieve radiometric calibration and the precise co-registration of images to spatially align them in the time series. Furthermore, high-resolution imagery may be sensitive to local noise and color variation, which requires specialized processing and mapping methods such as object-based image analysis (OBIA; Blaschke 2010; Dronova 2015).

Another promising cost-effective monitoring strategy involves using in situ phenocams – small, inexpensive digital cameras that can record fixed-view images of specific locations within sites and monitor changes in vegetation phenology and status at a high temporal frequency. Networks

of such strategically placed small cameras have been widely adopted by wildlife ecologists for detecting occurrences of mobile species (e.g., Steenweg et al. 2017) and by environmental scientists monitoring vegetation greenness as an indicator of productivity and greenhouse gas sequestration (Sonnentag et al. 2012a), including in some local wetland restoration projects (Knox et al. 2017). Phenocams offer an important opportunity to detect the precise timing of plant phenological shifts, including periods falling between cloud-free satellite data acquisitions. Their views can be further equipped with fixed visual scale references to measure changes in plant height or water levels. Furthermore, the data from small cameras can be transmitted wirelessly to a receiving computer server station to automatically extract vegetation parameters such as greenness.

5 Conclusions

This synthesis of monitoring efforts across 42 wetland restoration projects from the San Francisco Bay-Delta estuary reveals a comprehensive effort to track wetland responses to restoration treatments. Current monitoring strategies rely primarily on field surveys to assess key aspects of vegetation recovery, habitat properties, and their change. In contrast, spatially comprehensive geospatial datasets, including remote sensing imagery, are still used sparingly, mainly for tracking plant cover and the extent of identifiable vegetation types. The nature of indicators commonly targeted by monitoring efforts makes it obvious that remote sensing and spatial tools can complement field surveys via instantaneous and repeated coverage of wetland sites but cannot replace the informative value of such ground-level assessments, particularly for parameters that are not easily perceivable by remote sensors. In particular, the increasing availability of remote sensing datasets enables characterizing the spatial extent, phenology, and, in some cases, biomass and vertical structure of dominant vegetation types and detecting signatures of plant invasions at whole-site and regional scales that are unfeasible for comprehensive field surveys, while also reducing site disturbance and trampling. Remote sensing data alone cannot provide a robust understanding of on-the-ground processes underlying the observed ecological dynamics and remains limited in the capacity to accurately map individual species or their diversity. To be robust, geospatial tools and analytical methods require training and validation using on-the-ground data. Making monitoring strategies informative, cost-effective, and reproducible thus calls for a complementary use of spatial/remote and field-based strategies to capitalize on their unique advantages. Increasing the use of geospatial tools and remote sensing data will also require new data exchange venues to allow managers to compare site progress, share relevant data, and measure the combined progress made towards goals.

6 References

Adam, E., O. Mutanga, and D. Rugege. 2010. Multispectral and hyperspectral remote sensing for identification and mapping of wetland vegetation: A review. Wetlands Ecology and Management 18:281–296.

Alcaraz-Segura, D., J. Cabello, and J. Paruelo. 2009. Baseline characterization of major Iberian vegetation types based on the NDVI dynamics. Plant Ecology 202:13–29.

Alibakhshi, S., T. A. Groen, M. Rautiainen, and B. Naimi. 2017. Remotely-sensed early warning signals of a critical transition in a wetland ecosystem. Remote Sensing 9.

Anderson, K., and K. J. Gaston. 2013. Lightweight unmanned aerial vehicles will revolutionize spatial ecology. Frontiers in Ecology and the Environment 11:138–146.

Andrew, M. E., and S. L. Ustin. 2008. The role of environmental context in mapping invasive plants with hyperspectral image data. Remote Sensing of Environment 112:4301–4317.

Andrew, M. E., and S. L. Ustin. 2009. Habitat suitability modelling of an invasive plant with advanced remote sensing data. Diversity and Distributions 15:627–640.

Andrew, M. E., M. a. Wulder, and T. a. Nelson. 2014. Potential contributions of remote sensing to ecosystem service assessments. Progress in Physical Geography 38:328–353.

Baker, C., R. L. Lawrence, C. Montagne, and D. Patten. 2007. Change detection of wetland ecosystems using landsat imagery and change vector analysis imagery and change vector analysis. Wetlands 27:610–619.

Barbier, E. B., I. Y. Georgiou, B. Enchelmeyer, and D. J. Reed. 2013. The Value of Wetlands in Protecting Southeast Louisiana from Hurricane Storm Surges. PLoS ONE 8:1–6.

Belluco, E., M. Camuffo, S. Ferrari, L. Modenese, S. Silvestri, A. Marani, and M. Marani. 2006. Mapping salt-marsh vegetation by multispectral and hyperspectral remote sensing. Remote Sensing of Environment 105:54–67.

Blaschke, T. 2010. Object based image analysis for remote sensing. ISPRS Journal of Photogrammetry and Remote Sensing 65:2–16.

Boers, A. M., and J. B. Zedler. 2008. Stabilized water levels and Typha invasiveness. Wetlands 28:676–685.

Botequilha Leitao, A., and J. Ahern. 2002. Applying landscape ecological concepts and metrics in sustainable landscape planning. Landscape and Urban Planning 59:65–93.

Boyer, K. E., and W. J. Thornton. 2012. Natural and Restored Tidal Marsh Communities. Pages 207–214 *in* A. Palaima, editor. Ecology, Conservation, and Restoration of Tidal Marshes: The San Francisco Estuary. University. Berkeley, CA.

Bradbury, R. B., R. a Hill, D. C. Aason, S. a Hinsley, J. D. Wilson, H. Balzter, G. Q. a Anderson, M. J. Whittingham, I. J. Davenport, and P. E. Bellamy. 2005. Modelling relationships between birds and vegetation structure using airborne LiDAR data: a review with case studies from agricultural and woodland environments. International Journal of Avian Science 147:443–452.

Bradley, B. A. 2014. Remote detection of invasive plants: A review of spectral, textural and phenological approaches. Biological Invasions 16:1411–1425.

Breaux, A., S. Cochrane, J. Evens, M. Martindale, B. Pavlik, L. Suer, and D. Benner. 2005. Wetland ecological and compliance assessments in the San Francisco Bay Region,

California, USA. Journal of Environmental Management 74:217–237.

Brudvig, L. A., R. S. Barak, J. T. Bauer, T. T. Caughlin, D. C. Laughlin, L. Larios, J. W. Matthews, K. L. Stuble, N. E. Turley, and C. R. Zirbel. 2017. Interpreting variation to advance predictive restoration science. Journal of Applied Ecology:1018–1027.

Byrd, K. B., L. Ballanti, N. Thomas, D. Nguyen, J. R. Holmquist, M. Simard, and L. Windham-Myers. 2018. A remote sensing-based model of tidal marsh aboveground carbon stocks for the conterminous United States. ISPRS Journal of Photogrammetry and Remote Sensing 139:255–271.

Byrd, K. B., J. L. O'Connell, S. Di Tommaso, and M. Kelly. 2014. Evaluation of sensor types and environmental controls on mapping biomass of coastal marsh emergent vegetation. Remote Sensing of Environment 149:166–180.

Byrd, K. B., L. Windham-Myers, T. Leeuw, B. Downing, J. T. Morris, and M. C. Ferner. 2016. Forecasting tidal marsh elevation and habitat change through fusion of Earth observations and a process model. Ecosphere 7:1–27.

Caldeira, M. C., A. Hector, M. Loreau, and J. S. Pereira. 2005. Species richness , temporal variability and resistance of biomass production in a Mediterranean grassland OIKOS 1:115–123.

California Department of Fish and Games. 2012. 2009 Vegetation Map Update for Suisun Marsh, Solano County, California.

Callaway, J. C., E. L. Borgnis, R. E. Turner, and C. S. Milan. 2012. Carbon Sequestration and Sediment Accretion in San Francisco Bay Tidal Wetlands. Estuaries and Coasts 35:1163–1181.

Callaway, J. C., and V. T. Parker. 2012. Current Issues in Tidal Marsh Restoration. Pages 253–262 *in* A. Palaima, editor. Ecology, Conservation, and Restoration of Tidal Marshes. University of California Press, Berkeley, CA.

Callaway, J. C., V. T. Parker, M. C. Vasey, L. M. Schile, and E. R. Herbert. 2011. Tidal Weltand Restoration in San Francisco Bay: History and Current Issues. San Francisco Estuary and Watershed Science 9.

Cardinale, B. J., J. E. Duffy, A. Gonzalez, D. U. Hooper, C. Perrings, P. Venail, A. Narwani, G. M. Mace, D. Tilman, D. a Wardle, A. P. Kinzig, G. C. Daily, M. Loreau, J. B. Grace, A. Larigauderie, D. S. Srivastava, and S. Naeem. 2012. Biodiversity loss and its impact on humanity. Nature 486:59–67.

Carpenter, S., B. Walker, J. M. Anderies, and N. Abel. 2001. From Metaphor to Measurement: Resilience of What to What? Ecosystems 4:765–781.

Chapple, D., and I. Dronova. 2017. Vegetation Development in a Tidal Marsh Restoration Project during a Historic Drought: A Remote Sensing Approach. Frontiers in Marine Science 4.

Chapple, D. E., P. Faber, K. N. Suding, and A. M. Merenlender. 2017. Climate Variability Structures Plant Community Dynamics in Mediterranean Restored and Reference Tidal Wetlands. Water 9:209–226.

Chust, G., I. Galparsoro, A. Borja, J. Franco, and A. Uriarte. 2008. Coastal and estuarine habitat mapping, using LIDAR height and intensity and multi-spectral imagery. Estuarine, Coastal and Shelf Science 78:633–643.

Costanza, J. K., A. Moody, and R. K. Peet. 2011. Multi-scale environmental heterogeneity as a predictor of plant species richness. Landscape Ecology 26:851–864.

Craft, C., P. Megonigal, S. Broome, J. Stevenson, R. Freese, J. Cornell, L. Zheng, and J. Sacco. 2003. The pace of ecosystem development of constructed Spartina alterniflora marshes. Ecological Applications 13:1417–1432.

Dahl, T. E. 2011. Status and Trends of Wetlands in the Contermious United States 2004 to 2009. Washington, DC.

Davidson, N. C. 2014. How much wetland has the world lost? Long-term and recent trends in global wetland area. Marine and Freshwater Research 65:934–941.

Davranche, A., G. Lefebvre, and B. Poulin. 2010. Wetland monitoring using classification trees and SPOT-5 seasonal time series. Remote Sensing of Environment 114:552–562.

Deland, M. R. 1992. No Net Loss of Wetlands: A Comprehensive Approach. Natural Resources & Environment 7:3–5.

Deverel, S. J., T. Ingrum, C. E. Lucero, and J. Z. Drexler. 2014. Impounded Marshes on Subsided Islands: Simulated Vertical Accretion, Processes, and Effects, Sacramento-San Joquin Delta, CA, USA. San Francisco Estuary & Watershed Science 12.

Díaz-Delgado, R., F. Lloret, X. Pons, and J. Terradas. 2002. Satellite Evidence of Decreasing Resilience in Mediterranean Plant Communities After Recurrent Wildfires. Ecology 83:2293–2303.

Diffenbaugh, N. S., D. L. Swain, and D. Touma. 2015. Anthropogenic warming has increased drought risk in California. Proceedings of the National Academy of Sciences 112:201422385.

Dronova, I. 2015. Object-Based Image Analysis in Wetland Research: A Review. Remote Sensing 7:6380–6413.

Dronova, I., and S. Taddeo. 2016. Canopy Leaf Area Index in Non-Forested Marshes of the California Delta. Wetlands 36:705–716.

Fortin, M. J., P. M. A. James, A. MacKenzie, S. J. Melles, and B. Rayfield. 2012. Spatial statistics, spatial regression, and graph theory in ecology. Spatial Statistics 1:100–109.

Gilmore, M. S., E. H. Wilson, N. Barrett, D. L. Civco, S. Prisloe, J. D. Hurd, and C. Chadwick. 2008. Integrating multi-temporal spectral and structural information to map wetland

vegetation in a lower Connecticut River tidal marsh. Remote Sensing of Environment 112:4048–4060.

Goals Project. 1999. Baylands ecosystem habitat goals. A report of habitat recommendations prepared by the San Francisco Bay Area Wetlands Ecosystem Goals Project. Oakland.

Grewell, B. J., E. K. Espeland, and P. L. Fiedler. 2013. Sea change under climate change : case studies in rare plant conservation from the dynamic San Francisco Estuary. Botany 91:309–318.

Guisan, A., and W. Thuiller. 2005. Predicting species distribution: Offering more than simple habitat models. Ecology Letters 8:993–1009.

Hestir, E. L., S. Khanna, M. E. Andrew, M. J. Santos, J. H. Viers, J. A. Greenberg, S. S. Rajapakse, and S. L. Ustin. 2008. Identification of invasive vegetation using hyperspectral remote sensing in the California Delta ecosystem. Remote Sensing of Environment 112:4034–4047.

Hiers, J. K., R. J. Mitchell, A. Barnett, J. R. Walters, M. MacK, B. Williams, and R. Sutter. 2012. The dynamic reference concept: Measuring restoration success in a rapidly changing no-analogue future. Ecological Restoration 30:27–36.

Hladik, C., J. Schalles, and M. Alber. 2013. Salt marsh elevation and habitat mapping using hyperspectral and LIDAR data. Remote Sensing of Environment 139:318–330.

Holmes, M. 2012. Policy: Achievements and Challenges. Pages 207–214 *in* A. Palaima, editor. Ecology, Conservation, and Restoration of Tidal Marshes: The San Francisco Estuary. University. Berkeley.

Hudak, A. T., J. S. Evans, and A. M. S. Smith. 2009. LiDAR utility for natural resource managers. Remote Sensing 1:934–951.

Jankowski, K. L., T. E. Törnqvist, and A. M. Fernandes. 2017. Vulnerability of Louisiana's coastal wetlands to present-day rates of relative sea-level rise. Nature Communications 8:1–7.

Jensen, J. R. 2007. Remote Sensing of the Environment: An Earth Resource Perspective. Second Edi. Prentice Hall, Upper Sadle River, NJ.

Johnson, C. R., R. H. Chabot, M. P. Marzloff, and S. Wotherspoon. 2017. Knowing when (not) to attempt ecological restoration. Restoration Ecology 25:140–147.

Jung, R., W. Adolph, M. Ehlers, and H. Farke. 2015. A multi-sensor approach for detecting the different land covers of tidal flats in the German Wadden Sea - A case study at Norderney. Remote Sensing of Environment 170:188–202.

Kearney, M. S., D. Stutzer, K. Turpie, and J. C. Stevenson. 2009. The effect of Tidal Inundation on the Reflectance Characteristics of Coastal Marsh Vegetation. Journal of Coastal Research 25:1177–1186.

Kentula, M. E. 2000. Perspectives on setting success criteria for wetland restoration. Ecological Engineering 15:199–209.

Kettenring, K. M., and C. R. Adams. 2011. Lessons learned from invasive plant control experiments: A systematic review and meta-analysis. Journal of Applied Ecology 48:970–979.

Khanna, S., A. Palacios-Orueta, M. L. Whiting, S. L. Ustin, D. Riaño, and J. Litago. 2007. Development of angle indexes for soil moisture estimation, dry matter detection and land-cover discrimination. Remote Sensing of Environment 109:154–165.

Khanna, S., M. J. Santos, J. D. Boyer, K. D. Shapiro, J. Bellvert, and S. L. Ustin. 2018. Water primrose invasion changes successional pathways in an estuarine ecosystem. Ecosphere 9:e02418.

Kimmerer, W. J., D. D. Murphy, and P. J. Angermeier. 2005. A Landscape-level Model for Ecosystem Restoration in the San Francisco Estuary and its Watershed. San Francisco Estuary & Watershed 3.

Knox, S. H., I. Dronova, C. Sturtevant, P. Y. Oikawa, J. H. Matthes, J. Verfaillie, and D. Baldocchi. 2017. Using digital camera and Landsat imagery with eddy covariance data to model gross primary production in restored wetlands. Agricultural and Forest Meteorology 237–238:233–245.

Kulawardhana, R. W., R. A. Feagin, S. C. Popescu, T. W. Boutton, K. M. Yeager, and T. S. Bianchi. 2015. The role of elevation, relative sea-level history and vegetation transition in determining carbon distribution in Spartina alterniflora dominated salt marshes. Estuarine, Coastal and Shelf Science 154:48–57.

Kulawardhana, R. W., S. C. Popescu, and R. A. Feagin. 2014. Fusion of lidar and multispectral data to quantify salt marsh carbon stocks. Remote Sensing of Environment 154:345–357.

Laba, M., R. Downs, S. Smith, S. Welsh, C. Neider, S. White, M. Richmond, W. Philpot, and P. Baveye. 2008. Mapping invasive wetland plants in the Hudson River National Estuarine Research Reserve using quickbird satellite imagery. Remote Sensing of Environment 112:286–300.

Lackey, L. G., and E. D. Stein. 2014. Selecting the optimum plot size for a California design-based stream and wetland mapping program. Environmental Monitoring and Assessment 186:2599–2608.

Lindborg, R., and O. Eriksson. 2004. Historical landscape connectivity affects present plant species diversity. Ecology 85:1840–1845.

Lund, J., E. Hanak, W. Fleenor, W. Bennett, and R. Howitt. 2010. Comparing Futures for the Sacramento-San Joaquin Delta. University of California Press, Berkeley.

Luoma, S. N., C. N. Dahm, M. Healey, and M. J. N. 2015. Challenges Facing the Sacramento-San Joaquin Delta: Complex, Chaotic, or Simply Cantankerous? San Francisco Estuary &

Watershed 13:1–25.

Markle, C. E., G. Chow-Fraser, and P. Chow-Fraser. 2018. Long-Term habitat changes in a protected area: Implications for herpetofauna habitat management and restoration. PLoS ONE 13:1–16.

Matthews, J. W. 2015. Group-based modeling of ecological trajectories in restored wetlands. Ecological Applications 25:481–491.

Matthews, J. W., and A. G. Endress. 2008. Performance criteria, compliance success, and vegetation development in compensatory mitigation wetlands. Environmental Management 41:130–141.

Matthews, J. W., and G. Spyreas. 2010. Convergence and divergence in plant community trajectories as a framework for monitoring wetland restoration progress. Journal of Applied Ecology 47:1128–1136.

McGarigal, K., S. Tagil, and S. a. Cushman. 2009. Surface metrics: An alternative to patch metrics for the quantification of landscape structure. Landscape Ecology 24:433–450.

McNicol, G., C. S. Sturtevant, S. H. Knox, I. Dronova, D. D. Baldocchi, and W. L. Silver. 2017. Effects of seasonality, transport pathway, and spatial structure on greenhouse gas fluxes in a restored wetland. Global Change Biology 23:2768–2782.

Miller, R. L., M. Fram, R. Fujii, and G. Wheeler. 2008. Subsidence Reversal in a Re-established Wetland in the Sacramento-San Joaquin Delta, California, USA. San Francisco Estuary & Watershed October.

Minor, E. S., and D. L. Urban. 2008. A graph-theory framework for evaluating landscape connectivity and conservation planning. Conservation biology : the journal of the Society for Conservation Biology 22:297–307.

Mishra, D. R., and S. Ghosh. 2015. Using Moderate-Resolution Satellite Sensors for Monitoring the Biophysical Parameters and Phenology of Tidal Marshes. Pages 283–314 *in* R. W. Tiner, M. W. Lang, and V. V Klemas, editors. Remote Sensing of Wetlands. Applications and Advances. CRC Press, Taylor & Francis Group, Boca Raton.

Mo, Y., M. S. Kearney, J. C. A. Riter, F. Zhao, and D. R. Tilley. 2018. Assessing biomass of diverse coastal marsh ecosystems using statistical and machine learning models. International Journal of Applied Earth Observation and Geoinformation 68:189–201.

Moffett, K. B., and S. M. Gorelick. 2016. Alternative stable states of tidal marsh vegetation patterns and channel complexity. Ecohydrology 1662:1639–1662.

Moffett, K. B., J. Law, S. M. Gorelick, N. Nur, and J. K. Wood. 2014. Alameda Song Sparrow Abundance Related to Salt Marsh Metrics Quantified from Remote Sensing Imagery. San Francisco Estuary & Watershed 12:1–19.

Moffett, K. B., W. Nardin, S. Silvestri, C. Wang, and S. Temmerman. 2015. Multiple stable

states and catastrophic shifts in coastal wetlands: Progress, challenges, and opportunities in validating theory using remote sensing and other methods. Remote Sensing 7:10184–10226.

Moorhead, K. K. 2013. A Realistic Role for Reference in Wetland Restoration. Ecological Restoration 31:347–352.

Moreno-Mateos, D., Ü. Mander, F. A. Comín, C. Pedrocchi, and E. Uuemaa. 2008. Relationships between Landscape Pattern, Wetland Characteristics, and Water Quality in Agricultural Catchments. Journal of Environment Quality 37:2170.

Moreno-Mateos, D., P. Meli, M. I. Vara-Rodríguez, and J. Aronson. 2015. Ecosystem response to interventions: Lessons from restored and created wetland ecosystems. Journal of Applied Ecology 52:1528–1537.

Moreno-Mateos, D., M. E. Power, F. A. Comín, and R. Yockteng. 2012. Structural and functional loss in restored wetland ecosystems. PLoS Biology 10:e1001247.

Mori, A. S., T. Furukawa, and T. Sasaki. 2013. Response diversity determines the resilience of ecosystems to environmental change. Biological Reviews 88:349–364.

Moyle, P. B., A. D. Manfree, and P. L. Fiedler. 2013. The Future of Suisun Marsh : Balancing Policy with Change. San Francisco Estuary & Watershed Science 11.

Muller-Karger, F. E., E. Hestir, C. Ade, K. Turpie, D. A. Roberts, D. Siegel, R. J. Miller, D. Humm, N. Izenberg, M. Keller, F. Morgan, R. Frouin, A. G. Dekker, R. Gardner, J. Goodman, B. Schaeffer, B. A. Franz, N. Pahlevan, A. G. Mannino, J. A. Concha, S. G. Ackleson, K. C. Cavanaugh, A. Romanou, M. Tzortziou, E. S. Boss, R. Pavlick, A. Freeman, C. S. Rousseaux, J. Dunne, M. C. Long, E. Klein, G. A. McKinley, J. Goes, R. Letelier, M. Kavanaugh, M. Roffer, A. Bracher, K. R. Arrigo, H. Dierssen, X. Zhang, F. W. Davis, B. Best, R. Guralnick, J. Moisan, H. M. Sosik, R. Kudela, C. B. Mouw, A. H. Barnard, S. Palacios, C. Roesler, E. G. Drakou, W. Appeltans, and W. Jetz. 2018. Satellite sensor requirements for monitoring essential biodiversity variables of coastal ecosystems. Ecological Applications 28:749–760.

Nagendra, H., R. Lucas, J. P. Honrado, R. H. G. Jongman, C. Tarantino, M. Adamo, and P. Mairota. 2013. Remote sensing for conservation monitoring: Assessing protected areas, habitat extent, habitat condition, species diversity, and threats. Ecological Indicators 33:45–59.

National Research Council. 2001. Compensating for Wetland Losses Under the Clean Water Act. National A. Washington, DC.

Noss, R. F. 1990. Indicators for Monitoring Biodiversity: A Hierarchical Approach. Conservation Biology 4:355–364.

O'Connell, J. L., D. R. Mishra, D. L. Cotten, L. Wang, and M. Alber. 2017. The Tidal Marsh Inundation Index (TMII): An inundation filter to flag flooded pixels and improve MODIS tidal marsh vegetation time-series analysis. Remote Sensing of Environment 201:34–46.

Parker, V. T., J. C. Callaway, L. M. Schile, M. C. Vasey, and E. R. Herbert. 2011. Climate Change and San Francisco Bay – Delta Tidal Wetlands. San Francisco Estuary and Watershed Science 9:1–15.

Perring, M. P., R. J. Standish, J. N. Price, M. D. Craig, T. E. Erickson, K. X. Ruthrof, A. S. Whiteley, L. E. Valentine, and R. J. Hobbs. 2015. Advances in restoration ecology : rising to the challenges of the coming decades. Ecosphere 6:1–25.

Pettorelli, N., J. O. Vik, A. Mysterud, J. M. Gaillard, C. J. Tucker, and N. C. Stenseth. 2005. Using the satellite-derived NDVI to assess ecological responses to environmental change. Trends in Ecology and Evolution 20:503–510.

St. Pierre, J. I., and K. E. Kovalenko. 2014. Effect of habitat complexity attributes on species richness. Ecosphere 5:art22.

Reaser, J. K., L. A. Meyerson, and B. von Holle. 2008. Saving camels from straws: How propagule pressure-based prevention policies can reduce the risk of biological invasion. Biological Invasions 10:1085–1098.

Rocchini, D., G. Bacaro, G. Chirici, D. Da Re, H. Feilhauer, G. M. Foody, M. Galluzzi, C. X. Garzon-Lopez, T. W. Gillespie, K. S. He, J. Lenoir, M. Marcantonio, H. Nagendra, C. Ricotta, E. Rommel, S. Schmidtlein, A. K. Skidmore, R. Van De Kerchove, M. Wegmann, and B. Rugani. 2018. Remotely sensed spatial heterogeneity as an exploratory tool for taxonomic and functional diversity study. Ecological Indicators 85:983–990.

Rocha, a. V., D. L. Potts, and M. L. Goulden. 2008. Standing litter as a driver of interannual CO2 exchange variability in a freshwater marsh. Journal of Geophysical Research: Biogeosciences 113:1–10.

Rosso, P. H., S. L. Ustin, and a. Hastings. 2006. Use of lidar to study changes associated with Spartina invasion in San Francisco Bay marshes. Remote Sensing of Environment 100:295–306.

Rudnick, D. A., S. J. Ryan, P. Beier, S. A. Cushman, F. Dieffenbach, C. W. Epps, L. R. Gerber, J. Harrter, J. S. Jenness, J. Kintsch, A. M. Merenlender, R. M. Perkl, D. V. Preziosi, and S. C. Trombulak. 2012. The Role of Landscape Connectivity in Panning and Implementing Conservation and Restoration Priorities. Page Issue in Ecology.

San Francisco Estuary Partnership. 2015. The State of the Estuary 2015.

Schaffer-Smith, D., J. J. Swenson, M. E. Reiter, and J. E. Isola. 2018. Quantifying shorebird habitat in managed wetlands by modeling shallow water depth dynamics. Ecological Applications 28:1534–1545.

Schile, L. M., K. B. Byrd, L. Windham-Myers, and M. Kelly. 2013. Accounting for non-photosynthetic vegetation in remote-sensing-based estimates of carbon flux in wetlands. Remote Sensing Letters 4:542–551.

Schmidt, K. S., and A. K. Skidmore. 2003. Spectral discrimination of vegetation types in a

coastal wetland. Remote Sensing of Environment 85:92–108.

Selwood, K. E., M. A. McGeoch, R. H. Clarke, and R. Mac Nally. 2017. High-productivity vegetation is important for lessening bird declines during prolonged drought. Journal of Applied Ecology:641–650.

Sen, S., C. E. Zipper, R. H. Wynne, and P. F. Donovan. 2012. Identifying Revegetated Mines as Disturbance/Recovery Trajectories Using an Interannual Landsat Chronosequence. Photogrammetric Engineering and Remote Sensing 78:223–235.

Shuman, C. S., and R. F. Ambrose. 2003. A Comparison of Remote Sensing and Ground-Based Methods for Monitoring Wetland Restoration Success. Restoration Ecology 11:325–333.

Simenstad, C., D. Reed, and M. Ford. 2006. When is restoration not? Incorporating landscape-scape processes to restore self-sustaining ecosystems in coastal wetland restoration. Ecological Engineering 26:27–39.

Sloey, T. M., J. M. Willis, and M. W. Hester. 2015. Hydrologic and edaphic constraints on Schoenoplectus acutus , Schoenoplectus californicus , and Typha latifolia in tidal marsh restoration. Restoration Ecology 23:n/a-n/a.

Sonnentag, O., K. Hufkens, C. Teshera-Sterne, A. M. Young, M. Friedl, B. H. Braswell, T. Milliman, J. O'Keefe, and A. D. Richardson. 2012. Digital repeat photography for phenological research in forest ecosystems. Agricultural and Forest Meteorology 152:159–177.

Sousa-Silva, R., P. Alves, J. Honrado, and A. Lomba. 2014. Improving the assessment and reporting on rare and endangered species through species distribution models. Global Ecology and Conservation 2:226–237.

Standish, R. J., R. J. Hobbs, M. M. Mayfield, B. T. Bestelmeyer, K. N. Suding, L. L. Battaglia, V. Eviner, C. V. Hawkes, V. M. Temperton, V. a. Cramer, J. a. Harris, J. L. Funk, and P. a. Thomas. 2014. Resilience in ecology: Abstraction, distraction, or where the action is? Biological Conservation 177:43–51.

Steenweg, R., M. Hebblewhite, R. Kays, J. Ahumada, J. T. Fisher, C. Burton, S. E. Townsend, C. Carbone, J. M. Rowcliffe, J. Whittington, J. Brodie, J. A. Royle, A. Switalski, A. P. Clevenger, N. Heim, and L. N. Rich. 2017. Scaling-up camera traps: monitoring the planet's biodiversity with networks of remote sensors. Frontiers in Ecology and the Environment 15:26–34.

Stralberg, D., M. P. Herzog, N. Nur, K. A. Tuxen, and M. Kelly. 2010. Predicting avian abundance within and across tidal marshes using fine-scale vegetation and geomorphic metrics. Wetlands 30:475–487.

Suding, K. N. 2011. Toward an Era of Restoration in Ecology: Successes, Failures, and Opportunities Ahead. Annual Review of Ecology, Evolution, and Systematics 42:465–487.

Ta, J., L. W. J. Anderson, M. A. Christman, S. Khanna, D. Kratville, J. D. Madsen, P. J. Moran,

and J. H. Viers. 2017. Invasive aquatic vegetation management in the Sacramento-San Joaquin River Delta: Status and recommendations. San Francisco Estuary and Watershed Science 15.

Taddeo, S., and I. Dronova. 2018. Indicators of vegetation development in restored wetlands. Ecological Indicators 94:454–467.

Turner, M. G., W. L. Baker, C. J. Peterson, and R. K. Peet. 1998. Factors Influencing Succession: Lessons from Large, Infrequent, Natural Disturbances. Ecosystems 1:511–523.

Tuxen, K. A., L. M. Schile, M. Kelly, and S. W. Siegel. 2008. Vegetation colonization in a restoring tidal marsh: A remote sensing approach. Restoration Ecology 16:313–323.

Tuxen, K., and M. Kelly. 2008. Multi-scale functional mapping of tidal wetlands: an object-based approach. Pages 415–442 *in* T. Blaschke, S. Lang, and G. J. Hay, editors. Object-Based Image Analysis. Springer.

Tuxen, K., L. Schile, D. Stralberg, S. Siegel, T. Parker, M. Vasey, J. Callaway, and M. Kelly. 2011. Mapping changes in tidal wetland vegetation composition and pattern across a salinity gradient using high spatial resolution imagery. Wetlands Ecology and Management 19:141–157.

Vasey, M. C., V. T. Parker, J. C. Callaway, E. R. Herbert, and L. M. Schile. 2012. Tidal Wetland Vegetation in the San Francisco Bay-Delta Estuary. San Francisco Estuary and Watershed Science 10.

Wang, A., J. Chen, C. Jing, G. Ye, J. Wu, Z. Huang, and C. Zhou. 2015. Monitoring the Invasion of Spartina alterniflora from 1993 to 2014 with Landsat TM and SPOT 6 Satellite Data in Yueqing Bay, China. Plos One 10:e0135538.

Wang, L., I. Dronova, P. Gong, W. Yang, Y. Li, and Q. Liu. 2012. A new time series vegetation-water index of phenological-hydrological trait across species and functional types for Poyang Lake wetland ecosystem. Remote Sensing of Environment 125:49–63.

Whipple, A., A. Grossinger, D. Rankin, B. Stanford, and R. Askevold. 2012. Sacramento-San Joaquin Delta Historical Ecology Investigation : Exploring Pattern and Process.

White, P. S., and J. L. Walker. 1997. Approximating Nature's Variation: Selecting and Using Reference Information in Restoration Ecology. Restoration Ecology 5:338–349.

Wilcox, D. a., J. E. Meeker, P. L. Hudson, B. J. Armitage, M. G. Black, and D. G. Uzarski. 2002. Hydrologic variability and the application of Index of Biotic Integrity metrics to wetlands: A great lakes evaluation. Wetlands 22:588–615.

Xie, Y., A. Zhang, and W. Welsh. 2015. Mapping Wetlands and Phragmites Using Publically Available Remotely Sensed Images. Photogrammetric Engineering & Remote Sensing 81:69–78.

Yachi, S., and M. Loreau. 1999. Biodiversity and ecosystem productivity in a fluctuating

environment: The insurance hypothesis. Proceedings of the National Academy of Sciences 96:1463–1468.

Zedler, J. B., J. C. Callaway, S. Diego, and S. M. Na-. 1999. Tracking Wetland Restoration : Do Mitigation Sites Follow Desired Trajectories ? Restoration Ecology 7:69–73.

Zhong, L., P. Gong, and G. S. Biging. 2012. Phenology-based Crop Classification Algorithm and its implications on Agricultural Water Use Assessments in California's Central Valley. Photogrammetric Engineering & Remote Sensing 78:799–813.

Zweig, C. L., M. A. Burgess, H. F. Percival, and W. M. Kitchens. 2015. Use of Unmanned Aircraft Systems to Delineate Fine-Scale Wetland Vegetation Communities. Wetlands 35:303–309.

7 Tables and figures

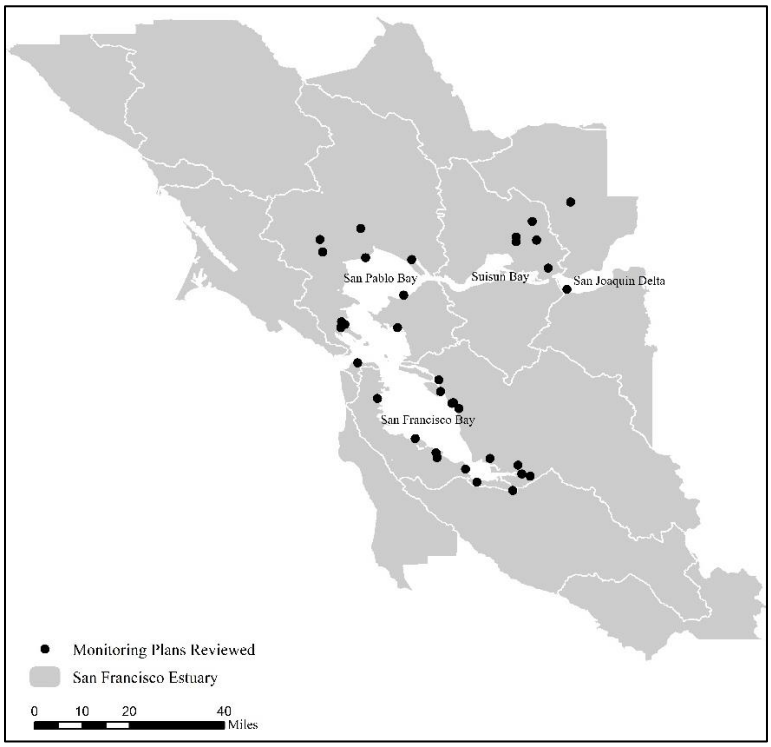

Figure 1. Study area and study sites

Table 1. Conservation documents for the estuary and their main habitat goals

Conservation Document	Restoration related-goals										
	Recover Endangered Species	Enhance species diversity	Control non-native species	Enhance ecosystem resilience	Enhance commercial and recreational harvest	Rehabilitate Ecological Processes	Enhance adaptability to climate change	Enhance habitat connectivity	Promote adaptive management	Erosion control and flood control	Improve water quality
CALFED I	X	X	X		X	X					
Bay-Delta Conservation Plan (2007)	X	X	X			X	X	X		X	X
Suisun Marsh Habitat Management, Preservation, and Restoration Plan (2011)					X						
California Water Fix (2016)	X			X		X	X		X		X
Delta Plan (2013)	X		X	X	X	X		X	X		X
California Water Action Plan (2014)	X	X				X	X	X		X	
Delta Conservation Framework (2017)	X	X	X	X	X	X	X	X	X		
San Francisco Bay Plan (2015)	X	X	X	X	X	X	X	X	X	X	X
Baylands Ecosystem Habitat Goals (1999)											
San Francisco Bay Joint Venture (2001)		X									X
Conservation Strategy for Restoration of the Sacramento-San Joaquin Delta, Sacramento Valley, and San Joaquin Valley Regions (CDFW et al. 2014).	X	X	X		X	X	X	X			X

Table 2. Summary of monitoring plans analyzed for this review

Restoration type	Wetland type	Restoration year	Number of projects	Mean project size (acres)	Restoration indicators	Mean monitoring length (yrs)
Compensatory mitigation	Brackish	1995	1	4	Vegetation cover, species composition, plant survival	5
	Diked	1993	1	94	Vegetation cover, vegetation composition	5
	Freshwater	1976-2009	9	39	Vegetation cover, species composition, plant height and height heterogeneity, stem density	6
	Salt marsh	1993-2007	2	6	Vegetation cover	5

	Tidal	1995-2004	13	83	Vegetation coverage, species composition, plant height, biomass, habitats mapping, community similarity	8
	Vernal pools	2005	2	534	Vegetation cover, species composition, habitat mapping	10
Non-mitigation	Brackish	1996-2003	2	1,077	Vegetation cover, plant height, species composition	10
	Diked	1998	1	72	Vegetation cover	10
	Tidal	1998-2015	10	205	Vegetation cover, species composition, habitat mapping, plant survival, plant height, rate of lateral expansion	10
	Wet Meadow	2002	1	492	Vegetation cover, rare species	10

Table 3. Examples of geospatial applications for measuring the progress made towards restoration goals in the San Francisco Bay-Delta estuary.

Restoration Goals	**Geospatial Applications**	**Local Examples**
Recover endangered species	Quantify suitable habitats using aerial and satellite images or 3D lidar products.	Stralberg et al. 2010 Tuxen and Kelly 2008 Schaffer-Smith et al. 2018
	Use ecological niche models to identify potential suitable habitats and target field monitoring.	Zhang & Gorelick 2014
	Use landscape metrics of habitat size, diversity, density, and connectivity.	Moffett et al. 2014 Tuxen and Kelly 2008
Control non-native species	Monitoring using repeated satellite images.	Hestir et al. 2008 Ta et al. 2017 Khanna et al. 2018 Andrew and Ustin 2008
	Use hyperspectral data to detect changes in extent and coverage of target plant species.	
Rehabilitate ecological processes	Upscale field measurements into site or regional estimates of ecosystem functions.	Byrd et al. 2014 Byrd et al. 2016 Byrd et al. 2018 Knox et al. 2017 McNicol et al. 2017
Enhance adaptability to climate change	Measure the impacts of climatic fluctuations on vegetation extent and productivity.	Chapple and Dronova 2017
Enhance habitat connectivity	Use landscape metrics to measure connectivity.	Zhang & Gorelick 2014
	Conduct connectivity analyses using network analysis or resistance kernel approach.	
Promote adaptive management	Use time series of satellite images to identify thresholds of ecosystem change for intervention.	Moffett and Gorelick 2016
	Use repeated aerial survey to detect early signs of ecosystem shifts.	

Erosion and flood control	Upscaling of field measurements into site or regional estimates of ecosystem functions.	Schaffer-Smith et al. 2018
	Identifying changes in terrain and hydrological properties using 3D lidar products.	Buffington et al. 2016

Table 4. Examples of common high-to-moderate resolution remote sensing data sources and their potential for the post-restoration assessments of wetlands.

	Sensor/Database	Agency	Temporal Scope	Spatial Resolution	Bands	Examples of Applications
Commercial	RapidEye	PlanetLabs	Every 1-6 days; 2008-Present	5m	5	Habitat mapping (Jung et al. 2015).
	World-View	DigitalGlobe	Every 1-2 day; 2009-Present	0.31 – 1.24m	8	Land cover mapping, quantify vegetation expansion (Chapple and Dronova 2017).
	IKONOS	DigitalGlobe	Every ~3 days; 1999-2015	0.82-4m	4	Mapping vegetation, detecting invasive species (Belluco et al. 2006).
	Quickbird	DigitalGlobe	1-3.5 days; 2001-2015	0.65-2.9m	4	Mapping vegetation (Gilmore et al. 2008; Laba et al. 2008), detecting invasive species.
Public	National Agriculture Inventory Framework	USDA	Every 2-3 years from 2003-Present	0.6 – 1 m	3-4	Inform sampling design (Lackey and Stein 2014), monitoring invasive species (Xie et al. 2015).
	Landsat	NASA	Every 16 days from 1972-Present	30 - 120 m	4-11	Base data for wetland elevation (Byrd et al. 2016) and carbon flux models (Knox et al. 2017; McNicol et al. 2017), phenological analyses (Knox et al. 2017).
	Sentinel-2	ESA	Every 5-10 days	10-60m	13	Estimate plant biomass and coverage (Mo et al. 2018).
	SPOT	ESA	Every 26 days since 1986	1.5-20m	4-5	Monitoring wetland vegetation (Davranche et al. 2010).

LiDAR	Variable	Variable	Variable	Base data for soil accretion model or carbon budget (Hladik et al. 2013; Kulawardhana et al. 2014), map certain non-native species (Rosso et al. 2006) and habitats (Bradbury et al. 2005).

8 Supplemental Information

Monitoring Plans and Reports Consulted for this Review

Anonymous. 1995. Fifth Monitoring Report. Central Avenue Wetland Mitigation Marsh. 6 p. [cited 2016 November 2]. Available from: https://www.ecoatlas.org/upfiles/1032/170190%20fifth%20year%20monitoring%20report.pdf

Anonymous. 1999. Charleston Slough Restoration Project. First Year Monitoring Results. ACOE Permit #195010. 4 p. [cited 2016 November 2]. Available from: https://www.ecoatlas.org/upfiles/1057/195010%20first%20year%20monitoring%20results.pdf

Anonymous. 1999. Mariner's Cove Fifth Year Monitoring Report. 4 p. [cited 2016 November 2]. Available from: https://ribits.usace.army.mil/ribits_apex/f?p=107:10:11462267296326::NO::P10_BANK_ID:374

Anonymous. 1997. San Leandro Shoreline Third Year Monitoring Report. 9 p. [cited 2016 November 2]. Available from: https://www.ecoatlas.org/upfiles/2960/SanLeandroShoreline179650%20third%20year%20monitoring%20report.pdf

Anonymous. 2005. Bayside Business Park – Phase II. Second Year Monitoring. ACOE permit #203390. 15 p. [cited 2016 June 2]. Available from: https://www.ecoatlas.org/upfiles/1026/203390%20%20second%20year%20monitoring%20report.pdf

Anonymous. 2003. Muzzi Marsh Monitoring Data. 42 p. [cited 10 January 2017]. Available from: http://ecoatlas.org/upfiles/2359/warm%20springs_muzzi_china%20camp_mon%20data.pdf

Bias MA, Woo I, Demers S, Takekawa JE, Reid F. 2003. Guadalcanal Tidal Marsh Restoration Progress Report. Prepared by Ecosystem Restoration Sciences, Inc., US Geological Survey, and Ducks Unlimited. Submitted to Chuck Morton, Department of Transportation, Office of

Environmental Planning. 12 p. [cited 10 January 2017]. Available from: https://www.ecoatlas.org/upfiles/1054/250060%20%202003%20monitoring%20report.pdf

California Department of Water Resources. 2006. Blacklock Restoration Project Monitoring Plan. Prepared in cooperation with U.S Bureau of Reclamation, California Department of Fish and Game, Suisun Resource Conservation District. 19 p. [cited 2016 November 2]. Available from: https://www.ecoatlas.org/upfiles/2339/Blacklock_Monitoring_Plan_2006.pdf

California Department of Fish and Game and Grizzly Island Wildlife Area. 2003. Island Slough Wetland Development Management and Monitoring Update. 2003. Prepared for the Army Corps of Engineers. Dept. of Water Resources. National Marine Fisheries Service. Regional Water Quality Control Board. San Francisco Bay Conservation and Development Commission. United States Fish and Wildlife Service. 9 p. [cited 2016 November 2]. Available from: https://www.ecoatlas.org/upfiles/2405/162230%20%202002%20monitoring%20report.pdf

California Fish and Game. 2003. Wetland Mitigation, Enhancement, and Monitoring Report for Belden's Landing Water Access Facility. Solano County. 5 p. [cited 10 January 2017]. Available from: https://www.ecoatlas.org/upfiles/2441/240300%20%20first%20year%20monitoring%20report.pdf

California Department of Transportation. 2009. Maintenance and Monitoring Report. Harvey Marsh Mitigation Site - Year 1. Cal Trans. Santa Clara County, California. 22 p. [cited 10 January 2017]. Available from: https://www.ecoatlas.org/upfiles/3072/Harvey%20Marsh%20M%26M%20Report%20Year%201.pdf

City of Foster. 2002. Lakeside Drive & Mariner's Island Extension Mitigation. Fourth Year Monitoring Report. 7 p. [cited 2016 November 2]. Available from: https://www.ecoatlas.org/upfiles/2424/197420%20fourth%20year%20monitoring%20report.pdf

Huffman & Associates, Inc. 1999. Madera del Presidio Project- Phase I and II. Fourth Year Monitoring Report. 16 p. [cited 2016 November 2]. Available from: https://www.ecoatlas.org/upfiles/2411/171740%20%20fourth%20year%20monitoring%20report.pdf

LFR Levine-Fricke. 2002. Montezuma Mitigation, Monitoring, and Reporting Plan. 298 p. [cited 2016 November 2]. Available from: https://www.ecoatlas.org/upfiles/4149/MMRP.pdf

LSA Associates. 1994. Galbraith Golf Course Wetland Mitigation Project. Success Criteria and Monitoring Plan. 5 p. [cited 2016 November 2]. Available from: https://www.ecoatlas.org/upfiles/1049/190660%20success%20criteria%20and%20monitoring%20plan.pdf

LSA Associates Inc., Tito Patri & Associates Inc. & Clearwater Hydrology. 1997. Final Bayfront Park Wetlands Restoration Project, City of Pinole, Contra Costa County. 1997. Prepared for City

of Pinole. LSA Project #COP630. 29 p. [cited 2016 November 2]. Available from: https://www.ecoatlas.org/upfiles/2903/BayfrontParkWetlands%20RestProj_RP_1997.pdf

LSA Associates Inc. 2001. Galbraith Golf Course Wetland Mitigation Project. Fifth Year Monitoring Report. 7 p. [cited 2016 November 2]. Available from: https://www.ecoatlas.org/upfiles/1050/190660%20fifth%20year%20monitoring%20report.pdf

LSA Associates. 2002. Citation Marsh. 3rd year monitoring report. Prepared for Citation Homes Central of Santa Clara, California. 11 p. [cited 2016 November 2]. Available from: https://www.ecoatlas.org/upfiles/2421/195480%20%20third%20year%20monitoring%20report.pdf

LSA Associates Inc. 2002. Deepwater Slough Island Mitigation Site. Year 1 Annual Monitoring Report. Pacific Shores Center. Redwood City. California. Submitted to Pacific Shores Center. 8 p. [cited 2016 November 2]. Available from: https://www.ecoatlas.org/regions/ecoregion/statewide/projects/1814#files

Marin Audubon Society. 2003. Triangle Marsh Restoration Project. Mitigation and Monitoring Plan. 8 p. [cited 2016 November 2]. Available from: https://www.ecoatlas.org/upfiles/2453/279842%20%20mitigation%20and%20monitoring%20plan.pdf

Olderbing Environmental. 1999. Oro Loma Marsh Mitigation Project. Project Description and Monitoring Plan. 38 p. [cited 2016 November 10]. Available from: https://www.ecoatlas.org/upfiles/1075/215901%20project%20description%20and%20monitoring%20plan.pdf

Santa Clara Valley Water District. 2015. Island Ponds Mitigation Monitoring and Reporting Year 10-2015. U.S Fish and Wildlife Service. Don Edwards National Wildlife Refuge. 75 p. [cited 2016 November 10]. Available from: http://www.southbayrestoration.org/monitoring/Island%20Ponds%20Year%2010%20Monitoring%20Report.pdf

San Pablo Bay National Wildlife Refuge. 1997. Final Tubbs Island Restoration Plan and Environmental Assessment. Mare Island. California. 12 p. [cited 2016 November 10]. Available from: https://www.cerc.usgs.gov/orda_docs/DocHandler.ashx?task=get&ID=133

S.S. Papadopulus & Associates, Inc. & Philip Williams and Associates, Inc. 2004. Cooley Landing. Third Year Monitoring Report. ACOE Permit #238870. 23 p. [cited 2016 November 10]. Available from: https://www.ecoatlas.org/upfiles/1139/238870%20third%20year%20monitoring%20report.pdf

Sunquest Properties, Inc. 2006. Brisbane Baylands Wetland Mitigation Plan. 5 p. [cited 2016 November 15]. Available from: https://www.ecoatlas.org/upfiles/2399/280500%20project%20description%20and%20performance%20criteria.pdf

Ward K, Ablog M. 2006. Crissy Field Restoration Project Summary of Monitoring Data 2000-2004. Golden Gate National Recreation Area. 102 p. [cited 2016 November 15]. Available from: https://www.nps.gov/goga/learn/management/upload/-1441-crissy-marsh.pdf

Wetlands Research Associates, Inc. 2003. Pacific Commons Preserve: 2003 Annual Monitoring Report. ACOE Permit #220851. 6 p. [cited 2016 November 15]. Available from: https://www.ecoatlas.org/upfiles/1165/220851%202003%20monitoring%20report%20and%20maps.pdf

Wildlands, Inc. 1999. Plummer Creek Wetlands Restoration Mitigation Project. Mitigation and Monitoring Plan. Rocklin. California. 12 p. [cited 2016 November 15]. Available from: https://www.ecoatlas.org/upfiles/1092/244150%20mitigation%20and%20monitoring%20plan.pdf

Wildlands, Inc. 2005. Kimball Island Mitigation Bank 2004 Monitoring Report. Rocklin. California. 28 p. [cited 2016 November 15]. Available from: https://ribits.usace.army.mil/ribits_apex/f?p=107:278:11462267296326::NO:RP,278:P278_BANK_ID:62

Wildlands, Inc. 2008. North Suisun Mitigation Bank. 2008 Monitoring Report. Rocklin. California. 9 p. [cited 2016 November 15]. Available from: https://www.ecoatlas.org/upfiles/2843/North%20Suisun%202008%20Monitoring%20Report.pdf

Wildlands, Inc. 2015. Liberty Island Conservation Bank & Liberty Island Preserve. 2015 Monitoring Report Year 4. Rocklin. California. 64 p. [cited 2016 November 15]. Available from: https://ribits.usace.army.mil/ribits_apex/f?p=107:278:11462267296326::NO:RP,278:P278_BANK_ID:4840

Conservation Plans Consulted for this Review

California Department of Fish and Wildlife, U.S. Fish and Wildlife Service, National Oceanic and Atmospheric Administration. 2014. Conservation Strategies for Restoration of the Sacramento-San Joaquin Delta, Sacramento Valley, and San Joaquin Valley Regions. 255 p. Available from: https://nrm.dfg.ca.gov/FileHandler.ashx?DocumentID=31232

Delta Stewardship Council. 2013. The Delta Plan. Ensuring a reliable water supply for California, a healthy ecosystem, and a place of enduring value. 322 p. Available from: http://deltacouncil.ca.gov/sites/default/files/documents/files/DeltaPlan_2013_CHAPTERS_COMBINED.pdf

ICF International. 2016. Final Environmental Impact Report/Environmental Impact Statement for the Bay Delta Conservation Plan/Water Fix. Prepared for California Department of Water Resources. U.S. Bureau of Reclamation. Sacramento. California. Available from: https://californiawaterfix.com/

Monroe M, Olofson PR, Collins JN, Grossinger RM, Haltiner J, Wilcox C. 1999. Baylands Ecosystem Habitat Goals. SFEI Contribution No. 330. U. S. Environmental Protection Agency,

San Francisco, California/S.F. Bay Regional Water Quality Control Board, Oakland, California. 328 p. Available from: https://baylandsgoals.org/

San Francisco Bay Conservation & Development Commission. San Francisco Bay Plan. 2015. [internet]. Available from: http://www.bcdc.ca.gov/plans/sfbay_plan

San Francisco Bay Joint Venture. 2001. Restoring the Estuary. Implementation Strategy of the San Francisco Bay Joint Venture. 108 p. Available from: https://www.sfbayjv.org/pdfs/strategy/Restoring_The_Estuary_Full.pdf

Sloop C, Jacobs B, Logsdon R, Wilcox C. 2017. Delta Conservation Framework. A Planning Framework for Integrated Ecosystem Conservation toward Resilient Delta Landscapes and Communities by 2050. California Department of Fish and Wildlife. Available from: https://www.wildlife.ca.gov/Conservation/Watersheds/DCF

U.S. Department of the Interior. Bureau of Reclamation, U.S. Fish and Wildlife Service. California Department of Fish and Game. 2013. Suisun Marsh Habitat Management, Preservation, and Restoration Plan. 176 p. Available from: https://www.wildlife.ca.gov/Regions/3/Suisun-Marsh

Chapter 2

Spatial indicators of post-restoration vegetation dynamics in wetland ecosystems

Abstract

To provide a long-term and broad scale monitoring of wetland restoration outcomes, it is pivotal to identify metrics that show rapid and predictable responses to restoration treatments. Remote sensing can help monitor such metrics at a large scale, high frequency, and low cost, but remains somewhat underutilized in practice. This study sought to identify a set of landscape metrics derived from aerial images that were most responsive to restoration treatments and vegetation dynamics across a subset of 21 restored and 5 reference sites in the Sacramento-San Joaquin Delta of California, USA. Breakpoint analysis was first leveraged to detect phases in the development of vegetated pixels within an 11-year time series of Landsat data as estimated from satellite-based vegetation indices. Landscape metrics were then generated from land cover classifications based on high resolution aerial images from USDA's National Agricultural Inventory Program. Using hierarchical clustering, we grouped phases in post-restoration vegetation development showing similar temporal characteristics. We identified a subset of landscape metrics that best described the spatial structure of vegetation and ongoing restoration processes in each of these phase types. Our analyses identified four distinct phases in vegetation development: (1A) rapid non-linear increase; (1B) non-linear decrease; (2A) low change; (2B) low change with fluctuations. Landscape metrics offered a significant response to time and vegetation dynamics in our study set, suggesting their potential to complement and extend the scope of current monitoring at low cost. Young sites and sites experiencing rapid increase in site greenness were characterized by a lower density of small patches and a low vegetation cover, while older sites, reference sites, and low variability sites were characterized by large, clustered patches. Our study demonstrates that publicly available remote sensing data can detect important patterns in wetland recovery. Studying these patterns enhances the current understanding of factors promoting wetland recovery and capacity to predict future restoration outcomes.

1 Introduction

Recent literature reports a substantial variability in wetland responses to restoration treatments (Matthews et al. 2009; Moreno-Mateos et al. 2015; Van den Bosch and Matthews 2017), with some projects falling short of restoration targets. Responses can range from rapid and linear (e.g., Craft et al. 2003; Staszak and Armitage 2013) to slow or chaotic (e.g., Zedler et al. 1999; Bullock et al. 2011; Moreno-Mateos et al. 2012). A thorough monitoring of remnant and restored sites could identify factors driving this variability (Kentula 2000, Brudvig 2011, Suding 2011) to inform the planning of future projects. However, ecological restoration has suffered from a lack of consistent and long-term monitoring (Zedler 2000; Brudvig 2011; Wortley et al. 2013), particularly at the landscape scale (Simenstad et al. 2006; Brudvig 2011). As a result, factors promoting the recovery of sites or explaining divergences in site trajectory are not always fully

understood (Brudvig et al. 2017) and long-term responses to restoration interventions sometimes become unpredictable (Suding 2011).

As plants show rapid responses to environmental fluctuations (e.g., Johnston et al. 2007; Chapple et al. 2017; McCoy-Sulentic et al. 2017), monitoring their characteristics can elucidate the role of local and regional factors on vegetation recovery. For example, tracking long-term fluctuations in plant coverage could highlight the role of site legacies and connectivity on successional processes (e.g., primary, secondary succession) following restoration treatments. A rapid increase in vegetation coverage or richness may signal that abiotic conditions have been undisturbed by previous or surrounding land uses. Constraining processes (e.g., lack of hydrological connectivity, biological invasions) or inadequate restoration treatments may slow the recovery of plant communities (Bullock et al. 2011, Suding 2011).

Most studies tracking long-term vegetation development in restored wetlands have focused on indicators measured in the field, such as vegetation coverage, species richness, and functional diversity (e.g., Doren et al. 2009, D'Astous et al. 2013). Tracking these indicators on the ground is pivotal to measuring a site's response to treatments and disturbances (e.g., Matthews and Spyreas, 2010) or highlighting the role of site legacies on vegetation colonization and persistence (Galatowitsch 2006). However, plot-level indicators can become labor-intensive in large and heterogeneous sites requiring extensive sampling (Taddeo and Dronova 2018). These challenges have motivated the applications of remote sensing data in restoration monitoring, yet in wetlands such efforts are still seldom utilized (but see Shuman and Ambrose 2003; Tuxen et al. 2008; Chapple and Dronova 2017).

Researchers have advocated for broadening the current spatiotemporal scale at which restoration efforts are undertaken, recognizing that the combined effect of multiple sites is needed to achieve landscape goals (Kentula 2000; Kimmerer et al. 2005; Simenstad et al. 2006). Landscape assessments would favor site comparisons and highlight the role of landscape context (i.e., nature and configuration of land uses surrounding a project) on site recovery. Remote sensing analyses can complement field efforts (Klemas 2013a) and expand the spatiotemporal scale of wetland monitoring (Taddeo and Dronova 2018) to enable a low-cost monitoring of whole site extents and their landscape context. Breakpoint analysis is an example of application of remote sensing products for the monitoring of vegetation dynamics central to restoration success. Breakpoint analysis has been used to monitor changes in pixel greenness (i.e., value of remote sensing-based vegetation indices responsive to vegetation biomass and cover; Box 1) (e.g., Browning et al. 2017). Mathematically, these breakpoints segment a time series into phases (Box 1) with distinct trends, slope, or frequency amplitude (Verbesselt et al. 2010) marking changes in the direction or rate of vegetation development within a pixel. Breakpoints may reflect successional changes in a site and their impact on vegetation coverage and density. In other cases, a breakpoint may reveal the effect of disturbances or climatic fluctuations on vegetation productivity (Kennedy et al. 2010; Browning et al. 2017). In both situations, changes in vegetation productivity, composition, and abundance will probably impact the value of vegetation indices derived from land surface reflectance data and used as a proxy of site greenness (Jensen 2007). Breakpoint analysis can detect vegetation response to ecosystem stressors including droughts, fire, and logging (e.g.,

Browning et al., 2017; Verbesselt et al., 2012), but to our knowledge, has only been marginally used to characterize post-restoration patterns of vegetation development.

Landscape metrics describing the spatial distribution, structure, and diversity of land covers (Turner 1989; Box 1) are frequently used in conservation biology to monitor habitat extents, ecosystem services (Colwell and Lees 2000; Botequilha Leitao and Ahern 2002), or landscape changes and their impacts on ecological processes (Dale and Beyeler 2001; Van Meter and Basu 2015). As such, they represent another interesting application of remote sensing products for post-restoration monitoring. In wetland ecosystems, landscape metrics can detect changes in vegetation structure and composition (e.g., Tuxen et al. 2008; Kelly et al. 2011; Chapple and Dronova 2017), measure ecosystem services (e.g., Almeida et al. 2016) and quantify faunal habitats (e.g., Moffett et al. 2014; Dronova et al. 2016). Additionally, they can unravel ongoing ecological processes impacting the post-restoration trajectory of a site. For example, a decrease in the distance between neighboring vegetated patches can impact water flows and their capacity to transport seeds, plant fragments, and nutrients (Meire et al. 2014). To date, landscape metrics have been sparsely used in practice despite recent studies showing their potential to track post-restoration vegetation expansion and responses to ecosystem stressors (e.g., Tuxen et al. 2008; Moffett and Gorelick 2016; Chapple and Dronova 2017).

To promote the use of remote sensing data and spatial analyses for the broad-scale monitoring of wetlands, we developed a methodological framework based on openly accessible aerial and satellite images. Our primary goal was to identify a set of landscape metrics most sensitive to vegetation dynamics and site characteristics that could be included in long-term monitoring plans. Such an effort could help direct project managers towards a few, but most informative, landscape metrics that could be monitored repeatedly across projects to characterize post-restoration ecosystem changes.

Box 1. Definitions of key terms used in this paper

Greenness. Remote-sensing based proxy of vegetation coverage and productivity based on the passive reflectance of solar energy by vegetation in electromagnetic regions sensitive to plant physiology.

Breakpoint analysis: Breakpoint analysis identifies points within a time series separating two segments with a distinct slope or direction. These segments might represent different vegetation dynamics including loss of biomass following a major disturbance or a gain of coverage via primary succession.

Phases: In this paper, phases are segments in time series of site greenness separated by breakpoints and showing distinct trends or directionality of change.

Temporal metrics: Temporal metrics are statistics describing the rate of change, directionality of change, degree of non-linearity, and presence of abrupt short-term fluctuations throughout the duration of a phase.

Landscape metrics: Landscape metrics describe the geometry and distribution of land cover patches within a site.

2 Methods

2.1 Study area

We monitored the vegetation dynamics of 21 restored wetlands and five reference sites located in the Sacramento-San Joaquin Delta of California (hereafter the Delta) and the adjacent Suisun Marsh, United States (Figure 1). The Delta is confined between the cities of Tracy (37.7397° N, 121.4252° W) and Sacramento (38.5816° N, 121.4944° W) at the confluence of the Sacramento and San Joaquin rivers. It includes freshwater marshes dominated by *Schoenoplectus acutus* and *Typha spp.* and tidal marshes dominated by *Sacocornia pacifica* and *Spartina spp.* The Suisun Marsh, adjacent to the Delta, is the largest remaining brackish wetland in the Western United States and includes sites dominated by *Schoenoplectus americanus* and *Bolboschoenus maritimus* (Vasey et al. 2012; Moyle et al. 2013).

A large-scale land reclamation during the 1850s has degraded wetland habitats of the region and impacted their capacity to fulfill critical ecosystem functions (SFEI-ASC, 2014; Whipple et al., 2012). These transformations have resulted in the loss of 98% of freshwater wetlands and 95% of tidal marshes (Whipple et al. 2012) endangering few species and increasing the vulnerability to sea level rise and saltwater intrusion (SFEI-ASC 2014; Luoma et al. 2015). In response, over 38.44 km^2 of wetland habitats have been restored in the region and an additional 9.09 km^2 is underway (CWMW,2018). The region includes restoration projects varying in age, size, and restoration treatments which provides a unique setting to compare site post-restoration trajectories.

2.2 Study sites

Using the EcoAtlas database summarizing major restoration projects in the study area (CWMW, 2018), we selected 21 wetlands restored between 1993 and 2014 which had well-defined spatial boundaries and, when possible, information on restoration treatments (SI Table S1). Our sample included both freshwater and tidal wetlands but excluded vernal pools and wet meadows. Restoration treatments included levee breaching to increase tidal fluctuations, removal of non-native vegetation, grading, and planting. These projects ranged in size from 0.01 to 6.01 km^2 (SI Table S1). We selected five additional remnant wetland sites to serve as a reference as they are managed or protected (SI Table S1). To assess the effect of site age on landscape metrics and mean greenness, we grouped sites by age class using five-year increments (i.e., <5, 5-10, 10-15, >15).

2.3 Remote sensing data

To characterize post-restoration vegetation dynamics, we used satellite data from NASA's Landsat archive and aerial images from the USDA's National Agricultural Inventory Program (NAIP). Combining these two datasets enabled us to enhance the temporal frequency and spatial detail of our analyses: the Landsat archive includes frequent data (revisit time of 16 days) but a medium-high spatial resolution (30m) while the NAIP dataset proposes detailed data (0.6 to 1m resolution) but a low temporal frequency (one image every 2-3 years).

Images from the Landsat archives were used to characterize changes in site greenness from the year of restoration to 2017. We used greenness as a proxy of change in vegetation biomass and coverage. We leveraged images captured by Landsat satellites 7 ETM+ (2004 to 2014) and 8 OLI (2013 to 2017; path 44, and rows 33 and 34). Google Earth Engine (Gorelick et al. 2017) was used to mask pixels with clouds, cloud shadow, or water within individual images using the quality assessment band of Landsat's surface reflectance products. We then calculated the enhanced vegetation index (EVI) of remaining cloud-free and water-free pixels which we used as an indicator of vegetation greenness. EVI is an index of vegetation abundance based on the ratio of red light absorbed by plant chlorophyll and the proportion of infrared light scattered by mesophyll cells, to which a correction factor is applied to account for soil and atmospheric conditions (Huete et al. 2002). As Landsat ETM+ and OLI have different spectral bandwidths for similar electromagnetic regions, we used conversion equations developed by Roy et al. (2016) to calibrate the spectral data of Landsat 8 OLI to Landsat 7 ETM+.

2.4 Time series analysis and breakpoint detection

We applied a cubic smoothing spline to all cloud- and water-free Landsat pixels in a site to generate continuous site-level time series of EVI from 2004 to 2017. We then utilized the bfast R package (Verbesselt et al. 2010) to identify breakpoints within these site-specific time series of EVI values (Fig. 2). Breakpoints separate two statistically distinct but adjacent segments in a time series, allowing the identification of different phases in vegetation trajectory (Verbesselt et al. 2010). Bfast, for Breaks for Additive Seasonal and Trend, is an algorithm commonly used to identify breakpoints in time series of vegetation indices (e.g., Verbesselt et al. 2010; Browning et al. 2017). This algorithm identifies the breakpoint distribution that minimizes the Akaike

Information Criterion by iteratively testing different combination of breakpoints after removing the seasonal trend (Verbesselt et al. 2010). The combination of segments and breakpoints satisfying the least squares residuals moving sum is kept. We allowed a minimum of four years between breakpoints and used a significance level of 0.05.

Using the R package Traj we generated a series of temporal statistics describing the rate of change, degree of non-linearity, and the magnitude of abrupt short-term fluctuations in greenness (Leffondré et al. 2004) within each phase (or time series segment) separated by breakpoints. Statistics describing change over time include: change (i.e., amplitude in EVI values over the duration of the phase), mean change per year, slope, and change relative to the first score, and the coefficient of variation in EVI. The degree of non-linearity in the trend of EVI is described by the maximum, mean, and standard deviation in the first differences in time series of EVI values (i.e., a linear trajectory would have a low standard deviation in first differences). The presence and magnitude of abrupt short-term fluctuations are described by the ratio of the mean absolute second difference to the mean absolute first difference and the ratio of the maximum absolute second difference to mean absolute first difference (Leffondré et al. 2004). We applied a principal component analysis (PCA) to the resulting matrix of temporal metrics (phases X temporal metrics) to identify a subset of temporal statistics most representative of phases in vegetation recovery. We applied an agglomerative hierarchical clustering on the resulting PCA scores to form clusters of phases showing similar temporal characteristics using Ward's method and the hclust function in R (R Core Team 2017).

2.5 Spatial analyses

The NAIP dataset was used to delineate vegetated patches within restored sites through a land cover classification of all available images between 2005 and 2016. From this land cover classification, we generated landscape metrics to describe changes in the extent, structure, and spatial distribution of vegetation within our sample of sites. Images captured in 2016 had a finer resolution than previous years and were consequently resampled at a 1m resolution for consistency.

We used an object-based image analysis to delineate and classify wetland patches within every site and NAIP image. Object-based image analysis (OBIA) uses information on texture, spatial context, and shape to form clusters of adjacent and relatively homogeneous pixels (Blaschke, 2010; Knight et al., 2015). OBIA is increasingly used in wetland change analyses to address the ecosystem's high heterogeneity in vegetation distribution and density, which makes it difficult to parse out noise in data from significant change (Dronova 2015). To segment the NAIP images, we used the multi-resolution segmentation algorithm of eCognition 8.7. This algorithm uses a bottom-up region-growing approach which iteratively merges adjacent pixels by assessing the degree of homogeneity in their spectral and spatial characteristics.

We used the support vector machine (SVM) algorithm to classify the resulting objects as bare soil, mudflat, vegetation, or water. The SVM utilizes a set of training samples to find the hyperplane that best separates a dataset into a predefined number of classes (Mountrakis et al. 2011). This approach has been successfully used to classify plant functional types and

distinguish vegetated patches from mudflats and open water in wetlands (Wang et al. 2012; Dronova et al. 2011). To train the algorithm, we visually identified 200 to 500 randomly dispersed points per site using the NAIP dataset. We then verified the output of this supervised classification and manually corrected misclassified objects. From this supervised classification, we generated six land cover maps (2005, 2009, 2010, 2012, 2014, and 2016) for every study site.

We then computed landscape metrics from each of these land cover maps to detect changes in the distribution and geometry of vegetated patches using the landscape analysis software Fragstats v.4 (McGarigal et al. 2012). We focused on eight landscape metrics, identified by Cushman et al. (2008) as the most robust and less redundant indicators of landscape composition as well as a few additional landscape metrics of significant importance (Table 1). We used the mean value of landscape metrics averaged over the duration of each phase length to analyze differences between phase types and age classes.

2.6 Statistical analysis

We conducted a series of Kruskal-Wallis tests with post-hoc Dunn tests and Bonferroni correction for multiple-comparison and a significance level of 0.05 to assess the significance of differences in landscape metrics among phase types, age classes, and in between restored and reference sites. Lastly, we used chi-square tests to assess whether site age had a significant incidence on the occurrence of different phase types.

3 Results

3.1 Breakpoints

The number of breakpoints per site ranged from zero to three, for a total of 52 time series segments identified throughout the study area. Seven sites showed no breakpoints between 2005 and 2017 suggesting that there was no significant change in the slope or direction of their trend. Thirteen sites experienced one breakpoint. Seven sites showed two breakpoints. Eight of the breakpoints we identified occurred in 2009, which corresponded to the last year of the 2007-2009 drought in California. Five breakpoints occurred in 2008, the first allowable year of breakpoint given the four-year length criteria we set for breakpoint identification. Four breakpoints occurred in 2012 and 2013, respectively, which corresponds to the first and second year of the 2012-2015 drought in the study area. Lastly, one breakpoint occurred in 2010, while two breakpoints occurred in 2011.

3.2 Cluster-based phase types

3.2.1 Temporal characteristics

The PCA used to identify temporal metrics that best distinguished phase types revealed that four axes could explain 90% of the variation in temporal characteristics among sites and their phases (Table 2). The first axis describes the degree of non-nonlinearity in trajectories (i.e., higher standard deviation in the first differences; Leffondré et al. 2004) and explains 42% of variance among all phases. This axis is strongly related to the standard deviation of the first difference in

EVI, the maximum of the absolute first difference, and the mean of the absolute first difference. The second axis describes the rate of change in EVI throughout the phase length and explains 23% of the total variance. This axis is best described by the mean change in EVI per year, the change in EVI relative to the first score, and the amplitude of change in EVI over the entire phase length. The third axis pertains to variability in EVI throughout a phase and describes 14% of the variance across phases. This axis is best described by the coefficient of variation in EVI values and the ratio of the maximum absolute difference to the mean-over-time, which is sensitive to important changes in trajectories (Leffondré et al. 2004). Lastly, the fourth axis described 11% of variation and was best represented by the ratio of the mean absolute second difference to the mean absolute first difference and the ratio of the maximum absolute second difference to mean absolute first difference which are both sensitive to fluctuations in the time series (i.e., peaks and dips around the trend; Leffondré et al. 2004).

A hierarchical clustering conducted on sites' ranking along these four PCA axes (Table 2) identified four phase types showing similar temporal patterns and nested in two distinct clusters (1 and 2; Fig.3). A Wilcox test revealed that Cluster 1 showed a significantly lower standard deviation in first differences (χ^2=19.527; df=1; p<0.0001) and a lower absolute rate of change than the second cluster (χ^2=15.86, df=1, p<0.001). Cluster 1 showed a significantly lower coefficient of variation and position along the third axis than the second cluster (χ^2=10.17, df=1, p<0.001). The first cluster showed a greater magnitude of peaks and dips as evidenced by a greater ratio of first to second differences (χ^2=15.86, df=1, p<0.001).

Sub-clusters 2A and 2B showed significant differences in their rate of change with cluster 2A exhibiting a rapid positive change in EVI over time, expressed by a higher position along the second axis (p<0.0001). Meanwhile, group 2B showed a negative rate of change (decrease). Sub-clusters 2A and 2B did not show significant differences in their coefficient of variation or in the presence and magnitude of peaks and dips (Fig. 3). Cluster 1B showed a greater standard deviation in first differences than cluster 1A (p=0.006). Clusters 1A and 1B were not significantly distinct in their rate of change over time. They did show, however, a significant contrast in their ratio of the maximum absolute difference to the mean-over-time, with sub-cluster 1B showing significantly greater values than group 1A (p=0.0009) revealing a greater frequency and magnitude of abrupt short-term fluctuations (Fig. 3). In sum, cluster 1 is characterized by a lower amplitude of change in greenness. Its two sub-clusters are distinguished as follows: cluster 1A shows little abrupt fluctuations while 1B shows a greater number and magnitude of short-term fluctuations. Cluster 2 is characterized by a greater amplitude of non-linear change, with 2A showing a positive change in greenness and 2B showing a negative change in greenness (Fig. 3).

3.2.2 Spatial characteristics

Phase types revealed significant contrasts in landscape metrics (Fig. 4), including patch density (χ^2=11.63, df=3, p=0.01; Fig. 4B) and mean patch area (χ^2=8.2987, df=3, p=0.04; Fig. 4C). In addition, phases with a greater absolute rate of change (2A – positive; 2B- negative) were characterized by a greater patch density (χ^2=9.81, df=1, p=0.002; Fig. 3A) and smaller patches (χ^2=4.47, df=1, p=0.03; Fig. 4C) than phase types 1A and 1B (little change over time). Phase

type 2A (rapid positive change) showed a lower percentage vegetated than any other phase types (sign. level=0.05). Lastly, phase type 1A and 1B (both characterized by a smaller density of larger patches) showed significant contrasts with phase type 1B showing a greater coefficient of variation in patch area (p=0.04; Fig. 4C), greater fractal index (p=0.02; Fig. 4A), but lower distance to neighbor than 1A (p=0.02; Fig. 4E). Phase type 1A was characterized by a lower distance to neighbors than any other phase types (sign. level=0.05).

3.3 Spatiotemporal patterns in the occurrence of phase types

3.3.1 Site age, temporal characteristics, and phase type occurrence

A chi-square test suggested a potential effect of site age on the occurrence of the different phase types (χ^2=15.22, df=5, p=0.009). Site age had a significant impact on the likelihood of occurrence of phase type 1 versus phase type 2, but this difference was mainly driven by younger sites (0-5-year-old) and reference sites. Site age also had a significant incidence on the occurrence of sub-phase types (χ^2=21.963, p=0.04). This relationship was mostly driven by young sites, which were more likely to experience phase type 2A (rapid non-linear increase). Meanwhile, sites at an intermediate level of restoration (10-15 years) showed a greater occurrence of phase type 2B (rapid non-linear decrease), as evidenced by a greater Pearson's residual. Finally, reference sites experienced a greater occurrence of phase type 1A (slow change with few fluctuations) as shown by a greater Pearson's residual.

Younger sites showed a significantly greater non-linearity than older and reference sites (p=0.01). Site age significantly impacted the absolute rate of change in greenness (χ^2=10.68, df=4, p=0.03). This contrast was driven by significant differences between young sites and intermediate age class (p=0.003), 5-10 and 10-15 years old (p=0.02) and older restored sites (p=0.01). All age classes experienced a greater coefficient of variation in greenness than reference sites (p=0.01). Lastly, site age did not have a significant incidence on the magnitude of abrupt short-term changes or the position of the different phases along the fourth PCA axis.

3.3.2 Restored versus reference sites

There was no statistical difference between restored and reference sites in their position along the first PC, indicating that they both exhibit linear and non-linear trajectories. There is no statistical difference in the rate of change either or the position along the second axis. Yet restored and reference sites significantly differed in their position along the third axis (Mann-Whitney test, W=120, p=0.03) and their coefficient of variation in EVI values (χ^2=5.24, df=1, p=0.02), with restored sites showing more fluctuations around their trend than reference ones.

3.4 Landscape metrics versus site age

Reference sites in our study were characterized by lower density (χ^2=3.70, df=1, p=0.05; Fig. 5B) of larger patches (χ^2=5.35, df=1, p=0.02; Fig. 5C) than restored sites but a greater coefficient of variability in patch area (χ^2=4.44, df=1, p=0.04; Fig. 5D). Their patches were generally more complex, as revealed by greater shape index (χ^2=3.70, df=1, p=0.009) but also showed greater variability in shape index (χ^2=6.35, df=1, p=0.001). Lastly, patches in restored sites were more

aggregated (χ^2=5.89, df=1, p=0.02; Fig. 5F) and clustered as revealed by a greater coefficient of variation in distance to the nearest neighbor (χ^2=12.76, df=1, p=0.0003; Fig. 5E).

Age classes showed significant contrasts in their patch density (χ^2=11.14, df=4, p=0.03; Fig. 5B), mean patch area (χ^2=12.80, p=0.01; Fig. 5C), coefficient of variation in distance to the nearest neighbor (χ^2=17.77, df=4, p<0.0001; Fig. 5E), and aggregation index (χ^2=9.39,df=4, p=0.05; Fig. 5F). Younger sites were characterized by a lower percent coverage and higher patch density than any other age class (p<0.02) and reference sites (p<0.0001), but these landscape metrics did not differ among other age classes. Younger sites had significantly smaller mean patch area than any other classes (sign. level=0.05). The coefficient of variation in distance to the nearest neighbor was also significantly different (p=0.05), with reference sites showing greater coefficient of variation than all other site types except oldest sites (sign. level=0.05), and younger sites showing a lower coefficient of variation than older sites and intermediate sites (10-15 yrs). Reference sites showed greater aggregation index than all other age types (sign. level=0.05) except the oldest restored sites.

4 Discussion

4.1 Landscape metrics to monitor vegetation dynamics

Previous studies have monitored spatiotemporal variations in landscape metrics describing the distribution and geometry of land cover types to depict landscape changes, habitat quality and quantity, and ecosystem services (e.g., Botequilha Leitao and Ahern 2002; Tuxen et al. 2008; Almeida et al. 2016) but landscape metrics remain somewhat under-utilized in the monitoring of restored wetlands (Taddeo and Dronova 2018). In this study, landscape metrics showed a significant response to time and vegetation dynamics revealing their potential to complement and extend the scope of site and regional-level monitoring at low cost. As landscape metrics are key predictors of species occupancy and abundance at different taxonomic levels (Paracuellos and Tellería 2004; Moffett et al. 2014), our results suggest that they could be used to establish compliance to habitat goals and at the same time track vegetation development for other purposes, such as monitoring ecosystem functions (Dronova & Taddeo 2016, Matthes et al. 2014). The most responsive metrics in our study set were percent vegetated cover, patch density, mean patch area, shape complexity, distance to the nearest neighbor, and aggregation.

4.1.1 Responses to vegetation dynamics

We identified in our sample of sites four phases in vegetation development with distinct trends, degree of nonlinearity, and amplitude of fluctuations around the trend. These phases were: stability (1A), low change with fluctuations (1B), non-linear increase (2A), and non-linear decrease (2B). Phase types showed significant contrasts in landscape metrics which might reflect their association to different successional stages or highlight the incidence of the spatial distribution of vegetation on wetland trajectory. Sites experiencing a rapid increase in EVI values (phase type 2A) were characterized by a low density of smaller patches, resulting in a lower percentage of vegetation cover than any other phase types. Meanwhile, the cluster showing a low change in EVI (cluster 1) was characterized by a lower density of larger patches, resulting in a greater vegetation cover. These contrasts may reflect different wetland successional stages: the

low vegetation cover in the 2A phase type likely provides unoccupied niche space promoting a rapid colonization of vegetation, as indicated by the emergence of few smaller patches. As sites "mature", patches likely become bigger resulting in an increase in percentage cover. This is consistent with previous studies showing that colonization decreases over time as less microsites are available for seed establishment (Matthews and Endress 2010). Feedbacks between litter accumulation, canopy cover, and their impacts on plant productivity and seedling establishment (Craft et al. 2003; Xiong et al. 2003) could further limit the lateral expansion of vegetated patches in sites with large patches and a high vegetation cover. For example, dense canopies promote litter accumulation which, in sites with a lack of tidal flushing, may impact productivity and diversity (Xiong et al. 2003; Rocha et al. 2008; Anderson et al. 2016).

Significant differences among the two phase-types showing the lowest change over time might further highlight the role of vegetation structure and spatial distribution on wetland processes. The phase type characterized by a greater stability in EVI values over time (1A) showed a lower heterogeneity in patch area, lower patch complexity (as evidenced by a smaller fractal index), and lower mesh size than phase type 1B (small change with abrupt short-term fluctuations around the trend). The phase type 1B was characterized by a greater magnitude of fluctuations around the trend as well as bigger patches and a greater variability in patch area. Although at the scale of this analysis it is difficult to identify the specific cause of these fluctuations, field evidence from previous studies suggest the following potential mechanisms. In sites with a lack of tidal flushing (Schile et al. 2013; Anderson et al. 2016) or dominated by reeds (Dronova and Taddeo 2016), litter accumulation and burial (Rocha et al. 2008; Schile et al. 2013; Dronova and Taddeo 2016) may affect seedling establishment and biomass production in a multi-year cyclical manner (Rocha et al. 2008; Anderson et al. 2016). Alternatively, fluctuations in presence of floating and submerged aquatic vegetation reported in previous regional studies (Ta et al. 2017; Khanna et al. 2018) may contribute to temporarily increasing greenness in sites with open water, potentially explaining some occurrences of phase type 1B (small changes, high fluctuations) in our study area.

4.1.2 Response to time

While younger sites showed the most unique landscape patterns and structure, we observed significant contrasts among other age classes as well. These differences may reveal a transition from a prevalence of seed dispersal (favoring an increase in the number of patches and characterized by smaller patches) to increased vegetative reproduction, which would likely result in fewer novel patches, and the expansion of existing patches (Combroux et al. 2002).

Older and reference sites showed a higher coefficient of variation in distance between patches, suggesting a greater clustering of their vegetated patches (Cushman et al. 2008), while younger sites (<5yrs) showed a lower coefficient of variation but a greater distance between patches, suggesting that their patches are further apart and more randomly dispersed. Increased patch clustering can reduce water flow thereby affecting the transport of sediments and seeds from hydrochorous species (Meire et al. 2014). This can explain why an increased in patch aggregation and clustering is linked in our sample to a low change in EVI values over time.

4.1.3 Difference between restored and reference sites

Overall, restored and reference sites in our study area showed distinct landscape spatial patterns. Reference sites maintained a lower density of bigger, more complex patches, with a lower coefficient of variation in distance to the nearest neighbor. For some of these landscape metrics —including percent cover and patch density— this difference was mainly driven by significant contrasts between newly restored sites and reference sites. Reference sites maintained greater aggregation index and coefficient of variation in distance to neighbors than any age group, except the oldest one (>15 yrs), which suggests that sites may tend towards a greater aggregation of vegetated patches through time.

4.2 Patterns in the spatiotemporal occurrence of phase types

The occurrence of these phase types in time and space seems to reflect the effect of restoration treatments, site characteristics, and landscape context on vegetation dynamics. Younger sites (<5 years old) were more likely to experience a rapid non-linear increase in EVI values (phase type 2A) than older or reference sites and showed a greater rate of change in site greenness overall. These results parallel field observations in restored wetlands revealing an early and rapid increase in vegetation coverage in early years resulting from colonization, seedbank emergence, and plantings (Bernhardt and Koch 2003; Craft et al. 2003; Matthews et al. 2009; Staszak and Armitage 2013). Interestingly, younger sites were characterized by more non-linearity than any other age type, which suggests that they might be experiencing an exponential growth in vegetation greenness. This may result from the combined expansion of existing patches through vegetative dispersal and the apparition of new patches through sexual reproduction allowing a more rapid growth as propagule availability increases with colonization.

While site age had a significant impact on the rate of change in greenness over time, it did not significantly affect the amplitude of abrupt short-term fluctuations around the trend. This suggests that both young and older sites can experience fluctuations in site greenness over time. Sites at an intermediate level of restoration (between 10 and 15 years old) showed a greater than expected occurrence of phase 2B (non-linear decrease). This type of response in vegetation coverage (initial increase followed by decrease) has been observed by field-based studies including Anderson et al. (2016) in a freshwater wetland of California, and Matthews et al. (2009) in Illinois. Meanwhile, reference sites were more likely to experience phase type 1A (little change, little fluctuations) but also showed some occurrence of phase 1B (little change, fluctuations). This supports observations made by previous studies (Hiers et al. 2012; Chapple et al. 2017) showing that conditions in reference sites are not static but rather fluctuating with their abiotic environment. A substantial variability in the vegetation dynamics of sites similar in age reveals that restoration outcomes cannot be easily predicted outside of their immediate context, as wind, channels, and surface flows transport plant material, nutrients, and pollutants from adjacent land covers onto the wetland likely impacts their recovery (Cook and Hauer 2007; Matthews et al. 2009; Soomers et al. 2013).

4.3 Limitations

Previous studies have demonstrated the impact of data scale and resolution on landscape metrics (Wu 1999; Kelly et al. 2011). While some landscape metrics show a linear response to change in resolution, others have a non-linear response to image scale. As such, caution is needed when comparing the latter landscape metrics across sites or landscape datasets using a different land cover classification or data resolution. Because some of the most responsive landscape metrics identified in our results —including patch area, shape index, contagion and contiguity — tend to linearly respond to changes in grain size (Kelly et al. 2011), their sensitivity to data resolution can be relatively more predictable. Yet it is still possible that other patterns could become apparent at a different scale of analysis and that the most responsive metrics here will behave differently when applied to a different resolution. Nonetheless, our study shows that significant changes can be observed when using open-access aerial images with a coarser resolution (in this case, 1m) and lower temporal frequency. This reveals promising applications for project managers overseeing large sites for landscape-scale assessments including multiple sites.

Lastly, an important limitation of this study was the lack of comprehensive data on the management history of some of these sites – a common challenge in restoration monitoring that has been highlighted by previous studies in river ecosystems (Kondolf 1998; Bernhardt et al. 2007). Thus, it is possible that some of the patterns we observed in terms of when and where phases in vegetation development were occurring in the landscape were not completely relatable to site age or location, but rather to unique management approaches. Nonetheless, the fact that we could observe significant differences in the vegetation dynamics of our study sites shows that cost-effective landscape metrics and remotely sensed vegetation greenness can enable an informative comparison of site trajectories and response to restoration treatments.

5 Conclusion

Landscape metrics in our study sites showed significant responses to time and vegetation dynamics, suggesting their potential to help monitor wetland ecosystems. The variability in trajectories observed throughout the study area — even among older, potentially more established wetlands — highlights the importance of long-term monitoring to detect arising ecosystem stressors or unexpected fluctuations in properties of interest. Differences in the characteristics and patterns of occurrences of the phase types identified in this study reveal the benefits of a flexible, long term approach to post restoration assessment. Current length of post-restoration recovery varies widely, with some compensatory mitigation only requiring five years of monitoring (Hill et al. 2013; Van den Bosch and Matthews 2017) which can lead to an overestimation of restoration success (Van den Bosch and Matthews 2017). In our sample, while some sites experienced a relative stability (phase type 1A) after an initial increase (phase type 2A), other experienced a rapid decline (2B) or substantial fluctuations around the trend (1B). Perhaps unsurprisingly, younger, more recently-restored sites showed a greater magnitude of change in greenness as revealed by a higher coefficient of variation in EVI and a steeper trend. Younger sites showed almost consistently distinct spatial patterns when compared to older sites, including a lower percent coverage, higher density of smaller and more regularly dispersed patches. This, together with significant differences in landscape metrics between restored and

reference wetlands, even among older sites, highlights the potential of public remote sensing datasets to support long-term monitoring. This monitoring could be extended to reference sites some of which showed substantial fluctuations as observed in previous publications (e.g., Chapple et al. 2017). When financial resources for long-term monitoring are limited, monitoring efforts may prioritize landscapes that are more likely to experience important fluctuations in vegetation properties (Matthews et al. 2009; Matthews and Spyreas 2010).

6 References

Almeida, D., J. Rocha, C. Neto, and P. Arsénio. 2016. Landscape metrics applied to formerly reclaimed saltmarshes: A tool to evaluate ecosystem services? Estuarine, Coastal and Shelf Science 181:100–113.

Anderson, F. E., B. Bergamaschi, C. Sturtevant, S. Knox, L. Hastings, L. Windham-myers, M. Detto, E. L. Hestir, J. Drexler, R. L. Miller, J. H. Matthes, J. Verfaillie, D. Baldocchi, R. L. Snyder, and R. Fujii. 2016. Variation of energy and carbon fluxes from a temperate freshwater wetland and implications for carbon market verification protocols. Journal of Geophysical Research: Biogeoscience 121:1–19.

Bernhardt, E. S., E. B. Sudduth, M. A. Palmer, J. D. Allan, J. L. Meyer, G. Alexander, J. Follastad-Shah, B. Hassett, R. Jenkinson, R. Lave, J. Rumps, and L. Pagano. 2007. Restoring rivers one reach at a time: Results from a survey of U.S. river restoration practitioners. Restoration Ecology 15:482–493.

Bernhardt, K., and M. Koch. 2003. Restoration of a salt marsh system : temporal change of plant species diversity and composition. Basic and Applied Ecology 4:441–451.

Van den Bosch, K., and J. W. Matthews. 2017. An Assessment of Long-Term Compliance with Performance Standards in Compensatory Mitigation Wetlands. Environmental Management 59:546–556.

Botequilha Leitao, A., and J. Ahern. 2002. Applying landscape ecological concepts and metrics in sustainable landscape planning. Landscape and Urban Planning 59:65–93.

Browning, D. M., J. J. Maynard, J. W. Karl, and D. C. Peters. 2017. Breaks in MODIS time series portend vegetation change: Verification using long-term data in an arid grassland ecosystem: Verification. Ecological Applications 27:1677–1693.

Brudvig, L. A. 2011. The restoration of biodiversity: where has research been and where does it need to go? American journal of botany 98:549–58.

Brudvig, L. A., R. S. Barak, J. T. Bauer, T. T. Caughlin, D. C. Laughlin, L. Larios, J. W. Matthews, K. L. Stuble, N. E. Turley, and C. R. Zirbel. 2017. Interpreting variation to advance predictive restoration science. Journal of Applied Ecology:1018–1027.

Bullock, J. M., J. Aronson, A. C. Newton, R. F. Pywell, and J. M. Rey-Benayas. 2011. Restoration of ecosystem services and biodiversity: Conflicts and opportunities. Trends in

Ecology and Evolution 26:541–549.

Chapple, D., and I. Dronova. 2017. Vegetation Development in a Tidal Marsh Restoration Project during a Historic Drought: A Remote Sensing Approach. Frontiers in Marine Science 4.

Chapple, D. E., P. Faber, K. N. Suding, and A. M. Merenlender. 2017. Climate Variability Structures Plant Community Dynamics in Mediterranean Restored and Reference Tidal Wetlands. Water 9:209–226.

Colwell, R. K., and D. C. Lees. 2000. The mid-domain effect: Geometric constraints on the geography of species richness. Trends in Ecology and Evolution 15:70–76.

Combroux, C. S., G. Bornette, and C. Amoros. 2002. Plant Regenerative Strategies After a Major Disturbance: the Case of a Riverine Wetland Restoration. Wetlands 22:234–246.

Cook, B. J., and F. R. Hauer. 2007. Effects of hydrologic connectivity on water chemistry, soils, and vegetation structure and function in an intermontane depressional wetland landscape. Wetlands 27:719–738.

Craft, C., P. Megonigal, S. Broome, J. Stevenson, R. Freese, J. Cornell, L. Zheng, and J. Sacco. 2003. The pace of ecosystem development of constructed Spartina alterniflora marshes. Ecological Applications 13:1417–1432.

Cushman, S. A., K. McGarigal, and M. C. Neel. 2008. Parsimony in landscape metrics: Strength, universality, and consistency. Ecological Indicators 8:691–703.

Dale, V. H., and S. C. Beyeler. 2001. Challenges in the development and use of ecological indicators. Ecological Indicators 1:3–10.

Deverel, S. J., C. E. Lucero, and S. Bachand. 2015. Evolution of Arability and Land Use, Sacramento-San Joaquin Delta, California. San Francisco Estuary and Watershed Science 13:1–34.

Dronova, I. 2015. Object-Based Image Analysis in Wetland Research: A Review. Remote Sensing 7:6380–6413.

Dronova, I., S. R. Beissinger, J. W. Burnham, and P. Gong. 2016. Landscape-level associations of wintering waterbird diversity and abundance from remotely sensed wetland characteristics of poyang lake. Remote Sensing 8:1–22.

Dronova, I., and S. Taddeo. 2016. Canopy Leaf Area Index in Non-Forested Marshes of the California Delta. Wetlands 36:705–716.

Galatowitsch, S. M. 2006. Restoring prairie pothole wetlands: does the species pool concept offer decision-making guidance for re-vegetation? Applied Vegetation Science 9:261.

Gorelick, N., M. Hancher, M. Dixon, S. Ilyushchenko, D. Thau, and R. Moore. 2017. Google Earth Engine: Planetary-scale geospatial analysis for everyone. Remote Sensing of Environment 202:18–27.

Hiers, J. K., R. J. Mitchell, A. Barnett, J. R. Walters, M. MacK, B. Williams, and R. Sutter. 2012. The dynamic reference concept: Measuring restoration success in a rapidly changing no-analogue future. Ecological Restoration 30:27–36.

Hill, T., E. Kulz, B. Munoz, and J. R. Dorney. 2013. Compensatory stream and wetland mitigation in North Carolina: An evaluation of regulatory success. Environmental Management 51:1077–1091.

Huete, A., K. Didan, T. Miura, E. P. Rodriguez, X. Gao, and L. G. Ferreira. 2002. Overview of the radiometric and biophysical performance of the MODIS vegetation indices. Remote Sensing of Environment 83:195–213.

Jensen, J. R. 2007. Remote Sensing of the Environment: An Earth Resource Perspective. Second Edi. Prentice Hall, Upper Sadle River, NJ.

Johnston, C. A., B. L. Bedford, M. Bourdaghs, T. Brown, C. Frieswyk, M. Tulbure, L. Vaccaro, and J. B. Zedler. 2007. Plant species indicators of physical environment in Great Lakes coastal wetlands. Journal of Great Lakes Research 33:106–124.

Kelly, M., K. a. Tuxen, and D. Stralberg. 2011. Mapping changes to vegetation pattern in a restoring wetland: Finding pattern metrics that are consistent across spatial scale and time. Ecological Indicators 11:263–273.

Kennedy, R. E., Z. Yang, and W. B. Cohen. 2010. Detecting trends in forest disturbance and recovery using yearly Landsat time series: 1. LandTrendr — Temporal segmentation algorithms. Remote Sensing of Environment 114:2897–2910.

Kentula, M. E. 2000. Perspectives on setting success criteria for wetland restoration. Ecological Engineering 15:199–209.

Khanna, S., M. J. Santos, J. D. Boyer, K. D. Shapiro, J. Bellvert, and S. L. Ustin. 2018. Water primrose invasion changes successional pathways in an estuarine ecosystem. Ecosphere 9:e02418.

Kimmerer, W. J., D. D. Murphy, and P. J. Angermeier. 2005. A Landscape-level Model for Ecosystem Restoration in the San Francisco Estuary and its Watershed. San Francisco Estuary & Watershed 3.

Klemas, V. 2013. Remote Sensing of Coastal and Wetland Biomass: An Overview. Journal of Coastal Research 29:1016–1028.

Kondolf, G. M. 1998. Lesson learned from river restoration projects in California. Aquatic conservation: Marine and Freshwater Ecosystems 8:39–52.

Leffondré, K., M. Abrahamowicz, A. Regeasse, G. A. Hawker, E. M. Badley, J. McCusker, and E. Belzile. 2004. Statistical measures were proposed for identifying longitudinal patterns of change in quantitative health indicators. Journal of Clinical Epidemiology 57:1049–1062.

Luoma, S. N., C. N. Dahm, M. Healey, and M. J. N. 2015. Challenges Facing the Sacramento-

San Joaquin Delta: Complex, Chaotic, or Simply Cantankerous? San Francisco Estuary & Watershed 13:1–25.

Matthews, J. W., and A. G. Endress. 2010. Rate of succession in restored wetlands and the role of site context. Applied Vegetation Science 13:346–355.

Matthews, J. W., A. L. Peralta, D. N. Flanagan, P. M. Baldwin, A. Soni, A. D. Kent, and A. G. Endress. 2009a. Relative influence of landscape vs. local factors on plant community assembly in restored wetlands. Ecological Applications 19:2108–2123.

Matthews, J. W., A. L. Peralta, A. Soni, P. Baldwin, A. D. Kent, and A. G. Endress. 2009b. Local and landscape correlates of non-native species invasion in restored wetlands. Ecography 32:1031–1039.

Matthews, J. W., and G. Spyreas. 2010. Convergence and divergence in plant community trajectories as a framework for monitoring wetland restoration progress. Journal of Applied Ecology 47:1128–1136.

Matthews, J. W., G. Spyreas, and A. G. Endress. 2009c. Trajectories of Vegetation-Based Indicators Used to Assess Wetland Restoration Progress. Ecological Applications 19:2093–2107.

McCoy-Sulentic, M. E., T. E. Kolb, D. M. Merritt, E. C. Palmquist, B. E. Ralston, and D. A. Sarr. 2017. Variation in species-level plant functional traits over wetland indicator status categories. Ecology and Evolution 7:3732–3744.

McGarigal, K., S. A. Cushman, and E. Ene. 2012. FRAGSTATS v4: Spatial Pattern Analysis Program for Categorical and Continuous Maps. University of Massachusetts, Ahmerst.

Meire, D. W. S. A., J. M. Kondziolka, and H. M. Nepf. 2014. Interaction between neighboring vegetation patches: Impact on flow and deposition. Water Resources Research 50:3809–3825.

Moffett, K. B., and S. M. Gorelick. 2016. Alternative stable states of tidal marsh vegetation patterns and channel complexity. Ecohydrology 1662:1639–1662.

Moffett, K. B., J. Law, S. M. Gorelick, N. Nur, and J. K. Wood. 2014. Alameda Song Sparrow Abundance Related to Salt Marsh Metrics Quantified from Remote Sensing Imagery. San Francisco Estuary & Watershed 12:1–19.

Moreno-Mateos, D., P. Meli, M. I. Vara-Rodríguez, and J. Aronson. 2015. Ecosystem response to interventions: Lessons from restored and created wetland ecosystems. Journal of Applied Ecology 52:1528–1537.

Moreno-Mateos, D., M. E. Power, F. A. Comín, and R. Yockteng. 2012. Structural and functional loss in restored wetland ecosystems. PLoS Biology 10:e1001247.

Mountrakis, G., J. Im, and C. Ogole. 2011. ISPRS Journal of Photogrammetry and Remote Sensing Support vector machines in remote sensing : A review. ISPRS Journal of

Photogrammetry and Remote Sensing 66:247–259.

Moyle, P. B., A. D. Manfree, and P. L. Fiedler. 2013. The Future of Suisun Marsh : Balancing Policy with Change. San Francisco Estuary & Watershed Science 11.

Paracuellos, M., and J. Tellería. 2004. Factors Affecting the Distribution of a Waterbird Community: The Role of Habitat Configuration and Bird Abundan. Waterbirds 27:446–453.

Pettorelli, N., J. O. Vik, A. Mysterud, J. M. Gaillard, C. J. Tucker, and N. C. Stenseth. 2005. Using the satellite-derived NDVI to assess ecological responses to environmental change. Trends in Ecology and Evolution 20:503–510.

R Core Team. 2017. R: A language and environment for statistical computing. R Foundation for Statistical Computing, Vienna, Austria.

Raab, D., and S. E. Bayley. 2012. A vegetation-based Index of Biotic Integrity to assess marsh reclamation success in the Alberta oil sands, Canada. Ecological Indicators 15:43–51.

Rocha, a. V., D. L. Potts, and M. L. Goulden. 2008. Standing litter as a driver of interannual CO2 exchange variability in a freshwater marsh. Journal of Geophysical Research: Biogeosciences 113:1–10.

Roy, D. P., V. Kovalskyy, H. K. Zhang, E. F. Vermote, L. Yan, S. S. Kumar, and A. Egorov. 2016. Characterization of Landsat-7 to Landsat-8 reflective wavelength and normalized difference vegetation index continuity. Remote Sensing of Environment 185:57–70.

San Francisco Estuary Institute-Aquatic Science Center. 2014. A Delta Transformed: Ecological Functions, Spatial Metrics, and Landscape Change in the Sacramento-San Joaquin Delta.

Schile, L. M., K. B. Byrd, L. Windham-Myers, and M. Kelly. 2013. Accounting for non-photosynthetic vegetation in remote-sensing-based estimates of carbon flux in wetlands. Remote Sensing Letters 4:542–551.

Shuman, C. S., and R. F. Ambrose. 2003. A Comparison of Remote Sensing and Ground-Based Methods for Monitoring Wetland Restoration Success. Restoration Ecology 11:325–333.

Simenstad, C., D. Reed, and M. Ford. 2006. When is restoration not? Incorporating landscape-scape processes to restore self-sustaining ecosystems in coastal wetland restoration. Ecological Engineering 26:27–39.

Soomers, H., D. Karssenberg, M. B. Soons, P. A. Verweij, J. T. A. Verhoeven, and M. J. Wassen. 2013. Wind and Water Dispersal of Wetland Plants Across Fragmented Landscapes. Ecosystems 16:434–451.

Staszak, L. a., and A. R. Armitage. 2013. Evaluating Salt Marsh Restoration Success with an Index of Ecosystem Integrity. Journal of Coastal Research 287:410–418.

Suding, K. N. 2011. Toward an Era of Restoration in Ecology: Successes, Failures, and Opportunities Ahead. Annual Review of Ecology, Evolution, and Systematics 42:465–487.

Ta, J., L. W. J. Anderson, M. A. Christman, S. Khanna, D. Kratville, J. D. Madsen, P. J. Moran, and J. H. Viers. 2017. Invasive aquatic vegetation management in the Sacramento-San Joaquin River Delta: Status and recommendations. San Francisco Estuary and Watershed Science 15.

Taddeo, S., and I. Dronova. 2018. Indicators of vegetation development in restored wetlands. Ecological Indicators 94:454–467.

Turner, M. G. 1989. Landscape ecology: the effect of patern on process. Annual Review of Ecology and Systematics 20:171–197.

Tuxen, K. A., L. M. Schile, M. Kelly, and S. W. Siegel. 2008. Vegetation colonization in a restoring tidal marsh: A remote sensing approach. Restoration Ecology 16:313–323.

Van Meter, K. J., and N. B. Basu. 2015. Signatures of human impact: size distributions and spatial organization of wetlands in the Prairie Pothole landscape. Ecological Applications 25:451–465.

van der Valk, A. G. 2012. The Biology of Freshwater Wetlands. Page Biology of Habitats Series. Second edition. Oxford University Press, Oxford.

Vasey, M. C., V. T. Parker, J. C. Callaway, E. R. Herbert, and L. M. Schile. 2012. Tidal Wetland Vegetation in the San Francisco Bay-Delta Estuary. San Francisco Estuary and Watershed Science 10.

Verbesselt, J., R. Hyndman, A. Zeileis, and D. Culvenor. 2010. Phenological change detection while accounting for abrupt and gradual trends in satellite image time series. Remote Sensing of Environment 114:2970–2980.

Verbesselt, J., A. Zeileis, and M. Herold. 2012. Near real-time disturbance detection using satellite image time series. Remote Sensing of Environment 123:98–108.

Whipple, A., A. Grossinger, D. Rankin, B. Stanford, and R. Askevold. 2012. Sacramento-San Joaquin Delta Historical Ecology Investigation : Exploring Pattern and Process.

Wortley, L., J.-M. Hero, and M. Howes. 2013. Evaluating Ecological Restoration Success: A Review of the Literature. Restoration Ecology 21:537–543.

Wu, J. 1999. Hierarchy and Scaling: Extrapolating Information Along a Scaling Ladder. Canadian Journal of Remote Sensing 25:367–380.

Xiong, S., M. E. Johansson, F. M. R. Hughes, A. Hayes, K. S. Richards, and C. Nilsson. 2003. Interactive effects of soil moisture, vegetation canopy, plant litter and seed addition on plant diversity in a wetland community. Journal of Ecology 91:976–986.

Zedler, J. B. 2000. Progress in wetland restoration ecology. Trends in Ecology & Evolution 15:402–407.

Zedler, J. B., J. C. Callaway, S. Diego, and S. M. Na-. 1999. Tracking Wetland Restoration : Do Mitigation Sites Follow Desired Trajectories ? Restoration Ecology 7:69–73.

7 Figures and Tables

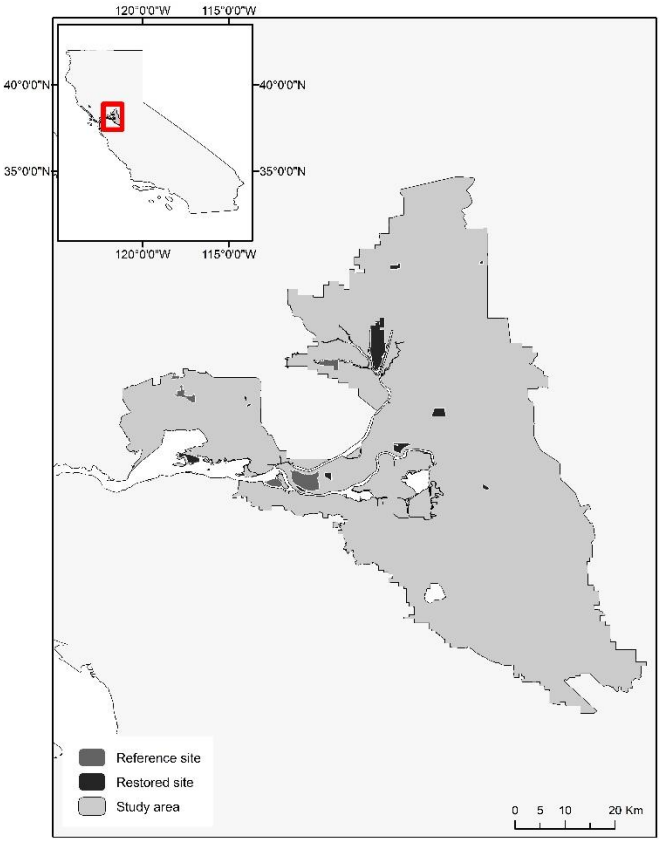

Figure 2. Study area and sites

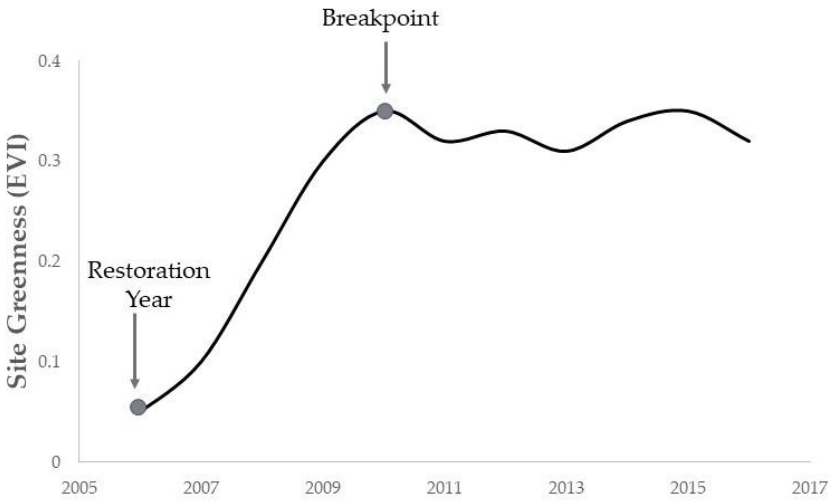

Figure 3. Demonstration of the breakpoint analysis. The breakpoint in this example separates two phases (or segments) with significantly different slope.

Table 1. Landscape metrics used in this study

Category	Landscape Metrics and acronym used in figures	Ecological Importance/Associated Processes
Patch Shape Complexity	Mean Fractal Index (FRAC)	Impacts edge effects
Aggregation	Aggregation Index (AI)	Uniformity of habitat distribution across the landscape, local connectivity of habitat
	Connectivity (CONNECT)	Dispersion of species, nutrients,
Nearest neighbor distance	Mean Euclidean Nearest Neighbor (ENN)	Impact on water flows, habitat connectivity
Patch dispersion	Coefficient of variation in Euclidean distance to nearest neighbor (ENN_CV)	Impact on water flows, metapopulation dynamics of species inhabiting vegetation patches
Large Patch Dominance	Largest Patch Index (LPI)	Habitat provisioning and local contiguity
Patch Density	Patch Density (PD)	The degree of habitat fragmentation
Patch size variability	Coefficient of variation in patch area (AREA_CV)	Non-uniformity in habitat size
Vegetation Coverage	Percent Cover (PLAND)	Contribution to photosynthetic carbon uptake, predictor of animal diversity and abundance

Table 2. Main principal component describing post-restoration phases

Principal component axis	Percentage of variance	Associated variables	Standardized loading
Nonlinearity	42%	Standard deviation of the first differences	0.95
		Maximum of the absolute first differences	0.97
		Mean of the absolute first differences	0.97
Rate of change in EVI (per year and overall)	23%	Mean change per year	0.96
		Change relative to first score	0.95
		Change overall	0.95
Variability	14%	Coefficient of variation	0.88
		Ratio of the maximum absolute difference to the mean-over-time	0.85
Short-term fluctuations	11%	Ratio of the mean absolute second difference to the mean absolute first difference	0.84
		Ratio of the maximum absolute second difference to mean absolute first difference	0.78

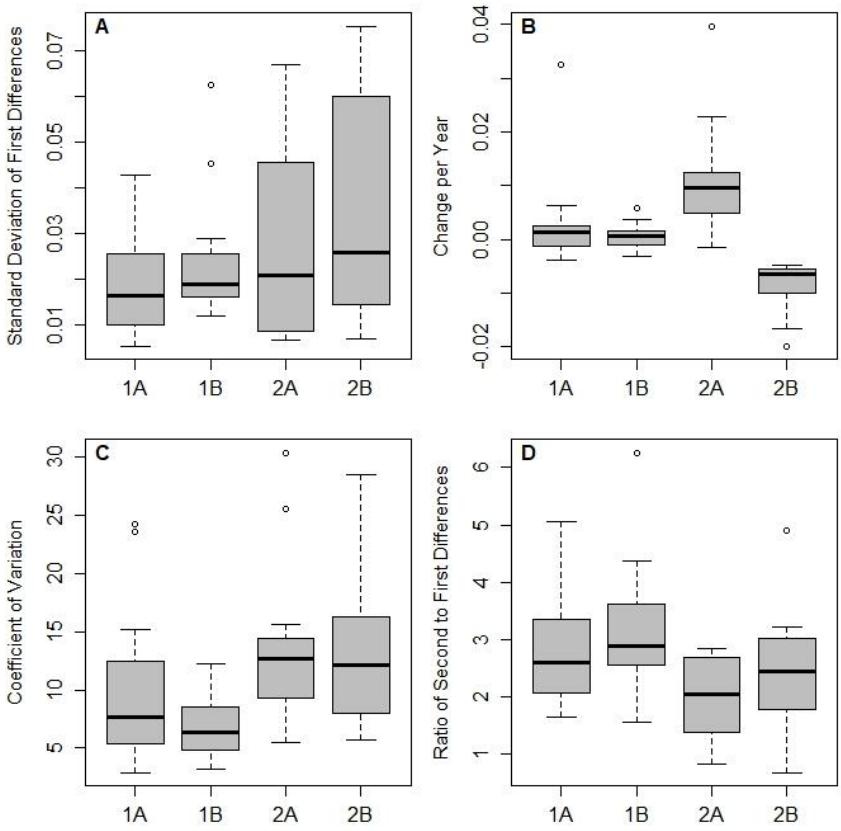

Figure 3. Temporal statistics describing the magnitude and direction of trends in greenness and fluctuations around the trend per cluster-based phase type identified through a hierarchical clustering. Standard deviation of first differences per cluster-based phase type (A), rate of change in EVI per year (B), coefficient of variation in EVI over phase length (C), and ratio of the mean absolute second difference to the mean absolute first difference (D) per cluster-based phase type.

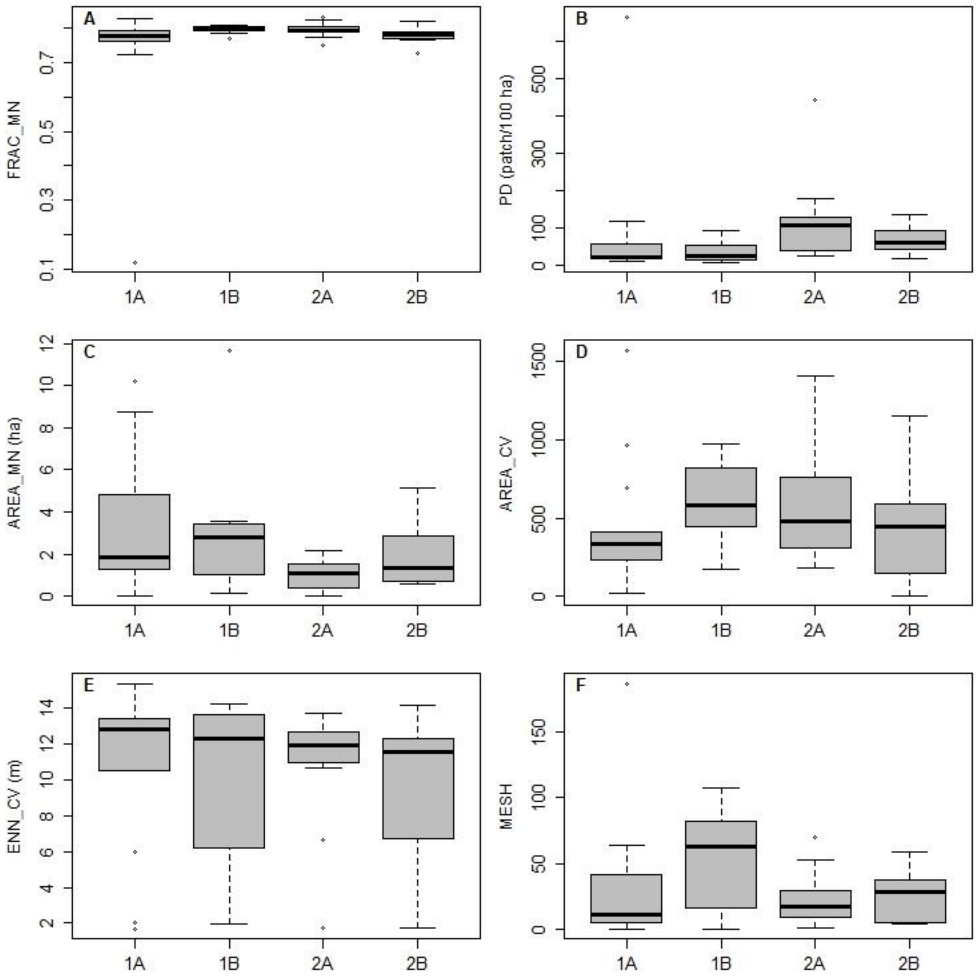

Figure 4. Landscape metrics per phase types (1A – small change, low fluctuations; 1B – small changes, with fluctuations, 2a: rapid positive change, 2B- rapid negative change). (A) mean fractal index, (B) density of vegetated patches (number of patches per 100 hectares), (C) mean area of vegetated patches, (D) coefficient of variation in the area of vegetated patches, (E) coefficient of variation in the distance between a vegetated patch and its nearest neighbor, (F) effective mesh size.

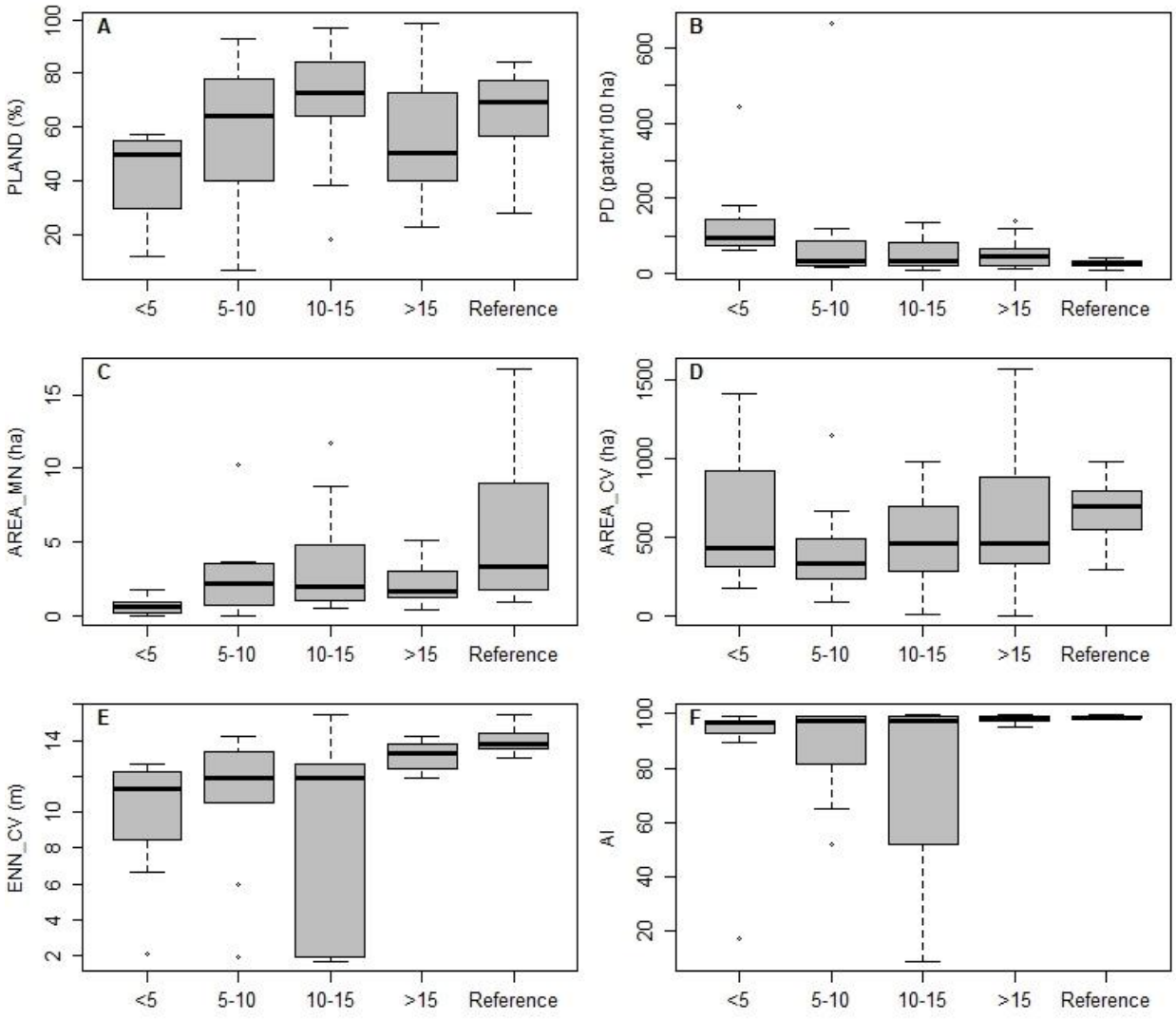

Figure 5. Landscape metrics by age class. (A) percentage of site vegetated, (B) density of vegetated patches (number of patches per 100 hectares), (C) mean area of vegetated patches, (D) coefficient of variation in the area of vegetated patches, (E) coefficient of variation in the distance between neighboring patches, (F) aggregation index.

Supplemental information

Table S1. Main properties of study sites and their landscape context. Proportion of wetlands in the landscape and dominant adjacent land covers were identified within a 500m radius from each site using the National Land Cover Dataset (NLCD).

Region	Type	Site	Restoration Year	Size (acres)	Proportion of Wetland in Landscape (%)	Dominant Adjacent Land Cover
Suisun Marsh	Reference	Rush Ranch	Reference	73	89.7	Wetland
		Peytonia	Reference	62	62.5	Wetland, Urban
		Hill Slough	Reference	275	37.2	Urban, wetland
	Restored	U.S. Maritime Administration Marsh	2006	28	36.8	Urban, wetland
		Fairfield	2009	0.02	0	Forest
		Ryer Island		376	41	Water, wetland
		Buckler	1993	20	35.2	Water, Wetland
		Calhoun Cut	Ref	398	1.1	Grasslands, croplands
		Blacklock	2006	26	79.1	Grassland, wetland
		Wheeler	2006	40	56	Grassland, Wetland
		Chipp	2004	60	41.6	Water, wetland
Central Delta	Reference	Brown	Reference	305	36.8	Water, Urban
		Lower Sherman Island	Reference	1,754	79.1	Croplands, grasslands
	Restored	Mayberry Farms	2010	307	76.3	Croplands, wetland
		Sherman Parcel	2005	6	73.4	Grasslands, Croplands
		West Pond	1997	8	1.2	Croplands
		East Pond	1997	7	1.2	Croplands
		East End	2013	740	3.8	Croplands
		Decker	2002	11	2	Croplands
		River Island		316	1.7	Croplands
		Fern	1999	79	17.2	Grassland, Cropland
		Kimball	2000	109	55.8	Grassland, wetland
North Delta	Reference	Calhoun Cut	2014	159	15	Grassland, cropland
	Restored	Liberty Island	1998	1,706	8	Water, Grassland

	Liberty Conservation	2010	165.7	31	Grassland, cropland
	Skyracker	2005	137	73	Croplands, wetland
	Beach Lake	2008	31	24.6	Grassland, cropland

Chapter 3
Phenological indicators of vegetation recovery in restored wetlands

Abstract

Landscape phenology is increasingly used to measure the impact of major disturbances on vegetation productivity and ecosystem functions. However, few studies have used phenology as a tool to monitor wetland recovery following restoration treatments. As plants show a rapid phenological response to changes in abiotic conditions, studying long-term variation in site phenology could help assess restoration success. To provide a low-cost approach to measuring restoration progress, we used open source remote sensing data from NASA's Landsat archives to characterize long-term phenological trends in restored wetlands of the Sacramento-San Joaquin Delta of California, USA. By tracking phenological changes across a 17-year period, we sought to identify a set of phenological metrics most responsive to time and restoration treatments. We compared phenological metrics derived from Landsat (16-day revisit), Sentinel-2 (5-day revisit), and MODIS (daily revisit) which enabled us to measure the sensitivity of these phenological metrics to data frequency and scale. Younger reference sites showed earlier start, midpoints, peak, and end of growing seasons than older and reference sites. Throughout post-restoration phases, sites continued to experience changes in the shape of their growing seasons, likely in response to variations in vegetation extent, water and bare ground exposure, and litter accumulation. These results demonstrate the potential of phenological analyses to measure restoration progress and detect landscape factors promoting wetland recovery. A thorough understanding of wetland phenology is key to quantifying ecosystem services including carbon sequestration and habitat provisioning.

1 Introduction

1.1 Wetland restoration and monitoring

Wetland restoration is increasingly used to counteract the large-scale degradation of wetland resources (Moreno-Mateos et al. 2012). Wetland restoration can be defined as the assisted recovery of a site towards a pre-determined ecological state or objective which include expanding wildlife habitats, providing ecosystem services critical to human well-being, or increasing regional resilience to global changes (SER 2004). Some ecosystem services targeted by wetland restoration efforts are bolstered by vegetation productivity and its resilience to disturbances. For example, plant accumulate carbon within their green and senescent biomass, promoting the sequestration of atmospheric carbon (Chmura et al. 2003; McLeod et al. 2011). Biomass production and sediment trapping by plant roots accelerate the soil build-up needed to counteract erosion and flooding (Nyman et al. 2006; Callaway et al. 2012). Vegetation recovery provides local wildlife species with resources and shelter (Zedler and Kercher 2005), making plant biomass, height, and structural heterogeneity key predictors of diversity in upper trophic levels (Zedler and Langis 1991; Spautz et al. 2006; Moffett et al. 2014; Quesnelle et al. 2015).

Indicators of plant productivity and composition are widely used for post-restoration site monitoring as they show rapid responses to site condition (Craft et al. 1999; Bernhardt and Koch 2003; Staszak and Armitage 2013) and provide base data to model ecosystem functions and services (Bradbury et al. 2005; Kollmann et al. 2016; Byrd et al. 2018). For instance, plants show a rapid response to environmental stressors, which can be detected through repeated morphological measurements (Raab and Bayley 2012; Mollard et al. 2013) or remote sensing analyses (Díaz-Delgado et al. 2002; Sen et al. 2012) to identify early ecosystem shifts warranting interventions. Current monitoring efforts in restored wetlands frequently leverage plot-level indicators (i.e., indicators measured in the field) of vegetation structure, composition, and diversity to measure compliance to restoration goals and targets (Taddeo and Dronova 2018). However, wetlands are highly heterogeneous and dynamic ecosystems which warrant repeated monitoring for a reliable assessment of restoration progress (Zedler et al. 1999; Matthews et al. 2009). Fluctuating water levels and difficult field access make on-site monitoring challenging and sometimes costly. These challenges, together with limited budgets, can result in short monitoring periods (Hill et al. 2013; Van den Bosch and Matthews 2017) which can lead to a skewed assessment of restoration progress or failure to detect arising ecosystem stressors (Van den Bosch and Matthews 2017).

1.2 Phenology as a restoration indicator

Remote sensing analyses can expand the spatiotemporal scale of monitoring and facilitate the upscaling of field observations into a regional understanding of wetland condition and ecosystem services (Adam et al. 2010; Klemas 2013b). A potential application of long-term, large scale remote sensing datasets includes landscape phenology which has been used to characterize plant response to local and regional changes from time series of satellite images (Liang and Schwartz 2009; Liang et al. 2011). The life cycle of plant communities controls the timing and intensity of several ecosystem processes including litter build-up and carbon cycles (Bellard et al. 2012; Cerdeira Morellato et al. 2016). Plant phenology can also impact the interaction, distribution, and abundance of multiple taxa including birds and small mammals (Butt et al. 2015; Burgess et al. 2018) as it determines the availability of food sources and habitat types required at different stages of a species' life cycle. Monitoring temporal variations in plant productivity and phenology can provide useful information on the presence and magnitude of disturbances such as extreme climatic events including fire, droughts, and hurricanes (e.g., Mo et al. 2015; Verbesselt et al. 2010; Buffington et al. 2018) as plants show a rapid morphological response to stress and environmental changes.

Previous studies have used an array of phenological indicators determined using the growing season trajectories, or curves, of satellite-based site greenness (i.e., spectral indices likely to strongly correlate with presence and coverage of vegetation based on satellite data; Huete et al. 1997, Shanahan et al. 2001, Pettorelli 2013). Short-term and long-term changes in the timing of phenological events (i.e., spring green-up, peak greenness, fall senescence; Fig. 1) or the shape of growing season curves (Fig. 1) can respond to site processes or regional factors. Short-term or long-term climatic changes including fluctuations in temperature, precipitations, or the frequency and magnitude of droughts can delay phenological events (Mo et al. 2015; Buffington et al.

2018). For example, Mo et al. (2015) showed that peak greenness could be delayed by two months in saline wetlands impacted by droughts. Similarly, climatic anomalies can also impact vegetation productivity, resulting in lower peak or mean annual greenness values (Buffington et al. 2018).

Landscape phenology can also respond to changes in species composition impacting biomass production, resource partitioning in time, and the duration of growing seasons. For example, ecosystem disturbances might favor stress-resistant species with a distinct phenological profile (Beaubien and Hall-Beyer 2003; Rigge et al. 2013). The proliferation of an introduced species can impact a site's growing season curve and the time needed for this site to reach peak greenness or senescence (Andrew and Ustin 2008; Bradley 2014). Fluctuations in species diversity might modulate maximum greenness (Taddeo et al. *in revision*) through a greater partitioning of resources which stimulates the vegetation productivity (Tilman et al. 2001; Hooper et al. 2012) captured by spectral vegetation indices (Castillo-Riffart et al. 2017; Madonsela et al. 2017). In addition, fluctuations in the spatial extent of plant coverage and the ratio of green vegetation to open water and bare soil can impact both median and maximum greenness as they modulate soil and water background effects on vegetation indices (Spanglet et al. 1998; Ollinger 2011; Li and Guo 2018).

1.3 Research objectives

The goal of this study was to provide a regional assessment of phenological changes in wetlands to test the potential application of landscape phenology for post-restoration monitoring. Specifically, this study compared the annual growing season curves of restored and reference wetlands to assess how their phenology responds to time, restoration interventions, and climatic fluctuations. Using a sample of restored wetlands from the Sacramento-San Joaquin Delta in California, we first assessed the sensitivity of different phenological indicators to the frequency of satellite images and to gaps in time series of satellite data. We then leveraged these phenological indicators to study the response of 20 wetlands to restoration treatments and climatic fluctuations.

2 Methods

2.1 Study sites and area

Our study focused on restored wetlands of the Sacramento-San Joaquin Delta in California, United States (here after referred to as the Delta; 725,000 acres) and the adjacent Suisun Marsh (116,000 acres). This study area is located at the confluence of the San Joaquin and Sacramento rivers and confined between the cities of Tracy (37.7397° N, 121.4252° W) and Sacramento (38.5816° N, 121.4944° W; Fig. 2). A hundred and fifty years of land conversion in the Delta has triggered the loss of 98% of freshwater marshes and 95% of tidal habitats historically found in the region (Whipple et al. 2012). This massive habitat loss has impacted wetland-dependent wildlife populations and eroded key ecosystem services (SFEI ASC 2014). Ecosystem services central to the region include flood and erosion control as well as carbon sequestration (Callaway et al. 2012; Deverel et al. 2015). Furthermore, the large-scale conversion of historical wetlands

has triggered a land subsidence throughout the region, with portions of the Delta now located 10 to 15 ft below sea level (Faunt and Sneed 2015). This land subsidence puts pressure on the levee system protecting the Delta against saltwater intrusion (Deverel et al. 2015) with important risks for freshwater access in California and the irrigation of 4.5 million acres of cropland.

Wetland restoration has emerged over the last few decades as a solution to environmental challenges in the Delta. Multiple projects implemented since the 1990s aim to promote soil build-up and carbon sequestration while improving wildlife habitats (Kimmerer et al. 2005; Siegel 2014). Over 30 wetland restoration projects have been initiated in the last twenty years (CWMW 2018). We selected among these different restoration projects, 20 restored and five reference sites (Fig. 2; SI Table S1) using the EcoAtlas database of wetland restoration projects in California (CWMW 2018). These sites have been restored between 1993 and 2014 and range in size from 0.01 to 6 km^2. Our study sites are included within four regions (Fig. 2): the Suisun Marsh, which shelters a greater concentration of wetlands, and the North, Central, and South Delta which are mostly covered by croplands.

2.2 Data

2.2.1 Satellite images

We used satellite images from the Landsat 7 ETM+ (2000-2014) and Landsat 8 OLI (2014-2017) surface reflectance products, path 44, and rows 33 and 34 which have a spatial resolution of 30m and a revisit time of 16 days (Fig.3). We identified a total of 321 images for row 33 (272 from Landsat 7 ETM+, 49 from Landsat 8) and 317 images for row 34 (266 from Landsat 7 ETM+, 51 from Landsat 8). We leveraged the quality assessment band of the Landsat Collection 1 Level 1 to mask clouds, cloud shadows, and open water in the cloud-based programming interface Google Earth Engine (Gorelick et al. 2017). We obtained an average of 15 cloud-free pixels per year with a minimum of 13 cloud-free pixel in 2003 and a maximum of 21 cloud-free pixel in 2016. As the Landsat ETM+ and OLI sensors have different band widths for similar regions of the electromagnetic spectrum, we applied conversion equations developed by Roy et al. (2016) to calibrate surface reflectance values in the blue, red, and infrared bands of the Landsat 8 OLI pixels to Landsat ETM+ values.

For each Landsat scene, we computed the enhanced vegetation index (EVI), an index based on red light absorption by plant chlorophyll and infrared light scattering by mesophyll cells. EVI uses correction factors to account for atmospheric scattering and soil background effect (Huete et al. 1997). As a result, EVI values do not saturate as quickly as the normalized difference vegetation index under high leaf area index conditions (Huete et al. 2002) and show a higher correlation to field measurements of leaf area index at low vegetation coverage (Mo et al. 2018).

2.3 Phenological model: fit and sensitivity analysis

2.3.1 Curve-fitting

We used a smoothing spline to fill gaps between Landsat scenes and diminish the effect of atmospheric scattering and temporary clouds on growing season curves (Pettorelli et al. 2005, Verbesselt et al. 2010; Fig. 3). Among the wide variety of fitting curve techniques used in the

literature (Pettorelli et al. 2005), we opted to use a smoothing spline as it offers a flexible approach for modeling the phenology of different growth forms, land cover types, and vegetation extents. We applied a smoothing spline to the entire set of pixels included within a study site to generate site-level growing season curves of greenness (Fig. 4). Splines were fitted using the smoothing.spline function of R 3.4.2 (R Core Team 2017). Data from Landsat 7 and Landsat 8 were fitted independently.

2.3.2 Phenological metrics

To identify the day of the year (DOY) corresponding to the start and end of the growing season, we used the EVI ratio thresholding method developed by White et al. (1997). We also determined for each growing season curve and site the DOY corresponding to the 10^{th}, 25^{th}, 30^{th}, 50^{th}, 75^{th}, and 90^{th} EVI percentile before (here after referred to as "pre") and after (here after referred to as "post") a site reaches its peak greenness value. We calculated the integrated EVI (IEVI) as the sum of all positive EVI values over a growing season and the relative annual range in EVI (here after referred to as "relative EVI") as the annual amplitude in EVI values divided by the IEVI (Pettorelli et al. 2005). Lastly, we identified for each annual growing season curve the mean, maximum, median, minimum EVI values as well as the range, standard deviation, skewness, and kurtosis in the distribution of EVI values.

2.3.3 Sensitivity analysis

As the number of cloud-free Landsat pixels varied by year and site, we tested the impact of gaps in the availability of Landsat data on a subset of nine sites (three sites from the Suisun Marsh, two sites from the North Delta, and four sites from the Central Delta; SI: Table S1). In each of these sites, we tested the sensitivity of phenological metrics to data gaps by incrementally removing two scenes per year, from the maximum to the minimum number of scenes available in the series (i.e., 21, 19, 17, 15, and 13 scenes). We then measured the difference (in number of days) between the timing of phenological indicators based on 21 Landsat scenes per year, and 19, 17, 15, 13 scenes per year. Lastly, we used an ANOVA test to assess whether phenological metrics or sites showed significant differences in their sensitivity to data gaps (i.e., a greater difference in phenological indicators based on 21 Landsat scenes versus 19, 17, 15, or 13).

2.4 Validation using near-surface remote sensing, Sentinel-2, and MODIS data

To validate phenological models derived from Landsat data, we used near-surface remote sensing in three of the study sites and conveyed phenological analyses in a subset of nine sites (the same sites used for gap analysis) using MODIS (daily revisit) and Sentinel-2 (revisit every 5 to 10 days) data. We used in situ digital photography of vegetation in three sites monitored for greenhouse gas fluxes by the Ameriflux Network. Digital cameras in these three sites are oriented West and permanently perched above the canopy. These three sites utilize a Canon Powershot Series A to generate jpeg images at a 30-minute interval for 12 hours a day (Knox et al. 2017). We used all images captured between 9 AM and 5 PM to generate growing season curves for each of the sites. We extracted within each image a region of interest (or "ROI") centered on vegetation and avoiding other non-vegetated types of land covers (i.e., bare soil, water). To reduce calculation time, we smoothed digital information in each ROI within a 3X3 pixel kernel. We used the phenopix package (Filippa et al. 2017) to extract vegetation indices

from the ROI and smooth the resulting phenological curves. For each image, we generated the green chromatic coordinate which has shown a strong correlation to gross primary productivity in two of our field study sites (Knox et al. 2017).

In addition, we compared the timing of phenological events derived from Landsat data with phenological events derived from MODIS and Sentinel-2 time series. As the MODIS dataset has a coarser resolution than Landsat, we compared phenological metrics across sites with varied degree of vegetation cover (Chapter 2) and throughout multiple years in order to assess whether the differences between phenological metrics derived from MODIS and Landsat data were impacted by the prevalence of mixed pixels. We generated phenological curves for every year of data between 2013 and 2017 using daily images from MODIS Terra Surface Reflectance product (MOD09GA; daily revisit, 500m spatial resolution) for nine sites representative of the area (the same sites used to analyze the sensitivity of phenological metrics to data gaps). We masked clouds and cloud shadows from every image using the quality assessment bands of MODIS scenes. We then computed for every image the EVI index based on the blue (459-479nm), red (620-670nm), and near-infrared (841-876nm) bands of the MODIS product. We used the same smoothing spline approach used for the Landsat and Phenocam data to generate annual growing season curves, from which a series of phenological metrics were then derived (Fig.1). We also used scenes from Sentinel-2 MSI: MultiSpectral Instrument which provides spectral information at a 10m resolution for the blue (centered at 496.6nm), red (centered at 664.5nm), and near infrared (centered at 835.1nm) bands every five days. We used all scenes available between January 1, 2016 and December 31, 2017 for images ID 10SEH and 10SFH. Prior to analyzing data, we masked clouds using the quality assessment bands of the Sentinel-2 data. This generated 77 to 86 images per site.

2.5 Statistical analyses

We used a principal component analysis to cluster phenological indicators showing similar patterns of fluctuations in the study area. We used a gap statistic analysis (Tibshirani et al. 2001) conducted using the fviz_nbcluster function of the factoextra package (Kassambara and Mundt 2017) to determine the maximal number of clusters. Accordingly, the HCPC function (Le et al. 2008) was leveraged to cluster the PCA results along the first six axis into eight clusters of phenological metrics (Table 1) using a hierarchical clustering approach based on the Ward's distance between points (Ward 1963).

We used analysis of variance (ANOVA) tests with Tukey Honest Significance post-hoc tests to assess whether phenological metrics were significantly impacted by data gaps (i.e., variation in the number of cloud free Landsat scenes available from one year to another) and data frequency (i.e., difference in timing of phenological events derived from Landsat and sensors with a shorter revisit time – Sentinel-2 and MODIS). We used Kruskall-Wallis tests with Dunn's post hoc tests to assess whether phenological indicators were significantly impacted by droughts. Specifically, we compared phenological indicators among years showing a positive value (i.e., 2000, 2003, 2005, 2006, 2010, 2011, 2017) for the Palmer Drought Severity Index (PDSI) and years showing a negative value (i.e., 2001, 2002, 2004, 2007, 2008, 2009, 2012, 2013, 2014, 2015, 2016). We

leveraged PDSI data for the Fairfield station (38.274, -122.068) extracted from the University of Nebraska's U.S. Drought Risk Atlas.

We utilized the Kruskal-Wallis test with the Dunn's Test with Bonferroni correction for multiple comparison to compare phenological metrics before and after restoration, throughout different time periods (i.e., first 5 years after restoration, 5-10 years, 10-15 years, and more than 15 years after restoration), and between restored and reference sites. Analysis were computed in R using the dunn.test package (Dinno 2017).

3 Results

3.1 Sensitivity of phenological indicators to data gaps and frequency.

3.1.1 Data gaps

An ANOVA test suggested that certain phenological indicators were more impacted by data gaps ($F=14.5470$, $df=6$, $p<0.0001$), but that sites and years did not differ significantly in their sensitivity to gaps in data. Specifically, data gaps impacted the timing of phenological events by an average of 12 days. Peak greenness, the first, and the last 75th percentile were the most impacted, as they showed an average difference of 18 days between iterations conducted using respectively 13, 15, 17, 19, and 21 images per year. The timing of the start and end of growing seasons, as well as the first and last 30th percentile showed an average difference of 4, 7, and 9 days. The timing of the first 50th percentile showed an average difference of 12 days, while the timing of the last 50th percentile showed an average difference of 8 days. Lastly, the number of cloud-free Landsat images did not have a significant impact on the mean, median, maximum, minimum, standard deviation, range, relative EVI or integrative EVI (significance level=0.05).

3.1.2 Data frequency

An ANOVA test with no-replication coupled to a Tukey Honest Significance post-hoc test showed that differences (or time delays) between phenological indicators derived from Landsat data and those derived from phenocams did not significantly differ from one year to another. They did, however, differ among the three sites monitored via phenocams. The site at an intermediate level of recovery (Mayberry Farms; 8 years old) showed a greater difference in phenophases ($p=0.02$), which differed by an average of 25 days. In turn, the older site, West Pond, showed an average difference of 12 days between phenological events based on phenocam data and phenological events based on Landsat data. The more recently restored site, East End, showed an average difference of 13 days between phenophases derived from Landsat and phenocam data.

An ANOVA test suggested that site ($F=14.208$,$df=7$,$p<0.0001$) and phenological indicators ($F=4.254$, $df=17$, $p<0.0001$) both had a significant effect on the difference (in number of days) between MODIS-based and Landsat-based phenological metrics, while this difference did not vary significantly from one year to another ($F=1.303$, $p=0.254$). In particular, the peak of the growing season, first and last 80th and 90th percentiles showed the greatest difference between MODIS and Landsat, as they differed by an average of 20 days. In contrast, the start of the

growing season, first 10th and 30th percentile differed by an average of 10 days. Sites varied significantly in their contrast between MODIS-based and Landsat-based phenological metrics.

Meanwhile, phenological indicators based on Sentinel-2 data did not differ significantly from Landsat-based phenology ($F=0.737$, $p=0.757$), but individual sites showed significant contrasts in the differences between phenological indicators based on Sentinel-2 and Landsat data ($F=9.312$, $p<0.0001$). Phenological metrics based on Sentinel-2 data and those based on Landsat data differed by an average of 10 days.

3.2 Redundancy among phenological indicators

A principal component analysis showed that the first six principal component axes could explain 81.48% of the variance in phenological metrics among all reference and restored sites. The productivity cluster (Table 1) included the minimum, maximum, mean, median and integrative EVI. Mean EVI highly correlated with maximum (Person correlation = 0.89, $p<0.0001$), median EVI values (Person correlation = 0.98, $p<0.0001$), and integrated EVI values (Person correlation = 0.97, $p<0.0001$) and showed a significant but lower correlation to minimum EVI (Person correlation = 0.62, $p<0.0001$). The range cluster included the relative EVI, range, and standard deviation which were all highly positively correlated (Pearson correlation >0.77, $p<0.0001$). The start of growing season cluster included the start of growing season and the DOY associated with the first 10th percentile of EVI values which were both significantly correlated (Pearson correlation = 0.60 $p<0.0001$), but negatively correlated to kurtosis (Pearson correlation = -0.29 $p<0.0001$), median (Pearson correlation = -0.35 $p<0.0001$), and maximum EVI (Pearson correlation = -0.18 $p<0.0001$). The peak of growing season cluster included the first 50th, 75th, and 90th percentiles, the peak of the growing season, last 50th, 75th and 90th percentiles which were all strongly correlated (Pearson correlation > 0.80 $p<0.0001$), but not significantly related to variables of the productivity cluster (sign level=0.05). The length of the growing season cluster included the length of growing season and kurtosis which showed a low, but significant, correlation coefficient (Pearson correlation = 0.18 $p<0.0001$) and both showed low but significant correlation with median EVI (Pearson correlation = 0.30 $p<0.0001$) but no significant relationship to maximum or minimum EVI. The end of growing season, last 10th and 30th percentiles positively correlated with the start of growing season (Pearson correlation = 0.55 $p<0.0001$), negatively correlated with minimum EVI value (Pearson correlation = -0.22, $p<0.0001$), but did not correlate with maximum or median EVI values.

3.3 Which phenological metrics show distinct values before and after restoration

Restored wetlands showed significant differences in their phenological indicators before and after restoration, with the start of the growing season (Kruskall-Wallis $\chi^2=37.551$, $p<0.0001$; Fig. 5A), first 50th percentile (Kruskall-Wallis $\chi^2=23.482$, $p<0.0001$; Fig. 5C), first 75th percentile (Kruskall-Wallis $\chi^2=25.9$, $p<0.0001$), first 90th percentile (Kruskall-Wallis $\chi^2=27.027$, $p<0.0001$), timing of peak biomass (Kruskall-Wallis $\chi^2=34.418$, $p<0.0001$; Fig. 5D), last 90th percentile (Kruskall-Wallis $\chi^2=30.095$, $p<0.0001$), last 50th percentile (Kruskall-Wallis $\chi^2=23.657$, $p<0.0001$), end of growing season (Kruskall-Wallis $\chi^2=25.04$, $p<0.0001$; Fig. 5B) occurring at a later date after restoration than before restoration intervention. Restoration also seems to have a

significant impact on the shape of growing season curves, with wetland sites showing a lower median (Kruskall-Wallis χ^2=4.7292, p=0.0335; Fig. 5E), mean EVI (Kruskall-Wallis χ^2=4.3226, p=0.0396), and integrated EVI (Kruskall-Wallis χ^2=4.5739,p=0.03424; Fig. 5F) after restoration, but no significant impact on their maximum EVI (Kruskall-Wallis χ^2=2.8987, p=0.0976), minimum (Kruskall-Wallis χ^2=0.4134, p=0.5202), standard deviation (Kruskall-Wallis χ^2=0.9063, p=0.3411). or skewness (Kruskall-Wallis χ^2=0.8082, p=0.3687).

3.4 How phenology metrics change with time

Across the global sample, we observed significant differences in the timing of phenological events with site age, but no significant differences in the shape of growing season curves (significance level of 0.05). Sites generally showed an earlier greening in their early stages of restoration (<5) than at later stages or than reference sites (significance level = 0.05). Site age had a significant effect on the end of the growing season as well (Kruskall-Wallis χ^2=16.9477, p=0.0007) with sites at an early stage of development showing an earlier end of growing season than older sites (significance level of 0.05). Consequently, younger sites reached their peak greenness earlier than sites that were 10-15 years old (p=0.0255) or more than 15 years old (p=0.0129). While the differences in the shape of the growing season curves were overall non-significant among the different age classes, older sites (>15 yr) showed more kurtosis in their EVI values than younger sites (p=0.0284).

We also used Kruskall-Wallis tests and linear regressions to assess, at the individual site level, whether sites significantly differed in their phenological metrics at early versus later stages of restoration. Few sites (except Blacklock Tidal, restored in 2006, and River Island, restored in 2009) showed a monotonic trend in their phenological metrics, as evidenced by a Mann-Kendall test with a significance level of 0.05. However, all but two sites showed significant changes in their phenological metrics over time, as indicated by linear regressions using time as an explanatory variable (Table 2). Specifically, we observed four different types of phenological changes in our study area: (A) no phenological change; (B) decrease in greenness; (C) increase in greenness with changes in the timing of phenological events, and (D) increase in greenness with no phenological changes.

The no phenological change category included two older sites — Ryer Island, restored in 2000, and Kimball, restored in 2000.The decrease in greenness category included the three oldest sites in our sample (Point Buckler restored in 1993 as well as West Pond and East Pond two adjacent sites restored in 1997), which all showed significant decreases in their maximum EVI and the relative range of their EVI. Nine sites —Blacklock (2006), Liberty Conservation (2010), Decker (2002), East End (2014), Fern (1999), Medford (2012), River Island (2009), and Sherman (2005), and Wheeler (2006)— showed significant increases in their productivity as well as a delay in the start, peak, and end of their growing season. Lastly, three sites —US Administration Marsh, Mayberry Farms, and French Camp Conservation Bank— showed significant increases in their productivity, but no linear increase in the timing of their phenological events. However, in all three cases, the first five years were significantly distinct from the following years by showing earlier start, peak, and end of their growing season.

3.5 Reference versus restored

Overall, restored sites showed phenological characteristics significantly distinct from reference sites, but these differences were mainly attributable to significant differences between younger sites (<5 yrs) and reference sites. Both the less than 5 years and 5-10 years old classes started their growing season earlier (<5yr — p=0.0050; 5-10 — p=0.0412; Fig. 6A). Sites at an early stage of restoration (<5 yr old), reached the first 50th percentile of their EVI (p=0.0024) and the last 50th percentile faster (p<0.0001), and ended their growing season earlier (p=0.0161; Fig. 6D) than reference sites. Meanwhile, older sites (i.e., sites within the 10-15 and more than 15 years old) did not significantly differ from reference sites.

3.6 Sensitivity to climate

Overall, sites showed significant differences in the timing of phenological events and shape of phenological curves during wetter years and dry years, as determined by the Palmer Drought Severity Index. Both restored and reference sites showed lower maximum greenness during dry years (F=32.088, p<0.0001; Fig.7A), Consequently, the range of EVI values was reduced during dry years (F=32.088, p<0.001; Fig. 7B), but this contrast was only significant during the early stage of restoration (p=0.0355). In terms of timing of phenological events, the start of the growing season occurred later during drought years than wetter years (F=4.854, p=0.0282; Fig. 7C), as well as the timing of the first 50th percentile (F=2.929, p=0.05; Fig. 7D). In addition, all the 19 sites showing a significant linear relationship between phenological metrics and time also showed a significant positive linear relationship between one of the clusters of phenological metrics and annual precipitations (significance level=0.05). An ANOVA test revealed that in 10 of these sites, including annual precipitations as a covariate significantly increased the fit of linear relationships between time since restoration and phenological metrics.

4 Discussion

Our analysis of landscape phenology in 25 wetland sites over a 17-year period reveals a significant phenological response of wetland sites to restoration treatments, although the nature of this response varied with the characteristics of individual sites. Across the study area, wetlands showed distinct phenological characteristics after restoration, which reflects for some of these sites a transition in land cover from previous crop or pasture to current wetland. Restored sites showed after restoration a delay in their growing season with their start, peak, midpoints, and end of growing season occurring later. This change in the timing of phenological events was accompanied by lower maximum, median, and integrated EVI values. Variations in the shape of growing season curves after restoration likely resulted from a change in species composition but also in certain sites from an increase in the prevalence of open water which is likely to decrease the magnitude of spectral vegetation indices (Kearney et al. 2009). Sites continued to experience phenological changes for up to 20 years after restoration. Sites at an early stage of restoration showed earlier start, midpoints, peak, and end of growing season than older wetlands or reference sites. In addition to changes in the timing of key phenological events, most sites also showed significant changes in the shape of their growing seasons, as revealed by their mean, maximum, and integrative EVI.

Our analyses suggest that using a subset of non-redundant phenological metrics responsive to restoration treatments and annual climatic fluctuations might help monitor vegetation dynamics following restoration treatments. The different phenological metrics of the productivity cluster (i.e., mean, median, minimum, maximum EVI, IEVI; Table 1) showed across all sites the most consistent response to time since restoration, likely as they reflect changes in the spatial distribution and productivity of vegetation. In addition, phenological metrics of the productivity cluster showed similar responses to data gaps, suggesting that any of these phenological metrics could be used to track vegetation dynamics. Among phenological metrics of the peak of growing season cluster (Table 1), metrics associated with the midpoints of growing seasons (i.e., first and last 50^{th} percentile) showed a significant response to time since restoration, while appearing to be less sensitive to data gaps. Meanwhile, the peak of the growing season, as well as the DOY associated with the first and last 90^{th} percentiles in EVI, showed the greatest phenological mismatches between Landsat and MODIS, which highlights the impact of both temporal and spatial resolution on the time needed to observe peak greenness in time series of satellite images. Lastly, phenological metrics included in the start and end of growing season clusters showed similar responses to data gaps, lower mismatches between Landsat and MODIS-based phenological metrics, and significant responses to time since restoration, suggesting that phenological metrics of these clusters could all provide valuable information on phenological changes in restored wetlands.

4.1 Trends and factors of phenological changes

While very few sites in our study area showed a monotonic phenological response to time, time since restoration nonetheless seems to have an impact on the timing of key phenological events and the shape of annual growing season curves as suggested by significant linear relationships between time since restoration and phenological metrics in all but two sites. In the global sample, sites at an early stage of restoration (i.e., less than 10 years old) maintained earlier start, peak, midpoints, and end of growing season than sites at a later stage of development (i.e., more than 15 years old) or reference sites. These phenological changes likely reveal the influence of plant growth and succession on site characteristics and satellite-based observations of wetland greenness.

As vegetation develops in these restored sites, plant expansion might impact site characteristics further modulating phenology and the surface reflectance of wetlands. Across our dataset, differences in phenological metrics between age groups were mostly attributed to contrasts between recently restored sites (<10 years) and the oldest sites (>15 years). At the site level, however, most restored wetlands experienced changes in the shape of their growing season curves, as revealed by significant responses of their minimum, maximum, median EVI, and integrative EVI to time since restoration. Changes in the shape of growing season curves likely reflect the incidence of restoration interventions and species succession on patterns of vegetation distribution and productivity. As revealed by previous studies, and further suggested by linear increases in phenological metrics observed here, plant succession in wetlands impacts their surface reflectance and, incidentally, the spectral vegetation indices used to measure vegetation cover (Zhao et al. 2009). At the scale of the Landsat dataset (30m) used in this study, the spectral

signature of vegetation in mixed pixels can be attenuated by the background effect of water or mudflat exposure where vegetation is absent or sparse (Zhao et al. 2009; Bradley 2014). As vegetated patches expand in some of these sites (Chapter 2) reducing the ratio of open water to vegetation, sites accumulate vegetation biomass which can in turn better mask water and soil background effects (Kearney et al. 2009; Mo et al. 2018).

Changes in the timing of the first and last 50^{th} percentile of greenness, the timing of peak biomass, maximum, and mean EVI could also reveal temporal changes in biomass production consistent with previous studies observing an increase in vegetation cover over the first 5-10 years following restoration treatments (Matthews et al. 2009; Berkowitz 2013). This increase in biomass production will likely impact maximum EVI values but also the time needed to reach this maximum EVI, as it requires more biomass production. In some of these sites, however, this initial increase in biomass production might eventually plateau or even decrease as a result of competition, the depletion of legacy nutrients, or shading via litter accumulation impacting biomass production and seedling recruitment (Raab and Bayley 2012; Berkowitz 2013; Anderson et al. 2016), which might explain why three of the oldest sites monitored here observed a decrease in phenological metrics of the productivity cluster. The impact of litter accumulation in one of these sites has been documented in a previous study monitoring gross primary productivity over time (Anderson et al. 2016). While not explored in this study, it is possible that phenological changes in some of these sites are caused by a transition in species dominance, particularly where non-native species with distinct phenological characteristics proliferate (Hestir et al. 2008; Bradley 2014).

Litter accumulation in some of these sites, as documented in previous studies (Schile et al. 2013; Anderson et al. 2016; Dronova and Taddeo 2016), could impact annual values of spectral vegetation indices, but also the timing of phenological events. The impact of litter is most noticeable in early spring and fall as standing litter or tick litter mats are more likely to mask the spectral signal of green emerging vegetation (Li and Guo 2018). This could partially explain why young sites were characterized by an earlier start and peak of the growing season; their green vegetation might simply be observable sooner as they have not yet accumulated a large quantity of litter. The abundance of litter might also delay plant phenology by shading seedlings (Xiong et al. 2003). The accumulation of litter in some of these sites might further impact minimum and maximum EVI values and the integrated EVI. Furthermore, the accumulation of senescent material (or litter) in wetlands can impact the strength of relationships between field observations of plant biomass or coverage and the values of satellite-based spectral indices, particularly when litter is taller or more abundant than green biomass (Schile et al. 2013; Dronova and Taddeo 2016).

Phenological changes in our study area were not perfectly linear. Significant increases in model fit with the inclusion of precipitation data and significant phenological contrasts among years with different PDSI are consistent with previous papers reporting that increased precipitation reduces salinity and promotes plant productivity (Buffington et al. 2018). In turn, prolonged droughts decrease plant productivity and can delay phenological events (Mo et al. 2015; Buffington et al. 2018). Throughout our study area, increased drought intensity, as determined by

the PDSI, was associated with lower maximum, standard deviation, and range of EVI values. Fluctuations in precipitation and drought severity impacted the phenological characteristics of almost all sites, modulating both the shape of their growing season curves and the timing of different phenological events. This impact of climatic characteristics might partially explain why very few sites showed monotonic trends in their phenological metrics, despite many of them showing a sensitivity to time since restoration. This reinforced the observation noted in local studies (Chapple et al. 2017; Chapple and Dronova 2017) and elsewhere (Matthews et al. 2009; Meyer et al. 2010; Brudvig et al. 2017) that post-restoration trajectories are not linear but may rather fluctuate in response to climatic fluctuations or change in management.

4.2 Sensitivity of phenological metrics to data frequency and gaps

In our dataset, the timing of key phenological metrics (e.g., start of growing season, end of growing season, position of peak) differed between Landsat (characterized by a revisit time of 16 days), MODIS (one image every day), and Sentinel-2 (one image every 5 days). These contrasts reveal the effect of temporal resolution on landscape phenology. For example, Villa et al. (2018) showed that decreasing the temporal frequency of satellite data could impact the timing of phenological events by up to seven days. Furthermore, significant differences among sites in the degree of phenological schedule mismatches suggest that the latter are not only attributable to issues of temporal resolution, but also to the spatial resolution of these different datasets and the spatial distribution of vegetation within test sites, consistent with observations made by Villa et al. (2018). As cells are larger in the MODIS dataset, the spectral signal of vegetation is more likely to be attenuated by the spectral influence of water, aquatic floating vegetation, or other land covers (roads, bare soil) which might impact the time needed to observe a significant change in greenness indicating the start of the growing season or its end.

Similarly, our results suggest that the strength of relationships between phenocam and satellite observations may be highly site-specific and impacted by site heterogeneity (i.e., variation in species density and open water) and litter accumulation. The site at an intermediate level of restoration —and characterized by a greater water-to-vegetation ratio— showed a greater discrepancy between phenocam and Landsat, which parallels observations made by Knox et al. (2017). This difference may be triggered by a greater variability in vegetation density and litter accumulation patterns in the site at an intermediate level of restoration. Presence of a dense layer of litter may explain the later start of the growing season observed within phenocams, as the satellite will not detect green vegetation growing under the canopy until it has emerged from the litter layer.

4.3 Phenological outliers

Basing phenological assessments on Landsat satellite images can be challenging due to gaps between acquisition dates and cloud cover. Landsat remains nonetheless very useful in tracking temporal changes in site phenology as one of the few sensors to provide repeated data prior to the 2000s. Furthermore, detecting phenological indicators at the scale of Landsat images (30m) can be particularly challenging in wetlands where some pixels overlap vegetation and open water. We somewhat circumvented this limitation by masking Landsat pixels labeled as “water”

in the quality assessment band, but smaller patches of open water or pixels overlapping vegetation and open water likely remain. Our analyses of outlier sites (i.e., sites in which phenological events occurred outside of the interquartile range of other sites) further reveals challenges in the use of phenological indicators in restored wetlands. In particular, few sites found themselves outside of the interquartile range during the year of their restoration or the first year following restoration treatments. This likely highlights challenges in accurately detecting growing season curves of fluctuations in greenness when sites are poorly vegetated. When sites are poorly vegetated, the background effect of water and bare soil likely decrease the value of vegetation indices including EVI, making it difficult to identify significant seasonal changes in site greenness. An additional issue with newly restored sites is that some transitioned from grasslands or crops into wetlands. During their restoration year(s), some of these sites maintained two or more different land covers (e.g., crops, wetlands) likely with different phenological schedules. In the year of restoration or the following one, it is possible that the signal of this other ecosystem type is stronger, explaining why some outlier site/year experienced earlier start, peak, and end of growing season. Despite these challenges, even sites with outlier phenological responses showed significant patterns of change in greenness, reflecting plant growth and succession.

5 Conclusion

Our analyses of 20 restored wetlands of the Sacramento-San Joaquin Delta in California showed a significant phenological response of sites to restoration interventions and interannual variation in climatic conditions. This phenological response might be best described by a set of non-redundant phenological indicators showing less sensitivity to data availability or the temporal resolution of datasets. Our analyses of outlier sites revealed challenges in the phenological-based analysis of newly restored sites with a very low vegetation cover, as many outlier sites where found during the year of their restoration when they were either flooded or mainly covered by bare soil. To further the use of phenological analyses in future studies, more near-surface phenological analyses or high-resolution and high-frequency analyses are needed to identify intrinsic site variables impacting site-wide growing season curves and facilitate their interpretation at broader scales.

6 Reference

Adam, E., O. Mutanga, and D. Rugege. 2010. Multispectral and hyperspectral remote sensing for identification and mapping of wetland vegetation: A review. Wetlands Ecology and Management 18:281–296.

Anderson, F. E., B. Bergamaschi, C. Sturtevant, S. Knox, L. Hastings, L. Windham-myers, M. Detto, E. L. Hestir, J. Drexler, R. L. Miller, J. H. Matthes, J. Verfaillie, D. Baldocchi, R. L. Snyder, and R. Fujii. 2016. Variation of energy and carbon fluxes from a temperate freshwater wetland and implications for carbon market verification protocols. Journal of Geophysical Research: Biogeoscience 121:1–19.

Andrew, M. E., and S. L. Ustin. 2008. The role of environmental context in mapping invasive plants with hyperspectral image data. Remote Sensing of Environment 112:4301–4317.

Beaubien, E. G., and M. Hall-Beyer. 2003. Plant phenology in western Canada: Trends and links to the view fromspace. Environmental monitoring and assessment 88:419–429.

Bellard, C., C. Bertelsmeier, P. Leadley, W. Thuiller, and F. Courchamp. 2012. Impacts of climate change on the future of biodiversity. Ecology Letters 15:365–377.

Berkowitz, J. F. 2013. Development of restoration trajectory metrics in reforested bottomland hardwood forests applying a rapid assessment approach. Ecological Indicators 34:600–606.

Bernhardt, K., and M. Koch. 2003. Restoration of a salt marsh system : temporal change of plant species diversity and composition. Basic and Applied Ecology 4:441–451.

Van den Bosch, K., and J. W. Matthews. 2017. An Assessment of Long-Term Compliance with Performance Standards in Compensatory Mitigation Wetlands. Environmental Management 59:546–556.

Bradbury, R. B., R. a Hill, D. C. Aason, S. a Hinsley, J. D. Wilson, H. Balzter, G. Q. a Anderson, M. J. Whittingham, I. J. Davenport, and P. E. Bellamy. 2005. Modelling relationships between birds and vegetation structure using airborne LiDAR data: a review with case studies from agricultural and woodland environments. International Journal of Avian Science 147:443–452.

Bradley, B. A. 2014. Remote detection of invasive plants: A review of spectral, textural and phenological approaches. Biological Invasions 16:1411–1425.

Brudvig, L. A., R. S. Barak, J. T. Bauer, T. T. Caughlin, D. C. Laughlin, L. Larios, J. W. Matthews, K. L. Stuble, N. E. Turley, and C. R. Zirbel. 2017. Interpreting variation to advance predictive restoration science. Journal of Applied Ecology:1018–1027.

Buffington, K. J., B. D. Dugger, and K. M. Thorne. 2018. Climate-related variation in plant peak biomass and growth phenology across Pacific Northwest tidal marshes. Estuarine, Coastal and Shelf Science 202:212–221.

Burgess, M. D., K. W. Smith, K. L. Evans, D. Leech, J. W. Pearce-Higgins, C. J. Branston, K. Briggs, J. R. Clark, C. R. Du Feu, K. Lewthwaite, R. G. Nager, B. C. Sheldon, J. A. Smith, R. C. Whytock, S. G. Willis, and A. B. Phillimore. 2018. Tritrophic phenological match-mismatch in space and time. Nature Ecology and Evolution 2:970–975.

Butt, N., L. Seabrook, M. Maron, B. S. Law, T. P. Dawson, J. Syktus, and C. A. Mcalpine. 2015. Cascading effects of climate extremes on vertebrate fauna through changes to low-latitude tree flowering and fruiting phenology. Global Change Biology 21:3267–3277.

Byrd, K. B., L. Ballanti, N. Thomas, D. Nguyen, J. R. Holmquist, M. Simard, and L. Windham-Myers. 2018. A remote sensing-based model of tidal marsh aboveground carbon stocks for the conterminous United States. ISPRS Journal of Photogrammetry and Remote Sensing 139:255–271.

Callaway, J. C., E. L. Borgnis, R. E. Turner, and C. S. Milan. 2012. Carbon Sequestration and Sediment Accretion in San Francisco Bay Tidal Wetlands. Estuaries and Coasts 35:1163–1181.

Castillo-Riffart, I., M. Galleguillos, J. Lopatin, and J. F. Perez-Quezada. 2017. Predicting vascular plant diversity in anthropogenic peatlands: Comparison of modeling methods with free satellite data. Remote Sensing 9:681.

Cerdeira Morellato, L. P., B. Alberton, S. T. Alvarado, B. Borges, E. Buisson, M. G. G. Camargo, L. F. Cancian, D. W. Carstensen, D. F. E. Escobar, P. T. P. Leite, I. Mendoza, N. M. W. B. Rocha, N. C. Soares, T. S. Freire Silva, V. G. Staggemeier, A. S. Streher, B. C. Vargas, and C. A. Peres. 2016. Linking plant phenology to conservation biology. Biological conservation 195:60–72.

Chapple, D., and I. Dronova. 2017. Vegetation Development in a Tidal Marsh Restoration Project during a Historic Drought: A Remote Sensing Approach. Frontiers in Marine Science 4.

Chapple, D. E., P. Faber, K. N. Suding, and A. M. Merenlender. 2017. Climate Variability Structures Plant Community Dynamics in Mediterranean Restored and Reference Tidal Wetlands. Water 9:209–226.

Chmura, G. L., S. C. Anisfeld, D. R. Cahoon, and J. C. Lynch. 2003. Global carbon sequestration in tidal, saline wetland soils. Global Biogeochemical Cycles 17:12.

Craft, C., J. Reader, J. N. Sacco, and S. W. Broome. 1999. Twenty-Five Years of Ecosystem Development of Constructed Spartina alterniflora (Loisel) Marshes. Ecological Applications 9:1405–1419.

Deverel, S. J., C. E. Lucero, and S. Bachand. 2015. Evolution of Arability and Land Use, Sacramento-San Joaquin Delta, California. San Francisco Estuary and Watershed Science 13:1–34.

Díaz-Delgado, R., F. Lloret, X. Pons, and J. Terradas. 2002. Satellite Evidence of Decreasing Resilience in Mediterranean Plant Communities After Recurrent Wildfires. Ecology 83:2293–2303.

Dinno, A. 2017. dunn.test: Dunn's Test of Multiple Comparisons Using Rank Sums.

Dronova, I., and S. Taddeo. 2016. Canopy Leaf Area Index in Non-Forested Marshes of the California Delta. Wetlands 36:705–716.

Faunt, C. C., and M. Sneed. 2015. Water Availability and Subsidence in California's Central Valley. San Francisco Estuary & Watershed 13:1–8.

Filippa, G., E. Cremonese, M. Migliavacca, M. Galvagno, M. Folker, A. D. Richardson, and E. Tomelleri. 2017. phenopix: Process Digital Images of a Vegetation Cover.

Gorelick, N., M. Hancher, M. Dixon, S. Ilyushchenko, D. Thau, and R. Moore. 2017. Google

Earth Engine: Planetary-scale geospatial analysis for everyone. Remote Sensing of Environment 202:18–27.

Hestir, E. L., S. Khanna, M. E. Andrew, M. J. Santos, J. H. Viers, J. A. Greenberg, S. S. Rajapakse, and S. L. Ustin. 2008. Identification of invasive vegetation using hyperspectral remote sensing in the California Delta ecosystem. Remote Sensing of Environment 112:4034–4047.

Hill, T., E. Kulz, B. Munoz, and J. R. Dorney. 2013. Compensatory stream and wetland mitigation in North Carolina: An evaluation of regulatory success. Environmental Management 51:1077–1091.

Hooper, D. U., E. C. Adair, B. J. Cardinale, J. E. K. Byrnes, B. A. Hungate, K. L. Matulich, A. Gonzalez, J. E. Duffy, L. Gamfeldt, and M. I. Connor. 2012. A global synthesis reveals biodiversity loss as a major driver of ecosystem change. Nature 486:105–108.

Huete, A., K. Didan, T. Miura, E. P. Rodriguez, X. Gao, and L. G. Ferreira. 2002. Overview of the radiometric and biophysical performance of the MODIS vegetation indices. Remote Sensing of Environment 83:195–213.

Huete, A. R., H. Q. Liu, K. Batchily, and W. VanLeeuwen. 1997. A comparison of vegetation indices global set of TM images for EOS-MODIS. Remote Sensing of Environment 59:440–451.

Kassambara, A., and F. Mundt. 2017. factoextra: Extract and Visualize the Results of Multivariate Data Analyses.

Kearney, M. S., D. Stutzer, K. Turpie, and J. C. Stevenson. 2009. The effect of Tidal Inundation on the Reflectance Characteristics of Coastal Marsh Vegetation. Journal of Coastal Research 25:1177–1186.

Kimmerer, W. J., D. D. Murphy, and P. J. Angermeier. 2005. A Landscape-level Model for Ecosystem Restoration in the San Francisco Estuary and its Watershed. San Francisco Estuary & Watershed 3.

Klemas, V. 2013. Using Remote Sensing to Select and Monitor Wetland Restoration Sites: An Overview. Journal of Coastal Research 289:958–970.

Knox, S. H., I. Dronova, C. Sturtevant, P. Y. Oikawa, J. H. Matthes, J. Verfaillie, and D. Baldocchi. 2017. Using digital camera and Landsat imagery with eddy covariance data to model gross primary production in restored wetlands. Agricultural and Forest Meteorology 237–238:233–245.

Kollmann, J., S. T. Meyer, R. Bateman, T. Conradi, M. M. Gossner, M. de Souza Mendonça, G. W. Fernandes, J.-M. Hermann, C. Koch, S. C. Müller, Y. Oki, G. E. Overbeck, G. B. Paterno, M. F. Rosenfield, T. S. P. Toma, and W. W. Weisser. 2016. Integrating ecosystem functions into restoration ecology-recent advances and future directions. Restoration Ecology:1–9.

Le, S., J. Josse, and F. Husson. 2008. FactoMineR: A package for Multivariate Analysis. Journal of Statistical Software 25:1–18.

Li, Z., and X. Guo. 2018. Non-photosynthetic vegetation biomass estimation in semiarid Canadian mixed grasslands using ground hyperspectral data, Landsat 8 OLI, and Sentinel-2 images. International Journal of Remote Sensing 39:6893–6913.

Liang, L., and M. D. Schwartz. 2009. Landscape phenology: An integrative approach to seasonal vegetation dynamics. Landscape Ecology 24:465–472.

Liang, L., M. D. Schwartz, and S. Fei. 2011. Validating satellite phenology through intensive ground observation and landscape scaling in a mixed seasonal forest. Remote Sensing of Environment 115:143–157.

Madonsela, S., M. A. Cho, A. Ramoelo, and O. Mutanga. 2017. Remote sensing of species diversity using Landsat 8 spectral variables. ISPRS Journal of Photogrammetry and Remote Sensing 133:116–127.

Matthews, J. W., G. Spyreas, and A. G. Endress. 2009. Trajectories of Vegetation-Based Indicators Used to Assess Wetland Restoration Progress. Ecological Applications 19:2093–2107.

McLeod, E., G. L. Chmura, S. Bouillon, R. Salm, M. Bj??rk, C. M. Duarte, C. E. Lovelock, W. H. Schlesinger, and B. R. Silliman. 2011. A blueprint for blue carbon: Toward an improved understanding of the role of vegetated coastal habitats in sequestering CO2. Frontiers in Ecology and the Environment 9:552–560.

Meyer, C. K., M. R. Whiles, and S. G. Baer. 2010. Plant Community Recovery following Restoration in Temporally Variable Riparian Wetlands. Restoration Ecology 18:52–64.

Mo, Y., M. S. Kearney, J. C. A. Riter, F. Zhao, and D. R. Tilley. 2018. Assessing biomass of diverse coastal marsh ecosystems using statistical and machine learning models. International Journal of Applied Earth Observation and Geoinformation 68:189–201.

Mo, Y., B. Momen, and M. S. Kearney. 2015. Quantifying moderate resolution remote sensing phenology of Louisiana coastal marshes. Ecological Modelling 312:191–199.

Moffett, K. B., J. Law, S. M. Gorelick, N. Nur, and J. K. Wood. 2014. Alameda Song Sparrow Abundance Related to Salt Marsh Metrics Quantified from Remote Sensing Imagery. San Francisco Estuary & Watershed 12:1–19.

Mollard, F. P. O., a. L. Foote, M. J. Wilson, V. Crisfield, and S. E. Bayley. 2013. Monitoring and Assessment of Wetland Condition Using Plant Morphologic and Physiologic Indicators. Wetlands 33:939–947.

Moreno-Mateos, D., M. E. Power, F. A. Comín, and R. Yockteng. 2012. Structural and functional loss in restored wetland ecosystems. PLoS Biology 10:e1001247.

Nyman, J. A., R. J. Walters, R. D. Delaune, and W. H. Patrick. 2006. Marsh vertical accretion

via vegetative growth. Estuarine, Coastal and Shelf Science 69:370–380.

Ollinger, S. V. 2011. Sources of variability in canopy reflectance and the convergent properties of plants. The New phytologist 189:375–94.

Pettorelli, N. 2013. Vegetation indices. Page The Normalized Difference Vegetation Index. Oxford University Press, Oxford.

Pettorelli, N., J. O. Vik, A. Mysterud, J. M. Gaillard, C. J. Tucker, and N. C. Stenseth. 2005. Using the satellite-derived NDVI to assess ecological responses to environmental change. Trends in Ecology and Evolution 20:503–510.

Quesnelle, P. E., K. E. Lindsay, and F. Leonore. 2015. Relative effects of landscape-scale wetland amount and landscape matrix quality on wetland vertebrates : a meta-analysis. Ecological Applications 25:812–825.

R Core Team. 2017. R: A language and environment for statistical computing. R Foundation for Statistical Computing, Vienna, Austria.

Raab, D., and S. E. Bayley. 2012. A vegetation-based Index of Biotic Integrity to assess marsh reclamation success in the Alberta oil sands, Canada. Ecological Indicators 15:43–51.

Rigge, M., A. Smart, B. Wylie, T. Gilmanov, and P. Johnson. 2013. Linking Phenology and Biomass Productivity in South Dakota Mixed-Grass Prairie. RANGELAND ECOLOGY & MANAGEMENT 66:579–587.

Roy, D. P., V. Kovalskyy, H. K. Zhang, E. F. Vermote, L. Yan, S. S. Kumar, and A. Egorov. 2016. Characterization of Landsat-7 to Landsat-8 reflective wavelength and normalized difference vegetation index continuity. Remote Sensing of Environment 185:57–70.

Schile, L. M., K. B. Byrd, L. Windham-Myers, and M. Kelly. 2013. Accounting for non-photosynthetic vegetation in remote-sensing-based estimates of carbon flux in wetlands. Remote Sensing Letters 4:542–551.

Sen, S., C. E. Zipper, R. H. Wynne, and P. F. Donovan. 2012. Identifying Revegetated Mines as Disturbance/Recovery Trajectories Using an Interannual Landsat Chronosequence. Photogrammetric Engineering and Remote Sensing 78:223–235.

Shanahan, J. F., J. S. Schepers, D. D. Francis, G. E. Varvel, W. W. Wilhelm, J. M. Tringe, M. R. Schlemmer, and D. J. Major. 2001. Use of remote-sensing imagery to estimate corn grain yield. Agronomy Journal 93:583–589.

Siegel, S. W. 2014. Suisun Marsh Today : Agents of Change. Page *in* P. B. Moyle, A. D. Manfree, and P. L. Fiedler, editors. Suisan marsh. Ecological Hisotry and Possibe futures. University of California Press, Berkeley.

Society for Ecological Restoration International Science & Policy Working Group. 2004. The SER International Primer on Ecological Restoration. Page Ecological Restoration. Tucson.

Spanglet, H. J., S. L. Ustin, and E. Rejmankova. 1998. Spectral reflectance characteristics of

California subalpine marsh plant communities. Wetlands 18:307–319.

Spautz, H., N. Nur, D. Stralberg, and Y. Chan. 2006. Multiple-Scale Habitat Relationships of Tidal-Marsh Breeding Birds in the San Francisco Bay Estuary. Studies in Avian Biology:247–269.

Staszak, L. a., and A. R. Armitage. 2013. Evaluating Salt Marsh Restoration Success with an Index of Ecosystem Integrity. Journal of Coastal Research 287:410–418.

Taddeo, S., and I. Dronova. 2018. Indicators of vegetation development in restored wetlands. Ecological Indicators 94:454–467.

Tibshirani, R., G. Walther, and T. Hastie. 2001. Estimating the number of clusters in a data set via the gap statistic. Journal of the Royal Statistical Society: Series B (Statistical Methodology) 63:411–423.

Tilman, D., P. B. Reich, J. Knops, D. Wedin, T. Mielke, and C. Lehman. 2001. Diversity and Productivity in a Long-Term Grassland Experiment. Science 294:843–845.

Verbesselt, J., R. Hyndman, A. Zeileis, and D. Culvenor. 2010. Phenological change detection while accounting for abrupt and gradual trends in satellite image time series. Remote Sensing of Environment 114:2970–2980.

Villa, P., M. Pinardi, R. Bolpagni, J.-M. Gillier, P. Zinke, F. Nedelcuţ, and M. Bresciani. 2018. Assessing macrophyte seasonal dynamics using dense time series of medium resolution satellite data. Remote Sensing of Environment 216:230–244.

Ward, J. H. 1963. Hierarchical Grouping to Optimize an Objective Function. Journal of the American Statistical Association 58:236–244.

Whipple, A., A. Grossinger, D. Rankin, B. Stanford, and R. Askevold. 2012. Sacramento-San Joaquin Delta Historical Ecology Investigation : Exploring Pattern and Process. Prepared for the California Department of Fish and Game and Ecosystem Restoration Program. A Report of SFEI-ASC's Historical Ecology Program, Publication #672, San Francisco Estuary Institute-Aquatic Science Center, Richmond, CA.

White, M. A., P. E. Thornton, and S. W. Running. 1997. A continental phenology model for monitoring vegetation responses to interannual climatic variability. Global Biogeochemical Cycles 11:217–234.

Xiong, S., M. E. Johansson, F. M. R. Hughes, A. Hayes, K. S. Richards, and C. Nilsson. 2003. Interactive effects of soil moisture, vegetation canopy, plant litter and seed addition on plant diversity in a wetland community. Journal of Ecology 91:976–986.

Zedler, J. B., J. C. Callaway, S. Diego, and S. M. Na-. 1999. Tracking Wetland Restoration : Do Mitigation Sites Follow Desired Trajectories ? Restoration Ecology 7:69–73.

Zedler, J. B., and S. Kercher. 2005. WETLAND RESOURCES: Status, Trends, Ecosystem Services, and Restorability. Annual Review of Environment and Resources 30:39–74.

Zedler, J. B., and R. Langis. 1991. Comparisons of Constructed and Natural Salt Marshes of San Diego Bay. Restoration & Management Notes 9:21–25.

Zhao, B., Y. Yan, H. Guo, M. He, Y. Gu, and B. Li. 2009. Monitoring rapid vegetation succession in estuarine wetland using time series MODIS-based indicators: An application in the Yangtze River Delta area. Ecological Indicators 9:346–356.

7 Table and figures

Figure 4. Phenological indicators commonly used in the literature.

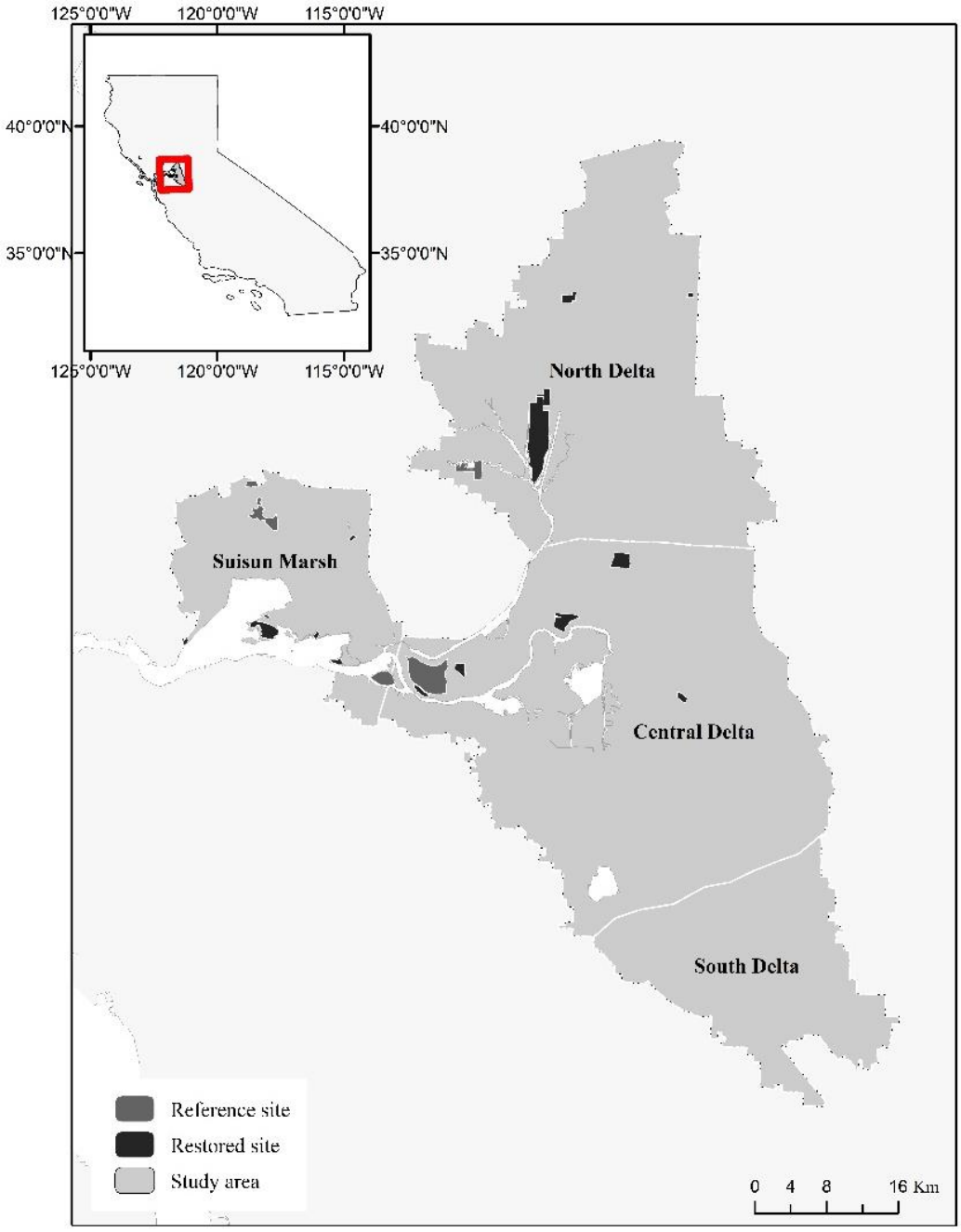

Figure 2. Study area including restored wetlands (in black) and reference sites (in dark grey).

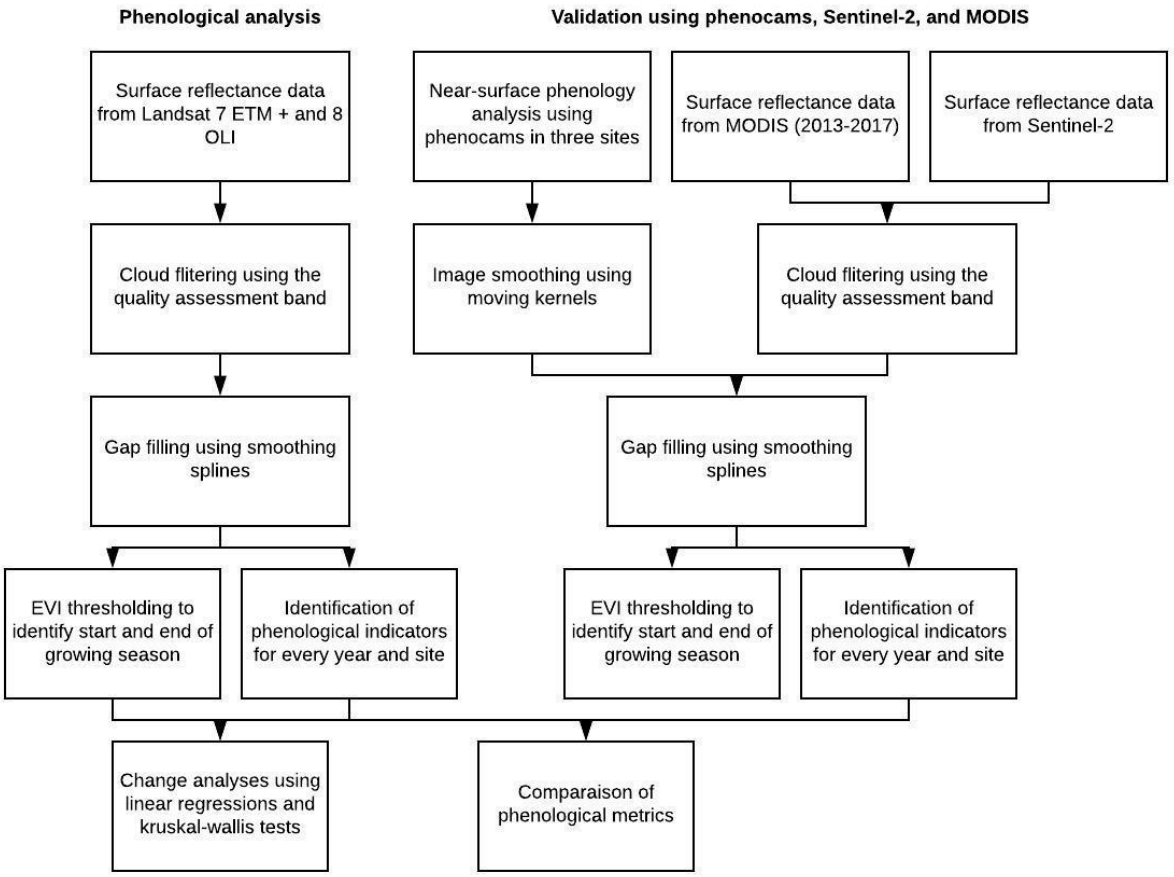

Figure 3. Flowchart of methodological steps for the phenological analyses of restored wetlands and reference sites and validation using phenocams, Sentinel-2, and MODIS images.

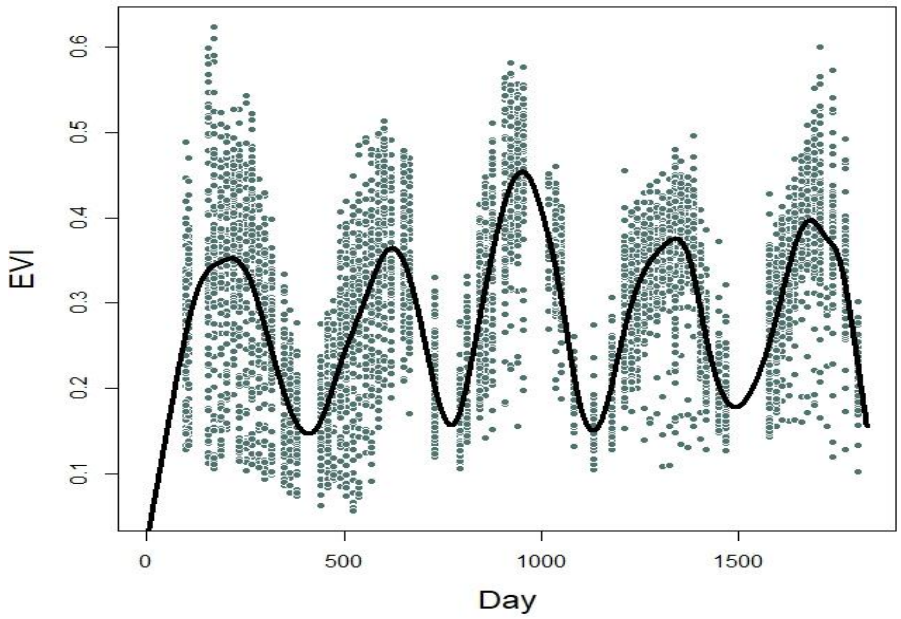

Figure 4. Example of generating a site-average phenological trajectory by applying a smoothing spline to all cloud-free Landsat 8 OLI pixels overlapping a restored wetland site.

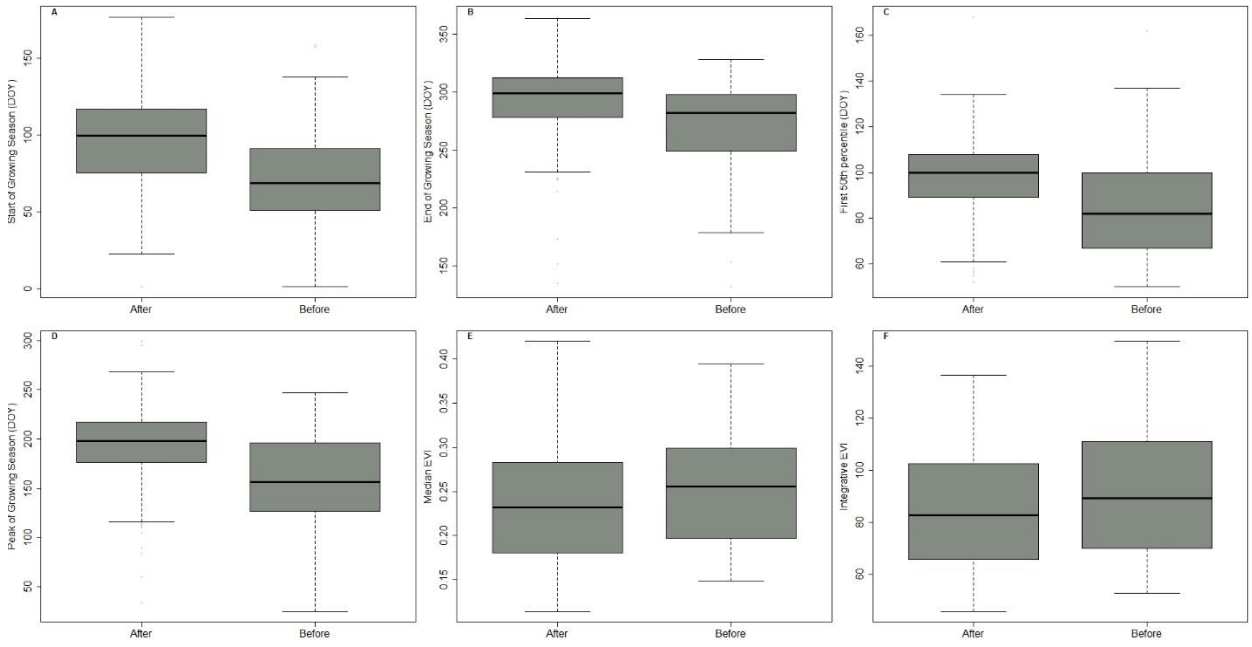

Figure 5. Phenological indicators before and after restoration. (A) Start of the growing season, in day of the year, before and after restoration. (B) End of the growing season, in day of the year, before and after restoration. (C) First 50th percentile of greenness, in day of the year, before and after restoration. (D) Peak of the growing season, in day of the year, before and after restoration. (E) Median EVI before and after restoration. (F) Integrative EVI before and after restoration.

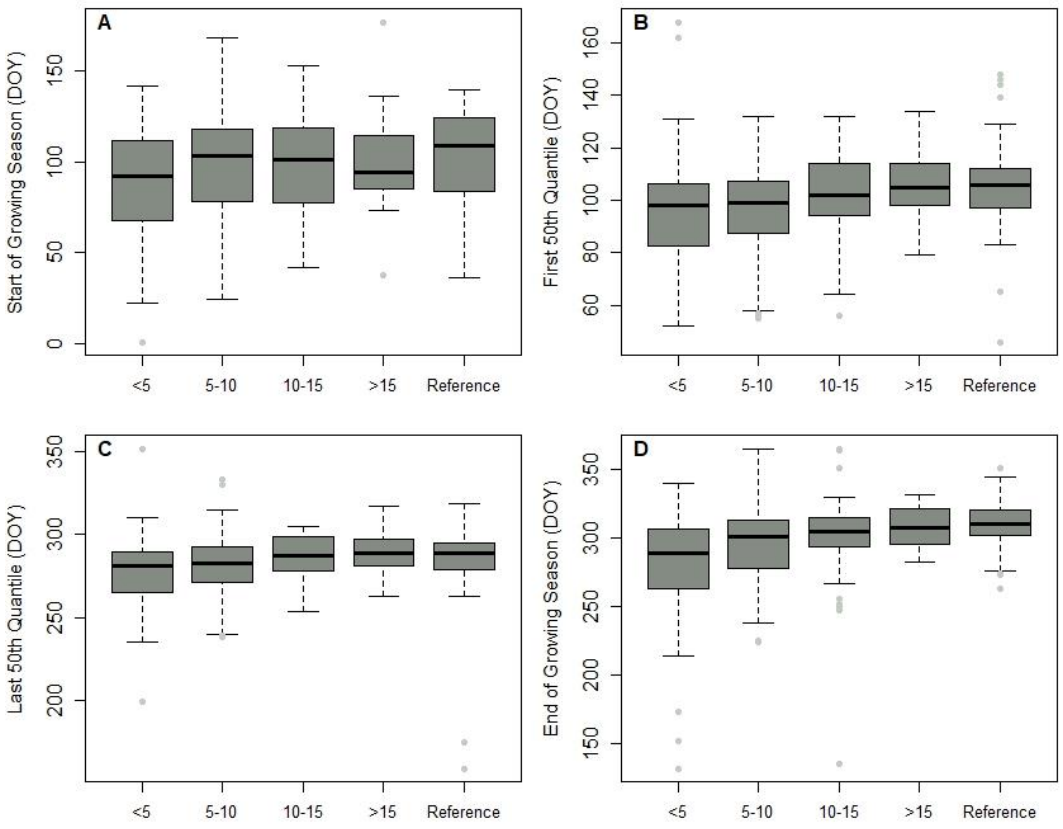

Figure 6. Difference between reference sites and restored sites grouped by age classes (i.e., less than 5 years old, 5-10 years old, 10-15 years old, and more than 15 years old). (A) Difference in the start of the growing season. (B) Difference in the first 50th percentile. (C) Difference in the last 50th percentile. (D) Difference in the end of the growing season.

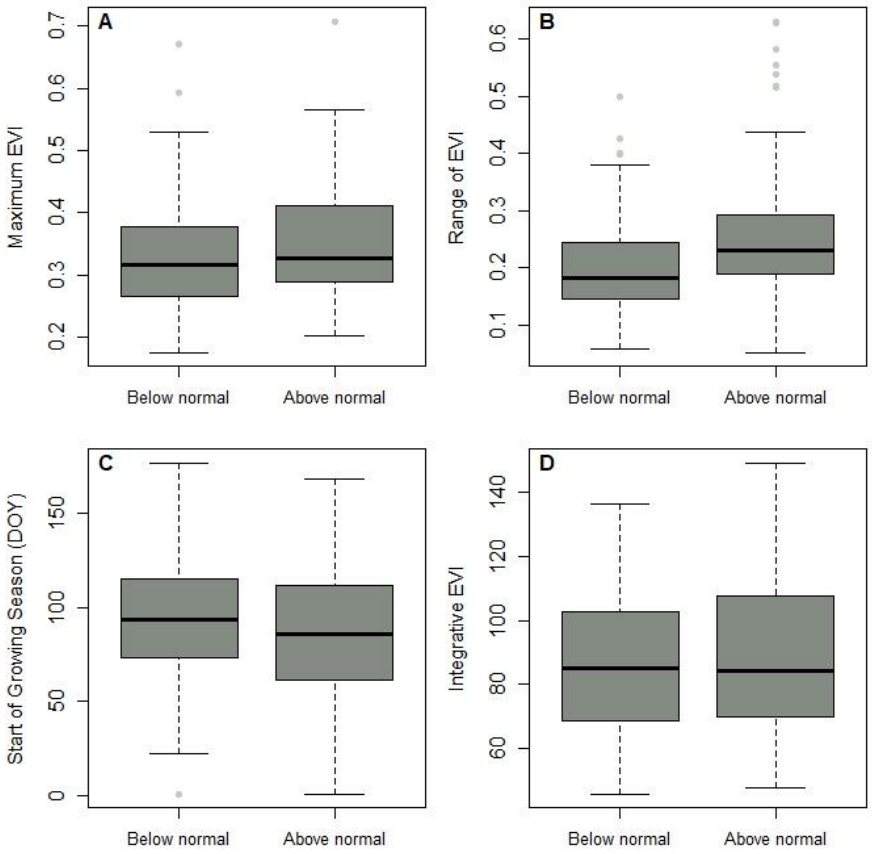

Figure 7. Phenological differences between dry years (i.e., years showing a negative Palmer Drought Severity Index value) and wetter years (i.e., years showing a positive Palmer Drought Severity Index value) across the entire dataset. (A) Difference in annual maximum EVI value between years showing a drought severity below normal or above normal. (B) Difference in annual range of EVI value between years showing a drought severity below normal or above normal. (C) Difference in the start of the growing season (in number of days) between years showing a drought severity below normal or above normal. (D) Difference in integrative EVI value between years showing a drought severity below normal or above normal.

Table 1. Cluster of phenological metrics, as identified by a hierarchical clustering using Ward's method (Ward 1963)

End of Growing Season	**MidPoint**	**Productivity**	**Range of EVI**
End of Growing Season Last 10th percentile Last 30th percentile	First 25th percentile First 30th percentile	Minimum EVI value Maximum EVI Median EVI value Mean EVI value IEVI	Relative EVI Range Standard deviation
Peak of Growing Season	**Start of Growing Season**	**Skewness**	**Length of Growing Season**
First 50th percentile First 90th percentile First 75th percentile First 80th percentile Last 90th percentile Last 80th percentile Last 50th percentile Last 25th percentile Peak of Growing season	Start of Growing Season First 10th percentile	Skewness	Kurtosis Length of growing season

Table 2. Trends in phenological indicators over time by site, as described by linear regressions where time since restoration is used as the explanatory variable. Arrows represent significant linear relationships (signif. level =0.05) between time since restoration and a given phenological metric.

Region	**Sites**	**Restoration Year**	**Productivity**	**Start of Growing Season**	**Peak of Growing Season**	**End of Growing Season**	**Length of Growing Season**	**Standard deviation**
Suisun Marsh	Blacklock	2006	↑	↑	↑	↑		
	Chipp	2004	↑	↓	↓			
	Point Buckler	1993	↓					
	Ryer Island	2000						
	US Administration Marsh	2006	↑	↑				
	Wheeler	2006	↑		↑	↑		
North Delta	Beach Lake	2008						
	Liberty Conservation	2010	↑	↑	↑			
	Liberty Island	1998	↑					
Central Delta	Decker	2002	↑	↑		↑	↑	
	East End	2014	↑	↑	↑	↑		
	East Pond	1997	↓				↓	
	Fern	1999	↑	↑	↑	↑		
	Kimball	2000		↑		↑		
	Mayberry Farms	2010	↑					
	Medford 1	2012	↑	↑	↑		↑	
	River Island	2009	↑		↑			↑
	Sherman	2005	↑	↑	↑	↑		↑
	West Pond	1997	↓			↑	↑	
South Delta	French Camp Conservation Bank	2006	↑			↑		

8 Supplemental information

Table S1. Study sites surveyed in this study. Dominant adjacent land covers and land uses are based on the MODIS land cover product and were identified within a 500m radius around every wetland.

Region	Temperature and precipitation (CalAtlAs)	Dominant adjacent land uses (MODIS)	Sites	Area (acres)	Restoration Year
Suisun Marsh	Min=8.6 ºC, Max = 24.0 ºC, 0.36 mm/day	Crops (15%), Wetlands (23%), Open water (19%), Urban (4%)	Hill Slough	275	Reference
			Peytonia	63	Reference
			Blacklock	26	2006
			Chipp	60	2004
			Point Buckler	20	1993
			Ryer Island	376	2000
			US Administration Marsh	28	2006
			Wheeler	40	2006
North Delta	Min = 8.8 ºC, Max = 24.9 ºC, 0.32 mm/day	Crops (78%), Urban (2%), Open Water (2%)	Calhoun Cut	1,112	Reference
			Beach Lake	31	2008
			Liberty Conservation	166	2010
			Liberty Island	1,706	1998
			Skyracker	137	2005
Central Delta	Min = 10.0 ºC, Max = 24.3 ºC, 0.28 mm/day	Crops (63%), Urban (10%), Water (3%)	Brown	305	Reference
			Lower Sherman Island	1,754	Reference
			Decker	11	2002
			East End	740	2014
			East Pond	7	1997
			Fern	79	1999
			Kimball	109	2000
			Mayberry Farms	307	2010
			Medford 1	60	2012
			River Island	316	2009
			West Pond	8	1997
South Delta	Min = 9.4ºC, Max = 24.6 ºC, 0.27 mm/day	Crops (88%), Urban (11%)	French Camp Conservation Bank	40	2006

Chapter 4

Spectral vegetation indices of wetland greenness and their response to vegetation structure, composition, and spatial distribution

Abstract

Land conversion and fragmentation threaten the resilience and biodiversity of wetland ecosystems which further hinders their provision of ecosystem services. Remote sensing datasets can provide frequent and consistent data to support wetland conservation efforts and facilitate monitoring from regional to national scales. However, wetlands present unique characteristics limiting the efficacy of remote-sensing based metrics developed for terrestrial ecosystems. Challenging characteristics of wetlands include land cover heterogeneity, soil and water exposure in less vegetated pixels, and dead biomass accumulation. To identify the factors impacting satellite-based measurements of wetland greenness, we tested how six spectral vegetation indices responded to the land surface characteristics and regional climatic and edaphic context of 1,138 wetlands sites surveyed by the U.S EPA's National Wetland Condition Assessment. Spectral vegetation indices (SVI) were estimated using all cloud-free surface reflectance data captured in 2011 by Landsat 5 TM and 7 ETM+. We tested two aggregation metrics —maximum and median greenness— for each vegetation index to facilitate the analysis of such a large dataset of satellite images. Using univariate and multivariate ordinary least square regression models, we assessed how the annual maximum and median value of each SVI responded to indicators of vegetation structure and composition, the presence of dead biomass, open water, bare soil, and climatic/edaphic variables. Results show that, in the global sample, NDVI and GNDVI are most responsive to field-based metrics of vegetation structure and composition. However, the responses of vegetation indices differed significantly among wetland types, suggesting that their use should be tailored to the specific characteristics of the wetland being monitored. Aggregation metrics showed different sensitivity to multivariate models, with median greenness being more sensitive to structure and composition, but also to confounding site variables including litter, open water, and bare soil. This study represents a first-time effort to study relationships between the on-site properties of wetlands and their spectral characteristics at a national scale.

1 Introduction

Long understudied (Dixon et al. 2016; Kingsford et al. 2016), wetland ecosystems provide critical ecological and human benefits (Chmura et al. 2003; Zedler 2003; Callaway et al. 2012; Pedersen et al. 2019); yet they have only recently gained consistent public awareness due to their dramatic loss and degradation (Bedford 1999; Davidson 2014). The extensive worldwide loss and fragmentation of wetlands threatens key ecosystem services including flood control, carbon sequestration, and water filtration (Nicholls et al. 1999; Chmura et al. 2003). These ecosystem services will become essential with climate changes exacerbating the vulnerability of coastal human populations to sea level rise and flooding (Nicholls et al. 1999) which, in turn, will

increase the need for carbon sequestration. The long-term, detailed, and consistent monitoring of wetlands is pivotal to the targeted conservation of their biological resources but is made difficult by challenging field conditions and a lack of accessibility to isolated sites (Adam et al. 2010; Klemas 2013). Wetlands warrant frequent monitoring due to their substantial spatiotemporal variability in plant composition and abundance (Zedler et al. 1999; Wilcox et al. 2002) resulting in sizeable logistical costs.

Readily available remote sensing datasets could increase the frequency and scope of current wetland monitoring efforts (Adam et al. 2010; Klemas 2013) to help prioritize conservation interventions and measure ecosystem functions at a large scale. However, wetland ecosystems present unique challenges limiting the efficacy of remote sensing tools and techniques developed for terrestrial ecosystems (Gallant 2015). Steep gradients in salinity, topography, and water level result in a high heterogeneity of plant cover and composition (Adam et al. 2010; Mishra and Ghosh 2015). The spectral properties of vegetation in pixels with a patchy plant distribution can be obscured by the absorption of visible light by open water or bare soil (Dronova 2015; Gallant 2015), which can negatively impact the value of spectral indices typically used to quantify wetland vegetation. Attenuation factors specific to aquatic ecosystems can further obscure the spectral signal of vegetation (Spanglet et al. 1998; Kearney et al. 2009; Schile et al. 2013). For example, litter accumulation (i.e., dead plant biomass) in sites with a lack of tidal flushing or with an abundant reed cover can attenuate the spectral signal of green vegetation, reducing the strength of linear relationships between ground biomass and spectral indices (Turner et al. 1999; Rocha et al. 2008; Schile et al. 2013; Dronova and Taddeo 2016). Similarly, fluctuations in water level impact the reflectance of vegetated surfaces in the red and infrared portions of the electromagnetic spectrum, particularly in pixels with a lower vegetation cover, low leaf area index, or erected leaves (Spanglet et al. 1998; Kearney et al. 2009; Byrd et al. 2014). Furthermore, the relationship between spectral indicators of vegetation (such as vegetation indices quantified from spectral reflectance in relevant electromagnetic regions) and field biomass varies with growth forms and canopy structure as they impact light scattering and absorption, exposure to non-vegetated background (Spanglet et al. 1998; Ollinger 2011), or the abundance of non-photosynthetically active plant material (Asner 1998).

In addition to these factors, wetlands often exhibit a substantial heterogeneity in growth forms and canopy structure, particularly where a coarse pixel overlaps low and high marshes, or where tall emergent species are found next to floating or submerged vegetation (Spanglet et al. 1998). Differences among wetland types may pose additional challenges. For example, estuarine wetlands tend to be more sparsely vegetated than inland wetlands due to their increased salinity resulting in difficult growing conditions. In these less vegetated sites, absorption of solar radiation by bare soil can reduce the value of vegetation indices (Spanglet et al. 1998). Dominant woody species in forested swamps might mask the spectral signal of the understory, impacting the strength of relations between plot-level diversity (Taddeo et al. *in revision*), coverage (Turner et al. 1999), and spectral vegetation indices. As such, it is critical to understand how relationships between spectral data and field-based indicators of plant coverage and biomass vary with the characteristics of dominant species, their spatial distribution, and density (Mishra and Ghosh 2015).

Spectral vegetation indices (here after SVIs), capturing differences in vegetation reflectance throughout the electromagnetic spectrum, are commonly used to map dominant vegetation types and estimate plant coverage and biomass (Huete et al. 1997; Gould 2000; Nagler et al. 2004) as they have shown significant relationships to indicators of plant vigor and productivity including leaf area index, biomass, and the fraction of absorbed photosynthetically active radiation (Myneni and Williams 1994; Gamon et al. 1995a; Nagler et al. 2004). Vegetation reflectance is influenced by both leaf-scale properties, such as chlorophyll and water content, and plant- and canopy-level structure, including leaf angle and density, the proportion of woody parts (Myneni and Williams 1994; Turner et al. 1999; Ollinger 2011). Plant chlorophyll, a green pigment responsible for photosynthesis, absorbs a strong proportion of light in the red portion of the electromagnetic spectrum (Sims and Gamon 2002; Blackburn 2006). Two plant pigments, carotene and xanthophyll, strongly absorb light in the blue portion of the electromagnetic spectrum which is noticeable during leaf senescence when plants lose chlorophyll (Jensen 2007). The green band has shown sensitivity to chlorophyll content across a greater range of chlorophyll a concentration than the red band (Gitelson et al. 1996; Gitelson and Merzlyak 1998). This band also shows sensitivity to plant stressors including pests, herbicides, and salinity (Carter 1993). The near-infrared light (NIR) is reflected by mesophyll cells but strongly absorbed by water, providing in heterogeneous wetlands a sharp contrast between green vegetation and water (Phinn et al. 1999; Lang et al. 2015). Lastly, the shortwave infrared portion of the electromagnetic spectrum (SWIR) is sensitive to soil and vegetation moisture, helping distinguish wet vegetation from senescent plant parts (Asner 1998; Jensen 2007). The shortwave infrared also shows a greater sensitivity to variations in woody species than NIR or visible bands (Asner 1998).

To better utilize the potential of wetland greenness to indicate associated ecosystem functions, it is critical to study how SVIs are impacted by the unique properties of wetlands and whether they perform consistently across wetland types, climates, and dominant growth forms (Huete et al. 1997; Turner et al. 1999). The normalized difference vegetation index (Rouse et al. 1973; NDVI; Table 1) is one of the most commonly used spectral vegetation indices. It determines the proportion of red light absorbed by plant chlorophyll to NIR light scattered by mesophyll cells (Tuker et al. 1979; Huete et al. 1985). Previous studies showed that NDVI saturates at medium to high leaf area index while at low leaf area index it is negatively impacted by soil brightness (Huete et al. 1997; Todd and Hoffer 1998; Pettorelli et al. 2005). The Enhanced Vegetation Index (EVI; Table 1) addresses these shortcomings by applying a soil adjustment factor and an atmospheric correction to the red and blue bands to minimize the incidence of atmospheric scattering and background noise (Huete et al. 2002). Similarly, the Soil-Adjusted Vegetation Index (SAVI; Table 1) incorporates a soil adjustment factor (Huete 1988) which proved useful in mapping low coverage vegetation in wetlands (Poulin et al. 2010). The green chromatic coordinate (GCC; Table 1) has been repeatedly used in studies leveraging near-surface remote sensing to characterize vegetation phenology (Sonnentag et al. 2012a; Keenan et al. 2014; Browning et al. 2017) or upscale ground-level phenocam data into site estimates of vegetation productivity (Knox et al. 2015; Browning et al. 2017). It also offers the advantage of using bands solely from the visible portion of the electromagnetic spectrum. Near-surface GCC showed strong relationships to eddy covariance-based gross primary productivity in previous studies (Browning et al. 2017; Knox et al. 2017). However, GCC computed from satellite data can be

highly sensitive to atmospheric scattering (Brown et al. 2017). The Green Normalized Difference Vegetation Index (GNDVI; Table 1), based on the normalized difference between the green and NIR bands, has been predominantly used to estimate crop productivity as it shows significant correlations to leaf chlorophyll, crop yield, and biomass in a variety of cultures (Shanahan et al. 2001; Eldaw Elwadie et al. 2005). The Land Surface Water Index (LSWI; Table 1), based on the SWIR and NIR portions of the electromagnetic spectrum (Tucker 1979), is sensitive to canopy water content (Toomey and Vierling 2005) and has consequently been successfully used to map rice paddies (Dong et al. 2016).

The central objective of this study was to identify the field characteristics (e.g., vegetation cover, composition, litter accumulation, proportion of open water) impacting wetland greenness as measured from broadband multispectral satellite images. At the resolution of Landsat pixels (30m), the spectral signature of vegetation in mixed pixels likely gets obscured by the background effects of water and soil. Despite this challenge, Landsat remains frequently used in regional and global wetland studies (e.g., Baker et al. 2007; Adam et al. 2010; Dronova et al. 2011) for its unparalleled spatiotemporal extent and temporal frequency compared to coarser (e.g., Moderate Resolution Imaging Spectroradiometer; MODIS), less frequent (e.g., National Agriculture Imagery Program; NAIP) or more costly (e.g., WorldView instruments) archival datasets. While certain vegetation properties might best be monitored at a finer spatial resolution, Landsat data present the undoubtable advantage of being globally and openly accessible at a scale relevant to policy-makers and landscape planners. Developing a better understanding of how land surface properties impact vegetation indices at the resolution of Landsat pixels would help produce more accurate estimation of vegetation extent and productivity and their related ecosystem functions.

To address this need, we tested across a sample of 1,138 wetland sites in the conterminous United States the response of six vegetation indices to the surface properties of wetlands. We considered three indices based on the normalized difference between the NIR band and the red, green, and SWIR bands, respectively (i.e., NDVI, GNDVI, LSWI; Table 1). We examined two vegetation indices that include a soil adjustment factor (i.e., EVI, SAVI; Table 1). Lastly, we included one index (i.e., GCC; Table 1) based solely on the visible portion of the electromagnetic spectrum. To reduce this national-wide dataset of Landsat images (>3,500 images) to a more computationally manageable dataset, we tested two aggregation metrics for these six SVIs (i.e., annual maximum and median greenness).

2 Methods

2.1 Study sites and area

We used field data from the U.S Environmental Protection Agency's National Wetland Condition Assessment (NWCA) to assess the relationships between vegetation properties (e.g., coverage, height, composition), non-photosynthetically active plant material (e.g., litter height and density), confounding site variables (e.g., proportion of open water, bare soil, and exposed gravel), climatic conditions, edaphic variables (Table 2) and SVIs (Table 1). The NWCA surveyed plant composition and abundance in 1,138 wetland sites of the conterminous United

States (Fig. 1; US EPA 2016a). It provides information on additional land covers including open water, exposed soil and gravel, as well as climatic, edaphic, and topographic data (Table 2). This wetland sample is stratified by state and wetland type to represent the broader population of wetlands in the conterminous United States (US EPA 2016b). Each state counts a minimum of eight sites sampled during the spring and summer of 2011 within five $100m^2$ plots included in a 0.5-hectare assessment area (US EPA 2016a). Sites are clustered by wetland types, classified on the basis of their hydrological characteristics and dominant growth form as follows (Figure 1): estuarine herbaceous (EH; n=272) and inland herbaceous (PRLH, n=358) dominated by emergent herbaceous species; estuarine woody (EW, n=73) dominated by small trees and shrubs (<6m tall), and inland woody forested and scrub-shrub wetlands (PRLW, n=435). Finally, sites are clustered in three groups along a disturbance gradient (i.e., least, intermediate, most) based on anthropogenic infrastructures, hydrologic disturbances, heavy metals, and alien species (US EPA 2016b). In this study, unless otherwise mentioned, we used the mean site value of land cover characteristics averaged across all five sampling plots.

2.2 Spectral data and vegetation indices

We used satellite images from the Landsat sensors 5 TM and 7 ETM+ (30m resolution and 16 days revisit) to estimate SVIs (Table 1). Both sensors have the same bandwidths and have been successfully combined in previous studies (e.g., Fernandes et al. 2003). We leveraged the surface reflectance products of these sensors which in previous studies showed a stronger correlation between field-based leaf area index and SVIs than top of atmosphere data (e.g., Turner et al. 1999). SVIs were calculated in the cloud-based programming interface Google Earth Engine (Gorelick et al. 2017) for all Landsat scenes overlapping the NWCA sites (Taddeo et al., *in revision*) between January 1 and December 31, 2011 and across 299 tiles (>3,500 scenes). We excluded pixels covered by clouds or cloud shadows using the quality assessment band of both Landsat 5 TM and 7 ETM + surface reflectance products. We obtained an average of 24 cloud-free images per pixel and year with a standard deviation of 12 images. We generated SVIs for the nine Landsat pixels included in a 3by3 window roughly corresponding to the 40m circular radius assessment area of each NWCA site. We then computed for each site (1) the spatial average of the annual maximum for each SVI (i.e., maximum SVI value averaged across all nine Landsat pixels overlapping a site; hereafter termed SVI year-maximum), and (2) the spatial average of the annual median value for each SVI (i.e., median SVI value averaged across all nine Landsat pixels overlapping a site, hereafter termed SVI year-median) (Taddeo et al., *in revision*).

2.3 Statistical analyses

All statistical analyses were conducted in R 3.4.2 (R Core Team 2017). We used the Shapiro-Wilk test to assess whether SVI year-maximums and year-medians were normally distributed across the global sample. We performed a series of ordinary least square linear regressions to assess the capacity of different explanatory variables (Table 2) to predict variations in SVI year-maximums and year-medians across the global sample and within specific wetland types. We used the Shapiro-Wilk test to measure the normality of residuals and applied log transformations to response variables when the residuals where not normally distributed. We tested the capacity of multivariate models including indicators of vegetation structure, composition, confounding

site variables, and landscape factors (Table 2) to predict variations in SVI year-maximums and year-medians. To construct these multivariate models, we began by measuring the correlation between each pair of variables using the Pearson's product moment correlation test of the cor.test function. We solely included in multivariate models the variables showing a coefficient of correlation inferior to 0.7. We identified four multivariate models: vegetation structure, vegetation composition, confounding site variables, and landscape factors. The vegetation structure multivariate model includes the following variables: total coverage by native species, total coverage by non-native species, mean plant height, number of canopy layers, maximum canopy height, coverage by forbs, coverage by shrubs, and coverage by trees. The composition multivariate model includes Shannon-Wiener diversity index, total species evenness, richness of graminoids, richness of forbs, richness of herbaceous species, richness of shrubs, and richness of trees. The confounding site variable multivariate model incorporates coverage by algae, coverage by submerged aquatic vegetation, coverage by floating aquatic vegetation, litter depth, litter coverage, open water coverage, bare group coverage, and exposed soil coverage. The landscape variable model includes mean elevation, maximum elevation, mean annual precipitation, coefficient of variation in total monthly precipitation, mean maximum precipitation, mean minimum precipitation, mean annual maximum air temperature, and standard deviation in mean annual air temperature. Lastly, we used analysis of variance (ANOVA) tests to assess whether certain models differed significantly in their capacity to predict variation in SVIs.

3 Results

3.1 Distribution by wetland types and correlation among SVIs

According to a Shapiro-Wilk normality test, none of the SVI year-maximum values were normally distributed (sign. level=0.05; SI Fig. S1A-F), but the low skewness value of EVI year-maximum (-0.22) suggested that its distribution was the closest to normality. NDVI, EVI, GNDVI, and LSWI year-maximum were all skewed towards larger values, with NDVI year-maximum (-1.04) and GNDVI year-maximum (-1.03) showing the most important skewness. Meanwhile, GCC year-maximum was positively skewed, indicating that a greater frequency of sites was included within the left tail of its distribution. NDVI, SAVI, EVI, and GNDVI all had low kurtosis values, while LSWI year-maximum (1.52) and GCC year maximum (105.37) both showed a greater kurtosis. While all SVI year-medians also failed the Shapiro-Wilk normality test, the low absolute skewness values (<|0.5|) of NDVI, LSWI, EVI, SAVI, and GCC year-medians suggested that their distributions were close to normality, while GNDVI year-median was moderately skewed (-0.651; SI Fig. S1 G-L). All SVI year-medians had an absolute kurtosis inferior to 1. All SVIs were significantly correlated (SI Table S1) but the year-median values of SVIs generally showed greater correlations than did their year-maximums. NDVI, GNDVI, SAVI and EVI were correlated particularly strongly, while both LSWI and GCC show lower correlations to other SVIs (SI Table S1).

ANOVA tests with Tukey Honest Significant Posthoc tests revealed significant contrasts among wetland types in their NDVI ($F_{3,1134}$=218.6, p<0.0001; Fig. 2A), GNDVI ($F_{3,1134}$=227.8, p<0.0001; Fig. 2B), LSWI ($F_{3,1134}$=47.01, p<0.0001; Fig. 2C), EVI ($F_{3,1134}$=251, p<0.0001; Fig.

2D), SAVI ($F_{3,1134}$=286.1, p<0.0001; Fig. 2E), and GCC ($F_{3,1134}$=57.52, p<0.0001; Fig. 2F) year-maximums, with inland woody wetlands showing greater SVI year-maximums, followed by inland herbaceous, estuarine woody, and estuarine herbaceous (sign.level=0.05) for all SVIs year-maximum except LWSI, which did not show significant differences between inland herbaceous sites and estuarine woody wetlands. Similarly, wetland types showed significant contrasts in their NDVI ($F_{3,1134}$=255.6, p<0.0001; Fig. 2G), GNDVI ($F_{3,1134}$=206.1, p<0.0001; Fig. 2H), LSWI ($F_{3,1134}$=94.72, p<0.0001; Fig. 2I), EVI ($F_{3,1134}$=245.1, p<0.0001; Fig. 2J), SAVI ($F_{3,1134}$=190.1, p<0.0001; Fig. 2K), and GCC ($F_{3,1134}$=165.4, p<0.0001; Fig. 2L) year-medians, with inland woody wetlands showing the greatest SVI year-median and estuarine herbaceous the lowest SVIs (sign.level=0.05), while the difference between inland herbaceous sites and estuarine woody wetlands was not significant.

3.2 General models

3.2.1 Univariate models of vegetation structure

The different indicators of canopy structure we considered (SI Table S2) differed in their capacity to explain variations in SVI year-maximums and year-medians. They had, overall, a greater capacity to explain variations in SVI year-medians than year-maximums (SI Table S2). Structural indicators had a better capacity to explain variation in NDVI year-maximum and year-median than any other SVIs (SI Table S2). The number of layers in the canopy and maximum canopy height showed the strongest explanatory power of all structural variables (SI Table S2) explaining 12 to 35% of variation in SVI year-maximums and 24 to 44% of variation in SVI year-medians, but both variables are categorical which partially explains the strength of their linear relationships to SVIs. Total species coverage could explain 4 to 19 % of variance in SVI year-maximums and 13 to 25% of variance in SVI year-medians (Fig. 3). NDVI, GNDVI, and LSWI all appear to show a saturation in the relationship between their year-maximum and total vegetation coverage (Fig.3 A-C), with index values no longer sensitive to changes in coverage beyond ~200% (in this dataset, vegetation coverage is measured as the sum of percent vegetation coverage in individual canopy layers, explaining why some sites exceed 100% coverage).

Graminoid and herb covers both negatively affected SVIs, explaining 10-26% of variation in their year-maximums and 19-29% of variation in their year-medians (SI Table S2). This might be due to a negative correlation between graminoid and tree cover (Pearson correlation coefficient=-0.5394, p<0.0001, df=1136) and herb and tree cover (Pearson correlation coefficient=-0.7274, p<0.0001, df=1136). Tree cover had a positive effect on SVIs, explaining 9-22% of variation in their year-maximums and 19-31% of variation in their year-medians. Similarly, shrub cover had a small but positive effect on SVIs, explaining 1-2% of variation in their year-maximums and 4-8% of variation in their year-medians. Vegetation cover among the >5 to 15m and 15 to 30 m classes consistently showed a greater explanatory power than other height classes, explaining 1 to 17% variation in year-maximums and 12 to 23% variation in year-medians (SI Table S2).

3.2.2 Univariate models of species composition

Total species diversity, evenness, and median species richness showed greater adjusted R^2 in their linear relationship to SVI year-medians than SVI year-maximums (SI Table S3). Meanwhile, the standard deviation in species richness across the five sampling plots of NWCA sites had a greater incidence on SVI year-maximums, explaining 3-16% of their variation, than their year-medians (3-12% of variation). The richness of forbs, graminoids, and herbs had a greater effect on SVI year-maximum, while the richness of taller growth forms (i.e., shrubs, trees) had a greater effect on SVI year-median (SI Table S3). Indicators of species composition had, overall, a greater capacity to explain variation in GNDVI and SAVI year-maximums and year-medians than other SVIs. Total species diversity showed the greatest explanatory power of all composition indices (Fig. 4). Evenness could explain 1-9% of the variation in year-maximums and 3-10% of variation in SVI year-medians. Lastly, of all growth forms, tree richness had the greatest explanatory power, explaining 9 to 33% of variation in year-maximums and 23 to 33% in year-medians.

3.2.3 Univariate models of confounding site variables

Overall, confounding site variables had a greater impact on the year-medians of SVIs than on their year-maximums (SI Table S4). Mean litter coverage could explain a significant proportion of variation in all SVI year-maximums (1 to 9%; SI Table S4) except LSWI. It had a significant impact on all SVIs year-medians, explaining 1 to 11% of their variation (SI Table 4). The proportion of bare ground explained a significant proportion of variation in all SVI year-maximums (0.3 to 6%) and year-medians (3 to 6%; SI Table S4). The proportion of open water significantly affected all SVIs year maximums except GCC year-maximum and all SVI year-medians except LSWI (SI Table S4). The coverage of submerged and floating vegetation did not significantly impact SVI year-maximums, except for LSWI year-maximum. However, it explained 0.2 to 1% of variation in NDVI, GNDVI, EVI, and SAVI year-medians. Algae coverage had a significant incidence on all SVIs year-maximums and year-medians except for LSWI, explaining up to 1% of their variation.

3.2.4 Univariate models of landscape variables

Across all climatic, edaphic, and topographic variables, the coefficient of variation in monthly precipitation, mean annual maximum air temperature, mean annual maximum air temperature, and mean site pH had the highest adjusted r-square for their linear relationship to SVIs (SI Table S5). The coefficient of variation in monthly precipitation and mean annual maximum air temperature had a greater incidence on SVI year-maximum than their year-median (SI Table S5).

3.2.5 Multivariate models

Overall, multivariate models of species composition and structure explained the greatest proportion of variation in SVI year-medians and year-maximums (Fig. 5; SI Table S6). Multivariate models of canopy structure had a greater explanatory power in the NDVI, LSWI, EVI, and GCC models, while indicators of species composition had a greater incidence on variation in the EVI and GNDVI models. (Fig. 5; SI Table S6). Multivariate models of vegetation structure and composition explained a greater proportion of variation in SVI year-medians than their year-maximums. The confounding site variable model explained 12 to 14 %

of variation in NDVI, GNDVI, EVI, and SAVI year-maximums, but a much smaller proportion of variation (1-2%) in GCC and LSWI year-maximums. The landscape models explained 13 to 24% of variation in SVI year-maximums and 11 to 20% of variation in SVIs year-medians.

3.3 Differences between different wetland types

In wetlands dominated by herbaceous species (i.e., estuarine and inland herbaceous wetlands), multivariate models of canopy structure, species composition, and confounding site variables explained a greater proportion of GNDVI year-maximums than any other SVIs (Fig. 6A and B, SI Table 7). Multivariate models of vegetation structure and landscape factors explained a greater proportion of variation in NDVI year-median within herbaceous-dominated wetlands than any other SVIs, while multivariate models of vegetation composition and confounding site variables were stronger with GNDVI year-medians as response. In estuarine woody wetlands, vegetation structure was a better predictor of LSWI and GCC year-maximums than any other SVIs (Fig. 6A), while the multimeric model of vegetation composition was a better predictor of GNDVI year-maximums than any other indices. Meanwhile, vegetation composition and structure had a greater capacity to explain variation in the LSWI year-median of estuarine woody wetlands than any other SVIs (Fig. 6B). In inland woody wetlands, multivariate models of vegetation structure explained a greater proportion of variation in NDVI year-maximum than any other SVIs while variations in SAVI year-maximums were best predicted by multivariate model of species composition. Overall, multivariate models of vegetation structure, composition, and confounding site variables explained a greater proportion of variation in NDVI year-median than any other SVI year-medians (Fig. 6B). Structure and landscape multivariate models had the greatest explanatory power on SVI year-maximum and year-median in inland woody wetlands, while abiotic multivariate models explained a small to non-significant portion of variation in SVI year-maximums (<3%) and year-medians (4-8%) (Figure 6A and B, SI Table S7).

3.4 Difference between high and low coverage

A partition of sites that showed lower total vegetation coverage than the sample average (<117%) and higher than average coverage (>117%) revealed significant differences in the predictive capacity of multimeric models at low versus high coverage, although responses were not consistent between the year-maximum of SVIs and their year-medians. Multivariate model of structure and confounding site variables (Table 3) had a greater explanatory power on SVI year-median at low total coverage than high coverage, while at high coverage, multivariate models of vegetation structure and composition had a greater incidence on SVI year-median than other multivariate models (Table 3).

4 Discussion

The substantial loss and degradation of wetlands has negatively impacted their ecosystem functions and contribution to global biological diversity (Gibbs 2011; Kingsford et al. 2016). Remote sensing datasets can provide frequent and consistent data to support conservation efforts at both national and continental scales. To ensure the accurate characterization of wetland properties, it is crucial to study how spectral vegetation indices respond to the land surface

characteristics of wetland sites including heterogeneity in land covers. We observed across a sample of 1,138 NWCA sites significant differences among wetland types in how SVIs respond to vegetation properties (e.g., coverage, height, composition), water and bare ground exposure, and landscape edaphic and climatic variables.

4.1 Variation among different SVIs in sensitivity to wetland ecosystem properties

SVIs showed significant contrasts in their responses to site and landscape characteristics, likely reflecting different spectral sensitivities to land surface properties. In the global sample of NWCA sites, NDVI and GNDVI, based on the normalized difference reflectance between the NIR and the red or green bands, were the most responsive SVIs to the surface properties of wetlands, with NDVI showing the greatest sensitivity to univariate and multivariate models of vegetation structure (e.g., height, cover). Meanwhile, univariate and multivariate models of species composition showed a greater capacity to predict variation in GNDVI year-maximum and year-median which reflects the sensitivity of the green band to fluctuations in chlorophyll a throughout a greater range of chlorophyll concentrations (Gitelson et al. 1996; Gitelson and Merzlyak 1998) and, consequently, the impact of vegetation diversity on GNDVI (Taddeo et al. *in revision*). The sensitivity of NDVI to wetland properties in our sample parallels observations by Mo et al. (2018) in which NDVI derived from Landsat ETM+ data showed a higher correlation to the leaf area index of marshes in Louisiana than EVI or SAVI. However, the shape of linear relationships between total species coverage and the year-maximum of NDVI and GNDVI suggest that both indices might saturate at high vegetation biomass or coverage. The saturation of NDVI under high coverage is well documented (Huete et al. 1997; Todd and Hoffer 1998; Pettorelli et al. 2005). Gamon et al. (1995b) also observed a saturation of the NIR band in dense vegetation which might impact GNDVI year-maximums under high coverage values. This indicates that for sites with a high biomass or leaf area index, it might be preferable to select an SVI that does not show the same saturation pattern. Alternatively, studies in high biomass areas could focus on the year-median of NDVI or GNDVI which does not show the same saturation pattern.

While the two indices incorporating a soil adjustment factor (EVI, SAVI) performed well, multivariate models of structure, composition, and confounding site variables could explain a lower proportion of their variance (between 1-16% less variance) than for NDVI or GNDVI. However, multivariate models of vegetation structure and composition showed a greater capacity to predict variations in EVI and SAVI at lower coverage, similar to observations made by Mo et al. (2018). Both EVI and SAVI year-maximums showed more sensitivity than NDVI to multivariate models of structure and composition in estuarine herbaceous wetlands, the wetland type characterized by the lowest vegetation coverage and SVI values. This suggest that under lower vegetation coverage, the use of a soil adjustment factor might help circumvent the effects of soil background on the reflectance of vegetation, as shown in wetlands (Mo et al. 2018) and terrestrial ecosystems (Huete et al. 1997; Huete et al. 2002; Pettorelli 2013).

While the relationship between GCC and vegetation coverage did not saturate at high values, its year-maximum showed less sensitivity to vegetation structure and composition than did other SVIs leveraging the NIR band. GCC has been previously used in near-surface phenology

analyses (Sonnentag et al. 2012b; Keenan et al. 2014; Knox et al. 2017), where it demonstrated significant correlations to leaf area index, plant biomass, and gross primary productivity. However, GCC computed from satellite-based surface reflectance data is sensitive to atmospheric scattering in the blue band (Brown et al. 2017). While EVI also includes the blue band, its use of a correction factor might reduce the incidence of atmospheric scattering, explaining why it performed significantly better than GCC.

LSWI showed less sensitivity to vegetation structure and composition. In univariate models, linear relationships between total vegetation coverage, species diversity and LSWI year-maximum or year-median showed the smallest slopes of all SVIs which may partially explain its lack of sensitivity to vegetation structure and composition. However, of all SVIs, LSWI was the least impacted by confounding variables including litter. This likely stems from its use of the SWIR band which is strongly reflected by cellulose and lignin in litter (Asner 1998; Nagler et al. 2000) facilitating the separation of wet vegetation from dead biomass (Adam et al. 2010).

These results show the importance of selecting the SVI most responsive to wetland properties of interest. In our dataset, NDVI showed greater sensitivity to structure, while GNDVI was most responsive to species composition. SVIs leveraging a soil adjustment factor (e.g., EVI, SAVI) offered a stronger signal of vegetation biomass at low coverage. Lastly, GCC and LSWI showed in the global sample a lower sensitivity to vegetation structure, composition, and confounding site variables than other SVIs.

4.2 Sensitivity of aggregation metrics to field characteristics

We observed significant differences in the capacity of models to predict SVI year-maximums and year-medians, which for some SVIs differed by as much as 24%. These contrasts may highlight the influence of atmospheric conditions and site properties on SVIs, with important implications for the use of aggregation metrics in future regional or global studies. Overall, multivariate models showed a more consistent capacity to predict year-medians across SVIs than their year-maximums. This might result from a greater contrast among SVIs in the distribution of their year-maximums: while most SVI year-medians showed similar skewness and kurtosis, year-maximums were characterized by lower correlations to one another and greater contrasts in the shape of their distribution. NDVI and GNDVI year-maximums showed the greatest skew towards higher values, likely highlighting their saturation at high vegetation coverage, while the distribution of EVI year-maximums was close to normality, consistent with Pettorelli (2013). Variations in the capacity of multivariate models to predict the different SVI year-maximums may also reflect different sensitivities to atmospheric conditions. While the annual median value of an SVI depends on its entire annual distribution, its maximum solely depends on the date, or Landsat image, that contains the greenest pixel of the time series highlighting the impact of atmospheric interference on certain SVIs (e.g., GCC; Brown et al. 2017).

Furthermore, models differed in their capacity to predict variations in the year-maximum of SVIs versus their year-medians. Structural and composition models had, overall, a greater capacity to predict variations in year-medians than year-maximums. However, at high vegetation coverage, species composition explained a greater proportion of fluctuations in both year-maximums and

year-medians than the multivariate model of vegetation structure. This suggests that, in wetlands with higher vegetation coverage, the identity of species may have more impact on their aggregated spectral characteristics than their coverage alone. This is likely due to species-specific differences in leaf structure, predominance of woody parts, and photosynthetic capacity affecting their reflectance in different portions of the electromagnetic spectrum. The role of species composition in modulating site greenness may also highlight the sensitivity of SVIs to diversity-productivity relationships as discussed in previous publications (e.g., Taddeo et al. *in revision*). Although the exact strength and shape of the diversity-productivity relationship varies among ecosystem types and disturbance levels, previous studies have shown that increased diversity can stimulate ecosystem productivity through a more effective partitioning of resources (Tilman et al. 1996; Hooper et al. 2005), which amounts to higher SVI values (Higgins et al. 2012; Maeda et al. 2014; Schweiger et al. 2018). At low coverage, it is possible that confounding factors, resulting in a greater occurrence of mixed pixels, mask the role of species identity in modulating SVIs. Lastly, the landscape model had a greater capacity to predict year-maximums than year-medians. This suggest that for a given vegetation coverage or diversity level, climatic and topographic controls are important in modulating maximum greenness. This result is consistent with previous studies showing in estuarine wetlands that increased precipitations can reduce salinity favoring productivity (Buffington et al. 2018) while higher temperatures positively impact NDVI values (Ichii and Yamaguchi 2001).

4.3 Confounding factors

The multivariate model of confounding site variables had a greater impact on SVIs at low vegetation coverage where gaps in between vegetated patches likely leave more bare ground, open water, and litter exposed (Myneni and Williams 1994; Spanglet et al. 1998; Kearney et al. 2009; Ollinger 2011). Similarly, the multivariate model of confounding site variables explained a greater proportion of variability in estuarine herbaceous wetlands (7-22% of year-maximum and 7-26% of year-median), characterized by a lower vegetation coverage, but a smaller proportion of variability in inland woody wetlands (<7% of year-maximum and 5-10% of year-median), the wetland type with the highest vegetation coverage. Overall, both univariate and multivariate models of confounding site variables had a greater capacity to explain variation in the year-medians of SVIs than on their year-maximums. This shows that at peak biomass, the influence of confounding factors is lessened as the vegetation is tall or dense enough to mask soil and water background effects. For example, litter coverage explained a greater proportion of variation in SVI year-median (2-11%) and a lower (<8%) to non-significant proportion of variation in SVI year-maximum. This is consistent with previous work showing that litter is more easily detectable at an early or late phenological state before peak greenness interferes with its reflectance in the SWIR (Li and Guo 2018). Similarly, the coverage of submerged vegetation and algae could explain a greater proportion of variation in SVI year-medians than SVI year-maximums and the proportion of bare ground had a greater incidence on the year-medians of SVIs than on their year-maximums. These results highlight the sensitivity of SVIs to both vegetation cover and productivity, but also to patterns of vegetation distribution in less vegetated sites. Stressors including salinity in estuarine wetlands or heavy metals in most disturbed sites can limit the lateral expansion of vegetation. When the spatial distribution of vegetation is

restricted, our analyses suggest that SVIs become increasingly sensitive to the presence of non-vegetated land covers, revealing that they indicate at the same time vegetation production and the extent of vegetation distribution within mixed pixels.

Spectral indices also showed significant differences in their sensitivity to univariate and multivariate models of confounding site variables including litter, open water, or bare soil exposure as the explanatory variable. NDVI, GNDVI, EVI, and SAVI all showed greater sensitivity than GCC and LSWI to the "confounding site variable" multivariate model. NDVI, GNDVI, EVI, and SAVI all seemed to be sensitive to litter coverage which explained 7-11% of the variation in their year-median and year-maximum. Litter accumulation impacts surface reflectance in visible bands thereby affecting SVI based on a ratio between visible bands and the NIR band (Todd and Hoffer 1998).

4.4 Differences among wetland types

Significant differences among SVIs in their response to the specific characteristics of wetland types identified here and in previous studies (Mo et al. 2018) suggest that future research efforts should select the SVIs most sensitive to the specific type of wetlands they are studying. These contrasts among relationships between site variables and SVIs likely result from differences among wetland types in their vegetation density, distribution, and the proportion of non-photosynthetically active plant parts (e.g., litter and woody parts).

In herbaceous-dominated sites (i.e., estuarine herbaceous and inland herbaceous), multivariate models of species composition, canopy structure, and confounding site variables explained a greater proportion of variation in GNDVI and NDVI than any other SVIs. Multivariate models in herbaceous-dominated sites showed, overall, a greater capacity to predict fluctuations in GNDVI year-maximums than other SVIs, and a greater capacity to predict variation in NDVI year-medians than other SVIs. This difference may stem from a contrast among GNDVI and NDVI in their sensitivity to vegetation properties. Overall, GNDVI is more sensitive to species composition as shown in previous studies (Gitelson et al. 1996; Gitelson and Merzlyak 1998; Taddeo et al. *in revision*), while composition generally had a greater contribution to maximum greenness than structure in the global model and under high vegetation coverage. GNDVI has shown better correlation to leaf chlorophyll, N content, and yield than other SVIs including NDVI and EVI in previous studies mapping productivity in diverse cultures including corn and wheat (e.g., Gitelson and Merzlyak 1998; Shanahan et al. 2001). Gitelson et al. (1996) showed that the green band is sensitive to chlorophyll a within a greater range of concentration than the red band. Similarities between the structural characteristics of some crops (i.e., erect leaves) and the herbaceous species dominating estuarine and inland herbaceous wetlands might partially explain the performance of GNDVI in these wetland types. Meanwhile, NDVI seemed to be more sensitive to vegetation structure which was a greater contributor to median greenness in the global sample, in sites dominated by herbaceous species, and at low vegetation coverage.

LSWI year-maximums and year-medians were, among all SVIs, the most responsive to indicators of canopy structure and composition in estuarine woody wetlands as evidenced by larger adjusted r-squares for their structure and composition multivariate models. The strength of

relationships between species composition and LSWI in sites dominated by woody species is consistent with observations made by Asner (1998) revealing a greater variability among woody species in SWIR reflectance. Furthermore, woody vegetation generally has a lower reflectance in visible bands than herbaceous species (Asner 1998), explaining the poor performance of vegetation indices leveraging visible bands in wetlands dominated by woody vegetation. However, LSWI previously showed limited efficiency in canopies with high density (Davranche et al. 2010) which might explain why LSWI performed better in estuarine woody wetlands than in the other, much denser, woody wetland type (i.e., inland woody wetlands). Interestingly, GCC year-maximum was strongly responsive to the multimeric model of vegetation structure in estuarine woody wetlands, but not to other site variables including species composition.

In inland woody wetlands, NDVI and EVI year-maximums and NDVI and GNDVI year-medians showed the greatest sensitivity to field variables (structure, composition). Yet the landscape multivariate model showed in inland woody wetlands the greatest explanatory power of all multivariate models and across all SVI year-maximums and year-medians. This highlights challenges in accurately detecting the full extent of vegetation richness and coverage in sites dominated by woody species which, when dominant, can obscure the spectral signal of understory species (Turner et al. 1999). This suggests that remote sensing of vegetation in inland woody wetlands might especially benefit from active remote sensing data which could help distinguish understory species below denser woody vegetation. In regions where such data is not available, our results indicate that the use of ancillary climate or elevation data, which can be found through free public databases, can improve the strength of linear relationships between field variables and SVIs.

4.5 Differences among disturbance gradient

Global, structure, composition, confounding site variable multivariate models generally showed a greater predictive capacity in the least disturbed sites than in intermediate and most disturbed ones. However, these models showed a greater capacity to predict variations in LSWI year-median and year-maximum in intermediate and most disturbed sites. This result might partially reflect the incidence of environmental stress on chlorophyll and water content, which impacts reflectance in the blue, red, NIR, and SWIR bands (Jensen 2007). As such, stressed vegetation – at a given coverage or leaf area index – should show lower SVI values than “healthy” plant communities.

Previous studies focusing on crops (Serrano et al. 2000) and grasslands (Wang et al. 2016) have shown that plant stress triggered by varying nitrogen exposure or water stress can impact the strength of relationships between field vegetation properties and SVIs. Differences in spectral properties and field composition among these three groups might further explain significant contrast in the predictive capacity of these different models. While least disturbed sites showed significantly lower SVIs year-maximum than intermediate and most disturbed sites, least disturbed sites also showed the greatest range in SVI year-maximum values. This could indicate a better capacity of SVIs to capture site variation in coverage and composition. Intermediate and most disturbed sites are characterized by a greater coverage and richness of native species, which in some cases might be spectrally dominant and negatively impact the strength of relationships

between field richness and SVIs (Taddeo et al. *in revision*). Lastly, most disturbed sites showed significantly greater litter and bare soil coverage (sign level=0.05) which might increase attenuation and reduce the strength of relationship between field-based vegetation characteristics and SVIs.

4.6 Implications for wetland monitoring and management

Vegetation structure and composition were, overall, the best predictors of wetland greenness as measured by SVIs estimated from broadband multispectral data. This reveals that both vegetation biomass and species identities modulate the overall greenness of wetland sites. While structure and composition were generally the best predictors of greenness, confounding site variables and landscape factors significantly impacted both median and maximum site greenness. The effect of confounding site variables, including litter coverage, bare ground exposure, algae, and submerged vegetation coverage was salient at low vegetation coverage and in wetland types in which stressors (e.g., salinity, inundation) limit vegetation productivity and lateral expansion. Meanwhile, at high vegetation coverage and in more productive wetland types, landscape climatic and edaphic variables described a substantial proportion of variability in site greenness sometimes explaining a greater percentage of variability than multivariate models of structure and composition (e.g., for some SVIs in estuarine and inland wetlands dominated by woody vegetation).

The importance of confounding site variables and landscape factors reveals strong regional controls on vegetation productivity, spatial distribution, and composition. Greenness is limited in some wetlands by the presence of stressors —including salinity and prolonged flooding— which restrict vegetation expansion in space and, consequently, its capacity to occupy large portions of pixels. In these wetlands, SVIs may never meet values recorded in inland sites because their SVIs are controlled by both the properties of vegetation and its spatial distribution. Meanwhile, in more productive wetlands or at peak greenness, climatic and edaphic factors can contribute to higher SVIs values. These patterns highlight the importance of interpreting SVIs patterns in their context; estuarine wetlands may not meet the SVI levels of inland woody wetlands but may nonetheless provide key ecosystem functions. As such, it is critical for future studies mapping vegetation properties at a regional or national scale to use previous SVIs values or the SVIs values of similar wetland sites as a reference to separate low values stemming from environmental constraints to vegetation distribution and significant responses to disturbances. These results also suggest that including regional variables (e.g., elevation, precipitation, temperature) within studies modeling vegetation characteristics at a large scale might enhance the robustness of models and their interpretation.

Our results also highlight the potential of broadband multispectral satellite data to track vegetation characteristics in wetlands at regional or national scales. In both highly and less productive wetlands, spectral vegetation indices were significantly impacted by indicators of vegetation abundance, composition, and spatial distribution. This shows that even coarser resolution data (30m) from Landsat sensors can be sensitive to changes in vegetation characteristics and their responses to environmental stressors. Furthermore, our study highlights the potential of aggregation metrics (in this case, mean and maximum greenness) as a mean to

reduce a large array of satellite images into a more computationally-efficient dataset. In our study area, mean and maximum greenness showed different sensitivities to site properties, indicating that they can be used in tandem for a thorough representation of wetland characteristics or by themselves in studies targeting a characteristic to which they are sensitive.

5 Conclusions

This study represents a first-time effort to assess relationships between the surface properties of wetlands and their spectral signature at a national scale. Our results indicate that vegetation properties and abundance may be best quantified using a spectral vegetation index sensitive to the specific properties of wetlands of interest. Important factors to identify the best vegetation index include dominant growth form, total vegetation cover, presence of open water and bare soil patches, and litter accumulation. In addition, the aggregation metrics studied here (i.e., maximum and median greenness) showed different responses to field characteristics, suggesting that their use should also be tailored to study objectives as they show different sensitivities to confounding factors and atmospheric conditions. Finally, our results support the need and opportunity to develop new vegetation indices or adapt existing ones to the specific properties of wetland ecosystems. For example, while indices including a soil adjustment factor (EVI and SAVI) performed well, they nonetheless showed less sensitivity to wetland properties than NDVI or GNDVI. Future research could assess whether the soil adjustment factor used by these two indices could be tailored to the soil properties of wetlands.

References

Adam, E., Mutanga, O., Rugege, D., 2010. Multispectral and hyperspectral remote sensing for identification and mapping of wetland vegetation: a review. Wetl. Ecol. Manag. 18, 281–296. doi:10.1007/s11273-009-9169-z

Asner, G.P., 1998. Biophysical and biochemical sources of variability in canopy reflectance. Remote Sens. Environ. 64, 234–253. doi:10.1016/S0034-4257(98)00014-5

Baker, C., Lawrence, R.L., Montagne, C., Patten, D., 2007. Change detection of wetland ecosystems using landsat imagery and change vector analysis imagery and change vector analysis. Wetlands 27, 610–619.

Bedford, B.L., 1999. Cumulative Effects on Wetland Landscapes: Links to Wetland Restoration in the United States and Southern Canada. Wetlands 19, 775–788.

Bell, D.M., Gregory, M.J., Kane, V., Kane, J., Kennedy, R.E., Roberts, H.M., 2018. Multiscale divergence between Landsat - and lidar - based biomass mapping is related to regional variation in canopy cover and composition. Carbon Balance Manag. 13, 1–14. doi:10.1186/s13021-018-0104-6

Blackburn, G.A., 2006. Hyperspectral remote sensing of plant pigments. J. Exp. Bot. 58, 855–867. doi:10.1093/jxb/erl123

Brown, L.A., Dash, J., Ogutu, B.O., Richardson, A.D., 2017. On the relationship between continuous measures of canopy greenness derived using near-surface remote sensing and satellite-derived vegetation products. Agric. For. Meteorol. 247, 280–292. doi:10.1016/j.agrformet.2017.08.012

Browning, D.M., Karl, J.W., Morin, D., Richardson, A.D., Tweedie, C.E., 2017. Phenocams bridge the gap between field and satellite observations in an arid grassland ecosystem. Remote Sens. 9. doi:10.3390/rs9101071

Buffington, K.J., Dugger, B.D., Thorne, K.M., 2018. Climate-related variation in plant peak biomass and growth phenology across Pacific Northwest tidal marshes. Estuar. Coast. Shelf Sci. 202, 212–221. doi:10.1016/j.ecss.2018.01.006

Byrd, K.B., O'Connell, J.L., Di Tommaso, S., Kelly, M., 2014. Evaluation of sensor types and environmental controls on mapping biomass of coastal marsh emergent vegetation. Remote Sens. Environ. 149, 166–180. doi:10.1016/j.rse.2014.04.003

Callaway, J.C., Borgnis, E.L., Turner, R.E., Milan, C.S., 2012. Carbon Sequestration and Sediment Accretion in San Francisco Bay Tidal Wetlands. Estuaries and Coasts 35, 1163–1181. doi:10.1007/s12237-012-9508-9

Carter, G.A., 1993. Responses of Leaf Spectral Reflectance to Plant Stress. Am. J. Bot. 80, 239–243.

Chmura, G.L., Anisfeld, S.C., Cahoon, D.R., Lynch, J.C., 2003. Global carbon sequestration in tidal, saline wetland soils. Global Biogeochem. Cycles 17, 12. doi:1111 10.1029/2002gb001917

Davidson, N.C., 2014. How much wetland has the world lost? Long-term and recent trends in global wetland area. Mar. Freshw. Res. 65, 934–941. doi:10.1071/MF14173

Davranche, A., Lefebvre, G., Poulin, B., 2010. Wetland monitoring using classification trees and SPOT-5 seasonal time series. Remote Sens. Environ. 114, 552–562. doi:10.1016/j.rse.2009.10.009

Department of the Interior, U.S Geological Survey, 2017. Product Guide. Landsat Surface Reflectance-Derived Spectral Indices. Version 3.6.

Dixon, M.J.R., Loh, J., Davidson, N.C., Beltrame, C., Freeman, R., Walpole, M., 2016. Tracking global change in ecosystem area: The Wetland Extent Trends index. Biol. Conserv. 193, 27–35. doi:https://doi.org/10.1016/j.biocon.2015.10.023

Dong, J., Xiao, X., Menarguez, M.A., Zhang, G., Qin, Y., Thau, D., Biradar, C., Moore, B., 2016. Mapping paddy rice planting area in northeastern Asia with Landsat 8 images, phenology-based algorithm and Google Earth Engine. Remote Sens. Environ. 185, 142–154. doi:https://doi.org/10.1016/j.rse.2016.02.016

Dronova, I., 2015. Object-Based Image Analysis in Wetland Research: A Review. Remote Sens. 7, 6380–6413. doi:10.3390/rs70506380

Dronova, I., Gong, P., Wang, L., 2011. Object-based analysis and change detection of major wetland cover types and their classification uncertainty during the low water period at Poyang Lake, China. Remote Sens. Environ. 115, 3220–3236. doi:10.1016/j.rse.2011.07.006

Dronova, I., Taddeo, S., 2016. Canopy Leaf Area Index in Non-Forested Marshes of the California Delta. Wetlands 36, 705–716. doi:10.1007/s13157-016-0780-5

Eldaw Elwadie, M., J. Pierce, F., Qi, J., 2005. Remote Sensing of Canopy Dynamics and Biophysical Variables Estimation of Corn in Michigan. Agron. J. - AGRON J 97. doi:10.2134/agronj2005.0099

Fernandes, R., Butson, C., Leblanc, S., Latifovic, R., 2003. Landsat-5 TM and Landsat-7 ETM+ based accuracy assessment of leaf area index products for Canada derived from SPOT-4 VEGETATION data. Can. J. Remote Sens. 29, 241–258. doi:10.5589/m02-092

Gallant, A.L., 2015. The challenges of remote monitoring of wetlands. Remote Sens. 7, 10938–10950. doi:10.3390/rs70810938

Gamon, J.A., Field, C.B., Goulden, M.L., Griffin, K.L., Hartley, A.E., Joel, G., Penuelas, J., Valenti, R., 1995a. Relationships between NDVI, canopy structure, and photosynthesis in three Californian vegetation types. Ecol. Appl. 5, 28–41. doi:10.2307/1942049

Gamon, J.A., Field, C.B., Goulden, M.L., Griffin, K.L., Hartley, A.E., Joel, G., Penuelas, J., Valenti, R., 1995b. Relationships between NDVI, canopy structure, and photosynthesis in three Californian vegetation types. Ecol. Appl. 5, 28–41. doi:10.2307/1942049

Gibbs, J.P., 2011. Loss and Biodiversity Conservation. Conserv. Biol. 14, 314–317. doi:10.1007/s10531-011-0010-7

Gitelson, A.A., Kaufman, Y.J., Merzlyak, M.N., 1996. Use of a green channel in remote sensing of global vegetation from EOS- MODIS. Remote Sens. Environ. 58, 289–298. doi:10.1016/S0034-4257(96)00072-7

Gitelson, A.A., Merzlyak, M.N., 1998. Remote sensing of chlorophyll concentration in higher plant leaves. Adv. Sp. Res. 22, 689–692. doi:10.1016/S0273-1177(97)01133-2

Gorelick, N., Hancher, M., Dixon, M., Ilyushchenko, S., Thau, D., Moore, R., 2017. Google Earth Engine: Planetary-scale geospatial analysis for everyone. Remote Sens. Environ. 202, 18–27. doi:10.1016/j.rse.2017.06.031

Gould, W., 2000. Remote Sensing of Vegetation, Plant Species Richness, and Regional Biodiversity Hotspots. Ecol. Appl. 10, 1861–1870.

Higgins, S.I., Richardson, D.M., Cowling, R.M., Trinder-, T.H., 2012. Predicting the Distribution Landscape-Scale of Alien and Their Threat. Conserv. Biol. 13, 303–313.

Hooper, D.U., Chapin, F.S.I., Ewel, J.J., 2005. Effects of biodiversity on ecosystem functioning: a consensus of current knowledge. Ecol. Monogr. 75, 3–35. doi:10.1890/04-0922

Huete, A., Didan, K., Miura, T., Rodriguez, E.P., Gao, X., Ferreira, L.G., 2002. Overview of the radiometric and biophysical performance of the MODIS vegetation indices. Remote Sens. Environ. 83, 195–213. doi:https://doi.org/10.1016/S0034-4257(02)00096-2

Huete, A.R., 1988. A Soil-Adjusted Vegetation Index (SAVI). Remote Sens. Environ. 25, 295–309. doi:10.1016/0034-4257(88)90106-X

Huete, A.R., Liu, H.Q., Batchily, K., VanLeeuwen, W., 1997. A comparison of vegetation indices global set of TM images for EOS-MODIS. Remote Sens. Environ. 59, 440–451. doi:10.1016/S0034-4257(96)00112-5

Ichii, K., Yamaguchi, Y., 2001. Global monitoring of interannual changes in vegetation activities using NDVI and its relationships to temperature and precipitation AU - Kawabata, A. Int. J. Remote Sens. 22, 1377–1382. doi:10.1080/01431160119381

Jensen, J.R., 2007. Remote Sensing of the Environment: An Earth Resource Perspective, Second Edi. ed. Prentice Hall, Upper Sadle River, NJ.

Kearney, M.S., Stutzer, D., Turpie, K., Stevenson, J.C., 2009. The effect of Tidal Inundation on the Reflectance Characteristics of Coastal Marsh Vegetation. J. Coast. Res. 25, 1177–1186.

Keenan, T.F., Darby, B., Felts, E., Sonnentag, O., Friedl, M., Hufkens, K., O' Keefe, J.F., Klosterman, S., Munger, J.W., Toomey, M., Richardson, A.D., 2014. Tracking forest phenology and seasonal physiology using digital repeat photography: a critical assessment. Ecol. Appl. 24, 140206175103002. doi:10.1890/13-0652.1

Kingsford, R.T., Basset, A., Jackson, L., 2016. Wetlands: conservation's poor cousins. Aquat. Conserv. Mar. Freshw. Ecosyst. 26, 892–916. doi:10.1002/aqc.2709

Klemas, V., 2013a. Using Remote Sensing to Select and Monitor Wetland Restoration Sites: An Overview. J. Coast. Res. 289, 958–970. doi:10.2112/JCOASTRES-D-12-00170.1

Klemas, V., 2013b. Remote sensing of emergent and submerged wetlands: an overview. Int. J. Remote Sens. 34, 6286–6320. doi:10.1080/01431161.2013.800656

Knox, S.H., Dronova, I., Sturtevant, C., Oikawa, P.Y., Matthes, J.H., Verfaillie, J., Baldocchi, D., 2017. Using digital camera and Landsat imagery with eddy covariance data to model gross primary production in restored wetlands. Agric. For. Meteorol. 237–238, 233–245. doi:10.1016/j.agrformet.2017.02.020

Knox, S.H., Sturtevant, C., Matthes, J.H., Koteen, L., Verfaillie, J., Baldocchi, D., 2015. Agricultural peatland restoration: Effects of land-use change on greenhouse gas (CO2 and CH4) fluxes in the Sacramento-San Joaquin Delta. Glob. Chang. Biol. 21, 750–765. doi:10.1111/gcb.12745

Lang, M.W., Purkis, S., Klemas, V. V, Tiner, R.W., 2015. Promising Developments and Future Challenges for Remote Sensing of Wetlands, in: Tiner, R.W., Lang, M.W., Klemas, V. V (Eds.), Remote Sensing of Wetlands. Applications and Advances. CRC Press, Taylor & Francis Group, Boca Raton, pp. 533–544. doi:doi:10.1201/b18210-30

Li, Z., Guo, X., 2018. Non-photosynthetic vegetation biomass estimation in semiarid Canadian mixed grasslands using ground hyperspectral data, Landsat 8 OLI, and Sentinel-2 images. Int. J. Remote Sens. 39, 6893–6913. doi:10.1080/01431161.2018.1468105

Maeda, E.E., Heiskanen, J., Thijs, K.W., Pellikka, P.K.E., 2014. Season-dependence of remote sensing indicators of tree species diversity. Remote Sens. Lett. 5, 404–412. doi:10.1080/2150704X.2014.912767

Mishra, D.R., Ghosh, S., 2015. Using Moderate-Resolution Satellite Sensors for Monitoring the Biophysical Parameters and Phenology of Tidal Marshes, in: Tiner, R.W., Lang, M.W., Klemas, V. V (Eds.), Remote Sensing of Wetlands. Applications and Advances. CRC Press, Taylor & Francis Group, Boca Raton, pp. 283–314. doi:doi:10.1201/b18210-18

Mo, Y., Kearney, M.S., Riter, J.C.A., Zhao, F., Tilley, D.R., 2018. Assessing biomass of diverse coastal marsh ecosystems using statistical and machine learning models. Int. J. Appl. Earth Obs. Geoinf. 68, 189–201. doi:10.1016/j.jag.2017.12.003

Myneni, R.B., Williams, D.L., 1994. On the relationship between FAPAR and NDVI. Remote Sens. Environ. 49, 200–211. doi:10.1016/0034-4257(94)90016-7

Nagler, P.L., Daughtry, C.S.T., Goward, S.N., 2000. Plant litter and soil reflectance. Remote Sens. Environ. 71, 207–215. doi:10.1016/S0034-4257(99)00082-6

Nagler, P.L., Glenn, E.P., Lewis Thompson, T., Huete, A., 2004. Leaf area index and normalized difference vegetation index as predictors of canopy characteristics and light interception by riparian species on the Lower Colorado River. Agric. For. Meteorol. 125, 1–17. doi:10.1016/j.agrformet.2004.03.008

Nicholls, R.J., Hoozemans, F.M.J., Marchand, M., 1999. Increasing flood risk and wetland losses due to global sea-level rise: Regional and global analyses. Glob. Environ. Chang. 9. doi:10.1016/S0959-3780(99)00019-9

Ollinger, S. V, 2011. Sources of variability in canopy reflectance and the convergent properties of plants. New Phytol. 189, 375–94. doi:10.1111/j.1469-8137.2010.03536.x

Pedersen, E., Weisner, S.E.B., Johansson, M., 2019. Wetland areas' direct contributions to residents' well-being entitle them to high cultural ecosystem values. Sci. Total Environ. 646, 1315–1326. doi:10.1016/j.scitotenv.2018.07.236

Pettorelli, N., 2013. Vegetation indices, in: The Normalized Difference Vegetation Index. Oxford University Press, Oxford. doi:10.1093/acprof:osobl/9780199693160.003.0002

Pettorelli, N., Vik, J.O., Mysterud, A., Gaillard, J.M., Tucker, C.J., Stenseth, N.C., 2005. Using the satellite-derived NDVI to assess ecological responses to environmental change. Trends Ecol. Evol. 20, 503–510. doi:10.1016/j.tree.2005.05.011

Phinn, S., Stow, D., Van Mouwerik, D., 1999. Remotely sensed estimates of vegetation structural characteristics in restored wetlands, Southern California. Photogramm. Eng. Remote Sensing 65.

Poulin, B., Davranche, A., Lefebvre, G., 2010. Ecological assessment of Phragmites australis wetlands using multi-season SPOT-5 scenes. Remote Sens. Environ. 114, 1602–1609. doi:https://doi.org/10.1016/j.rse.2010.02.014

R Core Team, 2017. R: A language and environment for statistical computing.

Rocha, a. V., Potts, D.L., Goulden, M.L., 2008. Standing litter as a driver of interannual CO2 exchange variability in a freshwater marsh. J. Geophys. Res. Biogeosciences 113, 1–10. doi:10.1029/2008JG000713

Rouse, J., Haas, R., Schell, I., Deering, D., Harlan, J., 1973. Monitoring the vernal advancement of retrogradation of natural vegetation. Greenbelt, Maryland.

Schile, L.M., Byrd, K.B., Windham-Myers, L., Kelly, M., 2013. Accounting for non-photosynthetic vegetation in remote-sensing-based estimates of carbon flux in wetlands. Remote Sens. Lett. 4, 542–551. doi:10.1080/2150704X.2013.766372

Schweiger, A.K., Cavender-Bares, J., Townsend, P.A., Hobbie, S.E., Madritch, M.D., Wang, R., Tilman, D., Gamon, J.A., 2018. Plant spectral diversity integrates functional and phylogenetic components of biodiversity and predicts ecosystem function. Nat. Ecol. Evol. 2, 976–982. doi:10.1038/s41559-018-0551-1

Shanahan, J.F., Schepers, J.S., Francis, D.D., Varvel, G.E., Wilhelm, W.W., Tringe, J.M., Schlemmer, M.R., Major, D.J., 2001. Use of remote-sensing imagery to estimate corn grain yield. Agron. J. 93, 583–589. doi:10.2134/agronj2001.933583x

Sims, D.A., Gamon, J.A., 2002. Relationships between leaf pigment content and spectral reflectance across a wide range of species, leaf structures and developmental stages. Remote Sens. Environ. 81, 337–354. doi:https://doi.org/10.1016/S0034-4257(02)00010-X

Sonnentag, O., Hufkens, K., Teshera-Sterne, C., Young, A.M., Friedl, M., Braswell, B.H., Milliman, T., O'Keefe, J., Richardson, A.D., 2012a. Digital repeat photography for phenological research in forest ecosystems. Agric. For. Meteorol. 152, 159–177. doi:10.1016/j.agrformet.2011.09.009

Sonnentag, O., Hufkens, K., Teshera-Sterne, C., Young, A.M., Friedl, M., Braswell, B.H., Milliman, T., O'Keefe, J., Richardson, A.D., 2012b. Digital repeat photography for phenological research in forest ecosystems. Agric. For. Meteorol. 152, 159–177. doi:10.1016/j.agrformet.2011.09.009

Spanglet, H.J., Ustin, S.L., Rejmankova, E., 1998. Spectral reflectance characteristics of California subalpine marsh plant communities. Wetlands 18, 307–319.

Tilman, D., Wedin, D., Knops, J., 1996. Productivity and sustainability influenced by biodiversity in grassland ecosystems. Nature 379, 718–720. doi:10.1038/379718a0

Todd, S.W., Hoffer, R.M., 1998. Responses of Spectral Indices to Variations in Vegetation Cover and Soil Background. Photogramm. Eng. Remote Sensing 64, 915–921.

Toomey, M., Vierling, L.A., 2005. Multispectral remote sensing of landscape level foliar moisture: techniques and applications for forest ecosystem monitoring. Can. J. For. Res. 35, 1087–1097. doi:10.1139/x05-043

Tucker, C.J., 1979. Red and Photographic Infrared Linear Combinations or Monitoring Vegetation. Remote Sens. Environ. 8, 127–150. doi:10.1016/0034-4257(79)90013-0

Turner, D.P., Cohen, W.B., Kennedy, R.E., Fassnacht, K.S., Briggs, J.M., Wisconsin, M., 1999. Relationships between Leaf Area Index and Landsat TM Spectral Vegetation Indices across Three Temperate Zone Sites. Remote Sens. Environ. 70, 52–68. doi:10.1111/j.1440-1746.2010.06530.x

US EPA, 2016a. National Wetland Condition Assessment: 2011 Technical Report. Washington, DC.

US EPA, 2016b. National Wetland Condition Assessment 2011: A Collaborative Survey of the Nation's Wetlands. Washington, DC.

Wilcox, D. a., Meeker, J.E., Hudson, P.L., Armitage, B.J., Black, M.G., Uzarski, D.G., 2002. Hydrologic variability and the application of Index of Biotic Integrity metrics to wetlands: A great lakes evaluation. Wetlands 22, 588–615. doi:10.1672/0277-5212(2002)022[0588:HVATAO]2.0.CO;2

Zedler, J.B., 2003. Wetlands at your service : reducing impacts of agriculture at the watershed scale. Front. Ecol. Environ. 1, 65–72.

Zedler, J.B., Callaway, J.C., Diego, S., Na-, S.M., 1999. Tracking Wetland Restoration : Do Mitigation Sites Follow Desired Trajectories ? Restor. Ecol. 7, 69–73.

6 Table and figures

Table 1. Vegetation indices used in this study and their formula. Spectral bands are based on the Landsat ETM+ designation, with the following bandwidths: ρ_B (B1 - blue; 0.45-0.52), ρ_G (B2 - green; 0.52-0.60); ρ_R (B3 - red; 0.63-0.69); ρ_{NIR} (B4 - near infrared – 0.77-0.90); ρ_{SWIR} (B5 - short-wave infrared; 1.55-1.75). The formulae for EVI and SAVI are based on USGS (2017).

Vegetation index	Formula	Range
Normalized Difference Vegetation Index (NDVI)	$\frac{\rho_{NIR} - \rho_R}{\rho_{NIR} + \rho_R}$	-1, +1
Green Normalized Difference Vegetation Index (GNDVI)	$\frac{\rho_{NIR} - \rho_G}{\rho_{NIR} + \rho_G}$	-1, +1
Land Surface Water Index (LSWI)	$\frac{\rho_{NIR} - \rho_{SWIR}}{\rho_{NIR} + \rho_{RSWIR}}$	-1, +1
Enhanced Vegetation Index (EVI)	$2.5 * \frac{\rho_{NIR} - \rho_R}{(\rho_{NIR} + 6\,x\,\rho_R - 7.5\,x\,\rho_B + 1)}$	-1, +1
Soil-adjusted Vegetation Index (SAVI)	$\frac{\rho_{NIR} - \rho_R}{(\rho_{NIR} + \rho_R + L)} * (1.5)$	-1, +1
Green Chromatic Coordinate (GCC)	$\frac{\rho_G}{\rho_G + \rho_R + \rho_B}$	0,1

Table 2. Field-based explanatory variables and their sources, by multivariate model.

Category	Variable	Units	Source
Structural	**Total coverage by native species:** sum of native vegetation percentage coverage by layers	Percentage	NWCA
	Total coverage by alien species: sum of alien vegetation percentage coverage by layers	Percentage	
	Coverage by submerged aquatic vegetation: mean proportion of coverage by submerged aquatic vegetation	Percentage	
	Coverage by floating aquatic vegetation: mean proportion of coverage by floating aquatic vegetation	Percentage	
	Coverage by algae: mean proportion of coverage by floating aquatic vegetation	Percentage	
	Mean height: mean height, by height class	Height class	
	Number of Layers: number of distinct height class	Height class	
	Max height; highest height class observed	Percentage	
	Coverage of Forbs: Total absolute coverage by forb species	Percentage	
	Coverage of Shrubs: Total absolute coverage by shrub species	Percentage	
	Coverage of Trees: Total absolute coverage by tree species	Percentage	
Composition	**Total Species Diversity**: Shannon-Wiener Diversity Index (calculated using all species)	Unitless	
	Evenness: evenness of all species	Unitless	
	Richness of Graminoids: number of graminoid species	Unitless	
	Richness of Forbs: number of forb species	Unitless	

	Richness of Herbaceous: number of herbaceous species	Unitless	
	Richness of Shrubs: number of shrub species	Unitless	
	Richness of Trees: number of tree species	Unitless	
Confounding site variables	**Litter depth**: Mean depth of litter across all plots	cm	NWCA
	Litter coverage: Mean percent cover by litter	Percentage	
	Open water coverage: Mean percent cover by open water	Percentage	
	Bare ground coverage: Mean percent cover by bare ground	Percentage	
	Exposed soil coverage: Mean percent cover by exposed soil	Percentage	
Landscape	**Mean elevation**	m	National Elevation Dataset (USGS)
	Maximum elevation	m	
	Mean annual precipitation, averaged over 30 years	cm	Parameter-elevation Relationships on Independent Slopes Mode (PRISM)
	Coefficient of variation in total monthly precipitations, over 30 years	cm	
	Mean maximum precipitation, averaged over 30 years	cm	
	Mean minimum precipitation, averaged over 30 years	cm	
	Mean annual maximum air temperature, average d over 30 years		
	Standard deviation of mean annual air temperature	Celsius	

Table 3. Adjusted R2 for the linear relationship between multivariate models and the year-maximum and year-median of spectral vegetation indices, for low vegetation coverage plots (<117%) and high vegetation coverage plots (>117%).

	Year-maximum						Year-median					
Group of variables	**NDVI**	**GNDVI**	**LSWI**	**EVI**	**SAVI**	**GCC**	**NDVI**	**GNDVI**	**LSWI**	**EVI**	**SAVI**	**GCC**
Low vegetation coverage												
Structure	0.2968***	0.2681***	0.0952***	0.2437***	0.2395***	0.166***	0.4063***	0.3014***	0.253***	0.326***	0.2803***	0.3371***
Composition	0.2693***	0.2958***	0.0509***	0.2907***	0.3105***	0.0898***	0.3717***	0.3559***	0.1767***	0.3288***	0.33***	0.2987**
Confounding	0.125***	0.1326***	0.0568***	0.0996***	0.1058***	0.0299**	0.153***	0.1459***	0.0774***	0.1536***	0.1335***	0.0902***
Landscape	0.2151***	0.1968***	0.1036***	0.1206***	0.1641***	0.0522***	0.173***	0.1318***	0.1561***	0.1028***	0.1144***	0.139***
High vegetation coverage												
Structure	0.3243***	0.3051***	0.1872***	0.2343***	0.2237***	0.0426**	0.3929***	0.2392***	0.2556***	0.2905**	0.2025***	0.2073***
Composition	0.305***	0.3456***	0.2012***	0.2951***	0.3296***	0.0435***	0.3837***	0.2982***	0.2811***	0.3005***	0.2481***	0.2349***
Confounding	0.0305**	0.0638***	0.0050	0.0382**	0.0493**	-0.0083	0.0366**	0.0811***	-0.0057	0.0483***	0.0567**	-0.0065
Landscape	0.2425***	0.2425***	0.1428***	0.1311***	0.1841***	0.1214***	0.1653**	0.0712***	0.14***	0.0789***	0.0402**	0.1678***

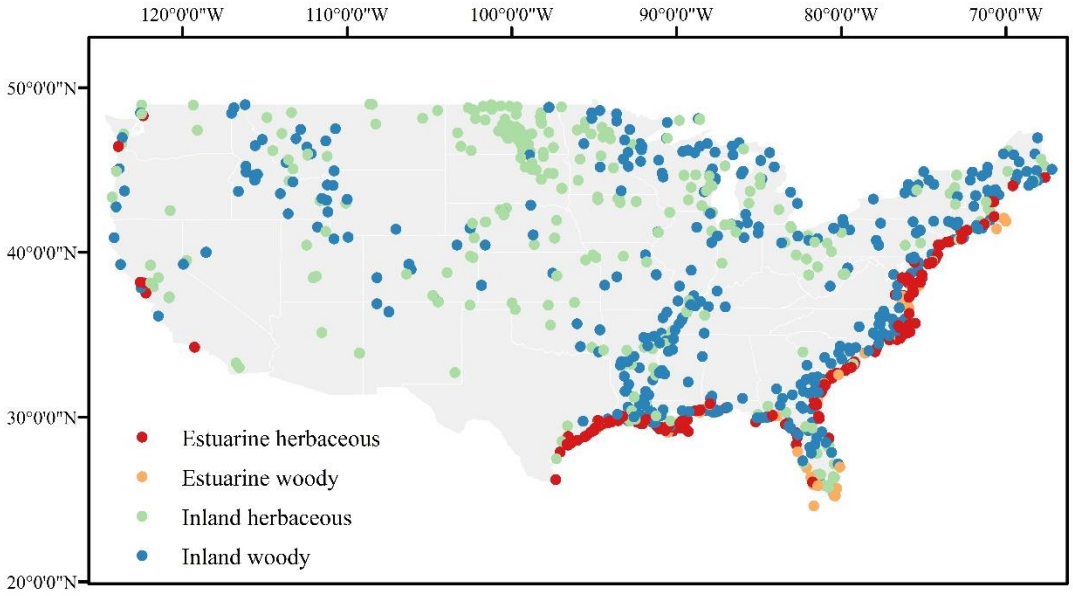

Figure 1. Spatial distribution of the 1,138 National Wetland Condition Assessment survey sites, by wetland type.

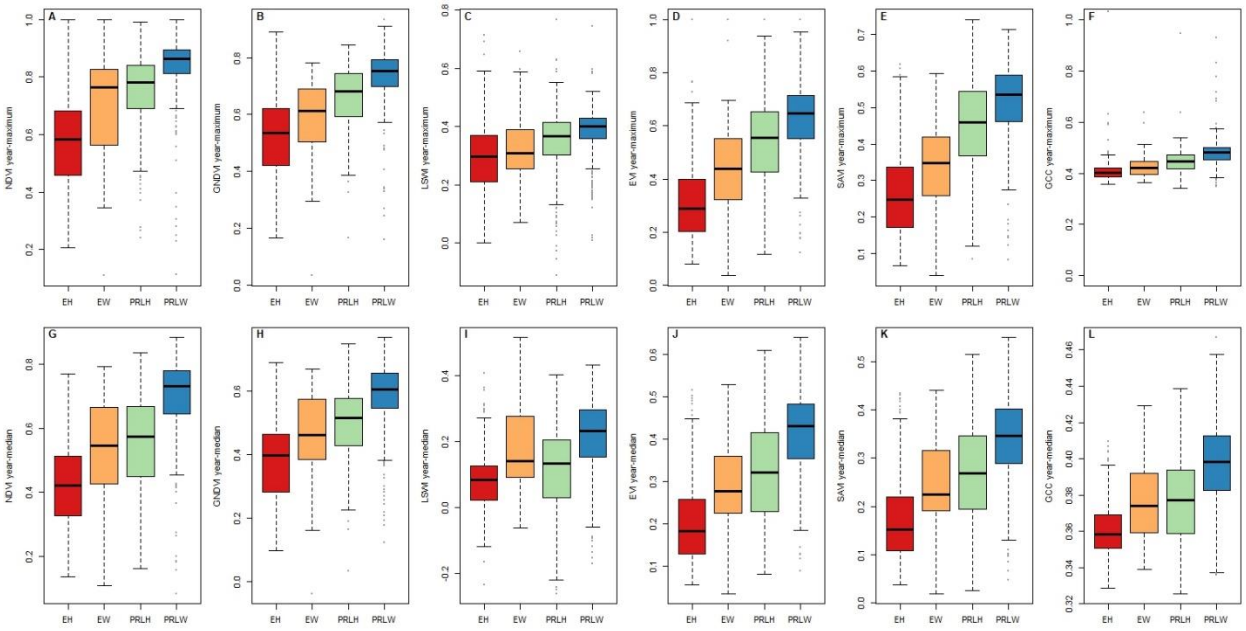

Figure 2. Distribution of year-maximum (top row) and year-median (bottom row) in site greenness by spectral vegetation indices (i.e., NDVI, GNDVI, LSWI, EVI, SAVI, GCC) and wetland types, where EH are estuarine herbaceous wetlands, EW are estuarine woody wetlands, PRLH are inland herbaceous wetlands, and PRLW are inland woody wetlands.

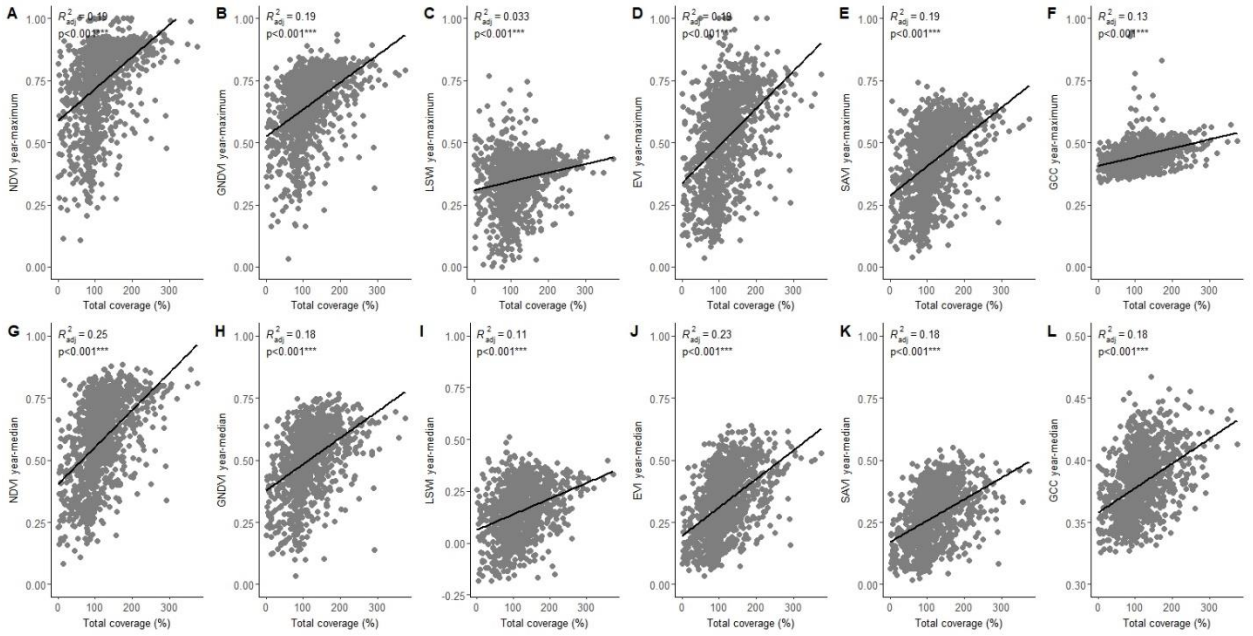

Figure 3. Linear relationships between total vegetation coverage and the year-maximum (top row) and year-median (bottom row) of spectral vegetation indices. Total coverage is measured as the sum of vegetation coverage in different layers (i.e., proportion of a layer occupied by photosynthetically-active vegetation) and can consequently exceed 100%.

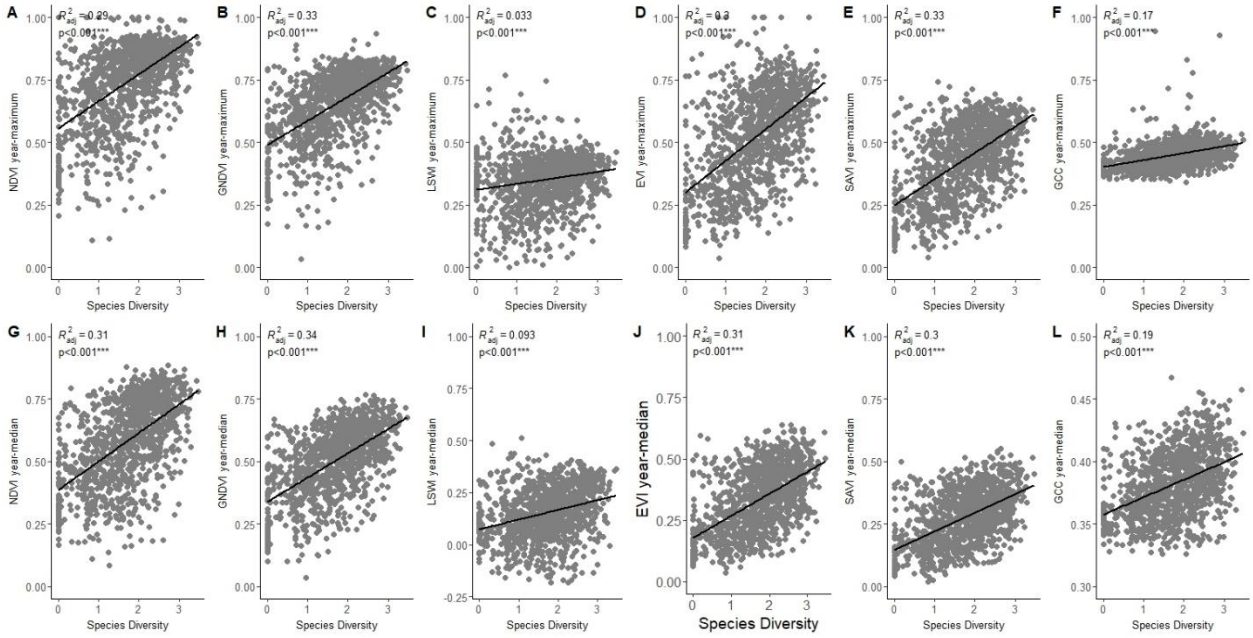

Figure 4. Linear relationships between the Shannon-Wiener Diversity Index and the year-maximum (top row) and year-median (bottom row) of spectral vegetation indices.

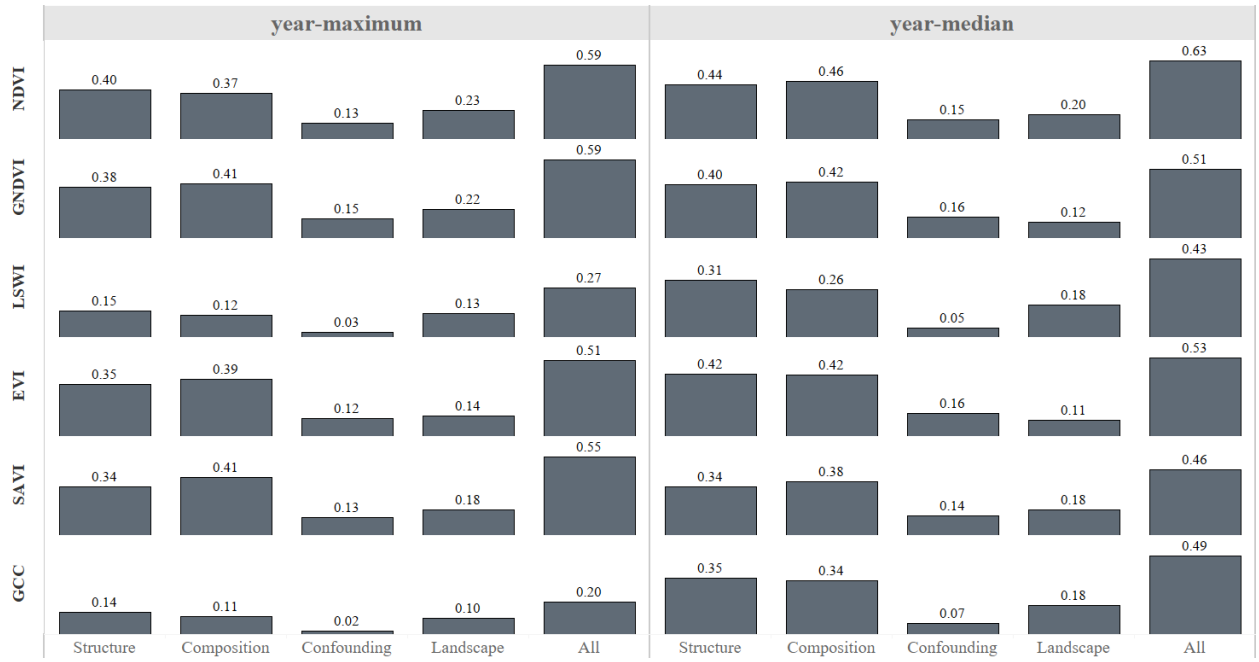

Figure 5. Adjusted R^2 for the linear relationships between multivariate models of canopy structure, vegetation composition, confounding site variables, and landscape variables and the year-maximum (left) and year-median (right) of spectral vegetation indices.

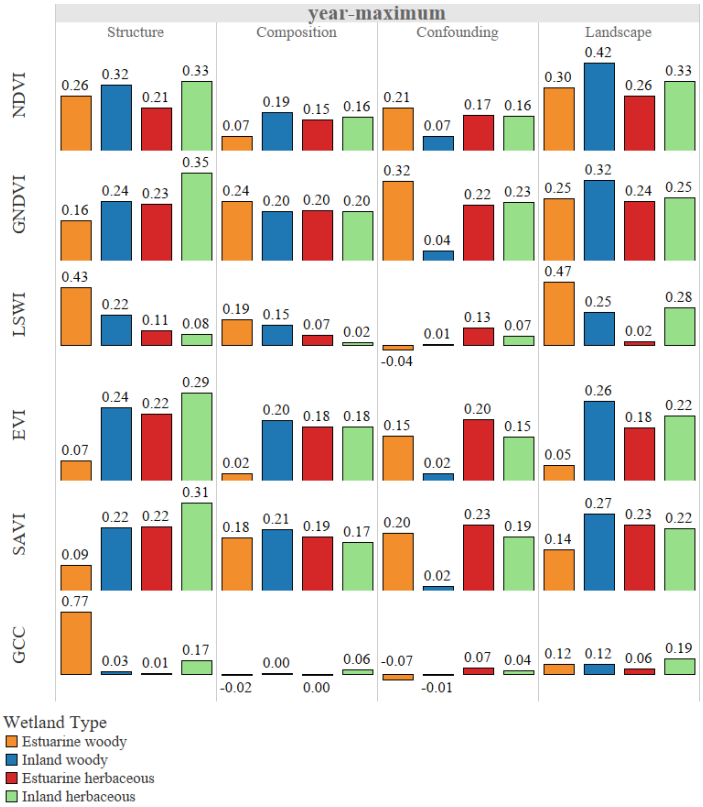

Figure 6A. Adjusted R^2 for the linear relationships between multivariate models of canopy structure, vegetation composition, confounding site variables, landscape variables and SVI year-maximum for estuarine herbaceous (red), estuarine woody (orange), inland herbaceous (green), and inland woody (blue) wetlands

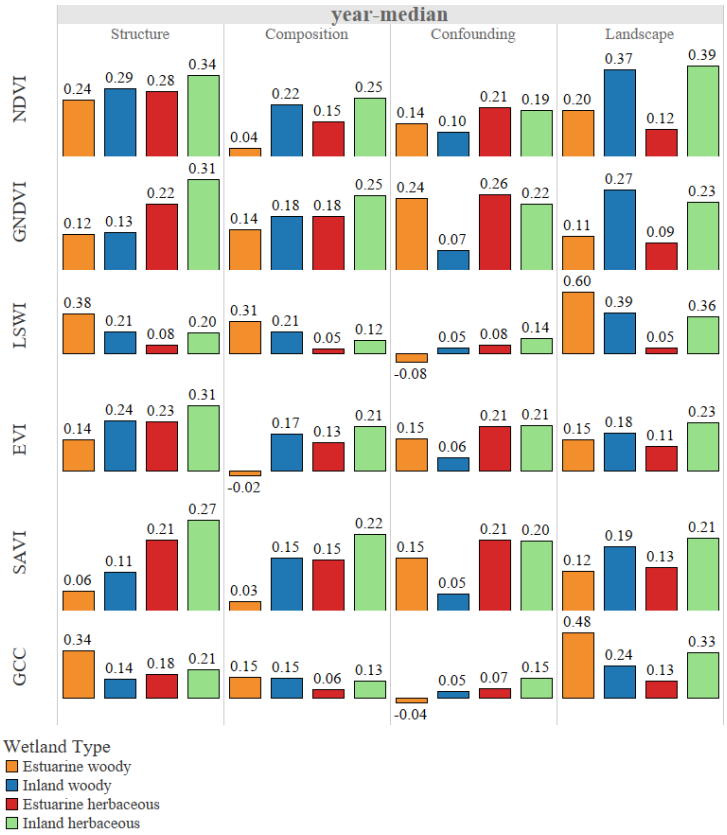

Figure 6B. Adjusted R^2 for the linear relationships between multivariate models of canopy structure, vegetation composition, confounding site variables, landscape variables and SVI year-median for estuarine herbaceous (red), estuarine woody (orange), inland herbaceous (green), and inland woody (blue) wetlands

7 Supplemental information

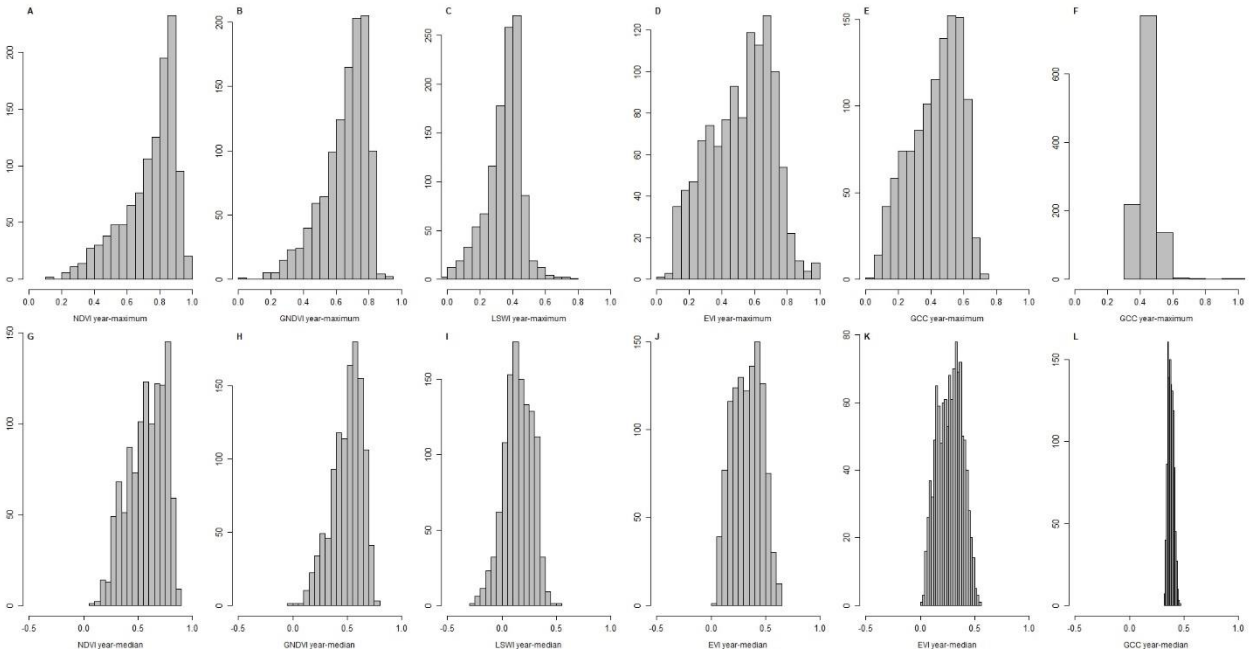

Figure S1. Distribution of site average of SVI year-maximum (histograms A-F) and year-median (G-L) across the global sample of NWCA sites.

Table S1. Pearson's correlation coefficient describing the correlation between each pair of SVI year-median (bottom half of table) and their year-maximum (upper half)

	NDVI	GNDVI	LSWI	EVI	SAVI	GCC
NDVI		0.9174***	0.4774***	0.8453***	0.8714***	0.5165***
GNDVI	0.8854***		0.3774***	0.8628***	0.9180***	0.4897***
LSWI	0.7219***	0.5406***		0.4634***	0.4622***	0.3908***
EVI	0.9285***	0.8763***	0.6820***		0.9527***	0.4727***
SAVI	0.8659***	0.9396***	0.6513***	0.9291***		0.4769***
GCC	0.8593***	0.6513***	0.8103***	0.8212***	0.7375***	1.0000

Table S2. Adjusted R^2 for the linear relationship between structural explanatory variables and spectral vegetation indices, across all study sites.

	Year-maximum						Year-median					
	NDVI	**GNDVI**	**LWSI**	**EVI**	**SAVI**	**GCC**	**NDVI**	**GNDVI**	**LWSI**	**EVI**	**SAVI**	**GCC**
Total canopy height and coverage												
Number of Layers	0.3545***	0.3442***	0.0939***	0.3106***	0.3055***	0.1138***	0.4358***	0.344***	0.2426***	0.3675***	0.3115***	0.2878***
Max height	0.3534***	0.3249***	0.1215***	0.2946***	0.2835***	0.1195***	0.4448***	0.3138***	0.2747***	0.3570***	0.2863***	0.3127***
Total species coverage	0.1945***	0.1857***	0.0358***	0.1918***	0.1915***	0.0977***	0.2481***	0.1851***	0.1288***	0.2343***	0.1831***	0.1837***
Coverage by growth form												

Forbs cover	-0.0004	-0.000	0.0131***	0.0031**	0.0060***	-0.0004	0.0069***	0.0000	0.0057***	0.0015	0.0004	0.0021
Graminoids Cover	0.2388***	0.2016***	0.1492***	0.2551***	0.2472***	0.0952***	0.2663***	0.2128***	0.1892***	0.2387***	0.2007***	0.2219***
Herb Cover	0.2327**	0.2016***	0.0938***	0.2201***	0.199***	0.0919***	0.2353***	0.2426***	0.2545***	0.2862***	0.2342***	0.2725***
Shrubs cover	0.0463***	0.0467***	0.0050***	0.02327***	0.0279***	0.0096***	0.0778***	0.0591***	0.0362***	0.0486***	0.0383***	0.0450***
Trees cover	0.2153***	0.2035***	0.0914***	0.1935***	0.1874***	0.0687***	0.3114***	0.2116***	0.1931***	0.2461***	0.1899***	0.228***
Coverage by layer												
< 0.5m	0.0087**	0.0042**	0.0231***	0.0060***	0.0031**	0.0062**	0.0032*	-0.0007	0.0178***	0.0007	0.0002	0.0073**
0.5 to 2m	-0.0005	0.0005	0.0076***	0.0009	0.0006	0.0017	-0.0002	0.0000	-0.0007	-0.0001	0.0004	-0.0006
2m to 5	0.1082***	0.0905***	0.0269***	0.0793***	0.077***	0.0406***	0.105***	0.0705***	0.0650***	0.0874***	0.0618***	0.0713***
5m to 15m	0.1659***	0.148***	0.0800***	0.15***	0.1413***	0.0623***	0.2284***	0.1517***	0.1588***	0.1957***	0.1493***	0.176***
15m to 30m	0.1415***	0.1379***	0.0694***	0.1396***	0.1285***	0.0523***	0.2003***	0.1162***	0.1256***	0.176***	0.1126***	0.151***
> 30m	0.0198***	0.0183***	0.0144***	0.0214***	0.0183***	0.0052**	0.0334***	0.0234***	0.0240***	0.0318***	0.0227***	0.0234***

Table S3. Adjusted R^2 for the linear relationship between different indicators of plant composition and spectral vegetation indices, across all study sites.

	Year-maximum						**Year-median**					
Explanatory variables	**NDVI**	**GNDVI**	**LSWI**	**EVI**	**SAVI**	**GCC**	**NDVI**	**GNDVI**	**LSWI**	**EVI**	**SAVI**	**GCC**
Total Diversity	0.2932***	0.3289***	0.0341***	0.2953***	0.326***	0.1734***	0.3103***	0.3355***	0.0942***	0.3093***	0.2955***	0.1926***
Evenness	0.0938***	0.0965***	0.0069**	0.0859***	0.0884***	0.0051**	0.0978***	0.1135***	0.0314***	0.0912***	0.0920***	0.0585***
Median Species Richness	0.254***	0.2901***	0.0385***	0.2248***	0.2917***	0.0742***	0.2774***	0.2757***	0.0927***	0.2776***	0.252***	0.2044***
Standard Deviation in Species	0.1306***	0.1479***	0.0277***	0.1561***	0.166***	0.0325***	0.1029***	0.1198***	0.0265***	0.1211***	0.1132***	0.0623***
Forb richness	0.1508***	0.1769***	0.0162***	0.1754***	0.2301***	0.0423***	0.122***	0.129***	0.0292***	0.1471***	0.1244***	0.102***
Graminoid richness	0.0583***	0.0781***	-0.0008	0.0598**	0.0791***	0.0062**	0.0309***	0.0609***	-0.0008	0.0479***	0.0524***	0.0102***
Herb richness	0.1336***	0.1617***	0.0133**	0.1511***	0.1803***	0.0315***	0.0990***	0.1199***	0.0144***	0.1255***	0.1125***	0.0716***
Richness of Shrubs	0.12***	0.1241***	0.0203***	0.0826***	0.0897***	0.0328***	0.1741***	0.1344***	0.0897***	0.1173***	0.1023***	0.1127***
Richness of Trees	0.2681***	0.2861***	0.0948***	0.2653***	0.2702***	0.0861***	0.3824***	0.3242***	0.2343***	0.3339***	0.3064**	0.2722***

Table S4. Adjusted R^2 for the linear relationship between confounding site variables and spectral vegetation indices, across all study sites.

	Year-maximum						**Year-median**					
Explanatory variables	**NDVI**	**GNDVI**	**LSWI**	**EVI**	**SAVI**	**GCC**	**NDVI**	**GNDVI**	**LSWI**	**EVI**	**SAVI**	**GCC**
Litter coverage	0.0794***	0.0896***	-0.0008	0.0744***	0.0787***	0.0123***	0.09***	0.11***	0.01***	0.11***	0.0781***	0.02***
Litter depth	-0.0008	-0.0006	0.0025	-0.0006	-0.0009	-0.0008	-0.00	-0.00	0.0011	-0.00	-0.0009	0.002
Proportion of bare ground	0.0451***	0.0310***	0.0027*	0.0105*	0.0159***	0.0073**	0.06***	0.04***	0.04***	0.03***	0.0261***	0.03***
Proportion of exposed gravel	-0.006	0.002	-0.0008	0.0004	0.0009	-0.0009	-0.0008	-0.0007	0.000	-0.0008	-0.0007	0.0000

Proportion of open water	0.0284***	0.0548***	0.0068**	0.0356***	0.0453***	0.0012	0.0450***	0.0688***	0.0016	0.0687***	0.0624***	0.0155***
Submerged cover	0.0008	0.0003	0.0140***	0.0018	0.0000	-0.0009	0.0026*	0.0072**	0.0002	0.0033*	0.0028*	0.0001
Floating vegetation cover	0.0017	-0.0001	0.0093***	0.0023	0.0030*	-0.0006	0.0007	0.0029*	0.001	0.0020	-0.0008	-0.0008
Algae cover	0.0072**	0.0117***	-0.0005	0.0118***	0.0112***	0.0013	0.0114***	0.0092***	0.0017	0.0147***	0.0099***	0.0053**

Table S5. Adjusted R^2 for the linear relationship between climatic, topographic, and edaphic explanatory indices and spectral vegetation indices, across all study sites.

Explanatory variables	Year-maximum						Year-median					
	NDVI	**GNDVI**	**LWSI**	**EVI**	**SAVI**	**GCC**	**NDVI**	**GNDVI**	**LWSI**	**EVI**	**SAVI**	**GCC**
Maximum elevation (m)	0.0004	-0.0008	0.0125***	0.0005	-0.0008	0.0009	0.0060**	-0.0004	0.0351***	-0.0002	0.0009	0.0073**
Mean annual precipitation	0.0035*	0.0002	0.005**	0.0022	-0.0005	0.0125***	0.0398***	0.0217***	0.0739***	0.0131***	0.0217***	0.0316***
Coefficient of variation in monthly precipitations	0.0953***	0.0939***	0.0507***	0.0564***	0.0649***	0.0136***	0.0993***	0.0521***	0.0727***	0.0446***	0.0337***	0.0614***
Mean maximum precipitation	0.0000	0.0021	0.0062**	0.0012	0.0057**	0.0132***	0.0097***	0.0035*	0.0405***	0.0003	0.0038*	0.0110***
Mean minimum precipitation	0.0022	0.0002	0.0000	0.0026*	-0.0009	0.0000	0.0158***	0.0073**	0.0258***	0.0020	0.0055**	0.0047*
Mean annual maximum air temperature	0.0910***	0.0948***	0.0327***	0.0469***	0.0798***	0.0222***	0.0269***	0.0162***	0.0051**	0.0221***	0.0099***	0.0327***
Standard deviation of mean annual air temperature	0.0137***	0.0126***	0.0049*	0.0052**	0.0135***	0.0031*	0.0070**	0.0029*	0.001	0.0036*	0.0017	0.0168***
Mean pH	0.0481***	0.0410***	0.0185***	0.0104***	0.0122**	0.0158***	0.0615***	0.0421***	0.0369***	0.0114***	0.0170***	0.0194***

Table S6. Adjusted R^2 for the linear relationship between different multivariate models and spectral vegetation indices, across all study sites.

	Year-maximum						Year-median					
Group of variables	NDVI	GNDVI	LSWI	EVI	SAVI	GCC	NDVI	GNDVI	LSWI	EVI	SAVI	GCC
Structure	0.3968***	0.377***	0.1467***	0.3494***	0.3433***	0.1361***	0.4931***	0.3987***	0.3116***	0.4202***	0.3433***	0.3545***
Composition	0.3692***	0.405***	0.1214***	0.386***	0.4105***	0.1093***	0.4608***	0.4182***	0.2633***	0.416***	0.3808***	0.3384***
Confounding	0.1327***	0.1469***	0.0294**	0.1178***	0.1255***	0.0191***	0.1536***	0.16***	0.0529***	0.1568***	0.1376***	0.0702***
Landscape	0.2352***	0.2163***	0.1321***	0.14***	0.1815***	0.1032***	0.1964***	0.1204***	0.1794***	0.1089***	0.1815***	0.1817***
All	0.5912***	0.5852***	0.2752***	0.5092***	0.5548***	0.2009***	0.6296***	0.511***	0.4313***	0.5308***	0.4621***	0.4925***

Table S7. Adjusted R^2 for the linear relationship between different multivariate models and spectral vegetation indices, by wetland type.

	Year-maximum						Year-median					
Group of variables	**NDVI**	**GNDVI**	**LSWI**	**EVI**	**SAVI**	**GCC**	**NDVI**	**GNDVI**	**LSWI**	**EVI**	**SAVI**	**GCC**
Estuarine herbaceous												
Structure	0.2071***	0.2252***	0.1084***	0.2218***	0.223***	0.0072	0.2771***	0.2241***	0.07889**	0.2332***	0.2074***	0.176***
Composition	0.1487***	0.2021***	0.0713***	0.1788***	0.1874***	-0.0008	0.1477***	0.1818***	0.0475**	0.1327***	0.1478***	0.0640***
Confounding	0.1719***	0.2215***	0.1291***	0.2031***	0.2285***	0.0738***	0.2069***	0.2562***	0.0783***	0.2072***	0.2054***	0.0697***
Landscape	0.2636***	0.2366***	0.0230*	0.1756***	0.2285***	0.06171***	0.1162***	0.0930***	0.0515**	0.1137***	0.1272***	0.1277***
All	0.4809***	0.5136***	0.3083***	0.4453***	0.4979***	0.0992***	0.3938***	0.3829***	0.2666***	0.3589***	0.3613***	0.273***
Estuarine woody												
Structure	0.2631***	0.1593**	0.4327***	0.0658	0.0901	0.7661***	0.241***	0.1202*	0.3796***	0.1445**	0.0576	0.3448***
Composition	0.0698	0.2394***	0.1876**	0.0246	0.1849**	-0.015	0.0359	0.1369*	0.3095***	-0.0244	0.0289	0.1505*
Confounding	0.2077***	0.3183***	-0.0379	0.1491*	0.2012**	-0.0736	0.142*	0.2423**	-0.084	0.1491*	0.1537*	-0.0361
Landscape	0.304***	0.2478**	0.4724***	0.0520	0.1441**	0.1233*	0.1952**	0.1141*	0.595***	0.1462**	0.116*	0.4801***
All	0.4499***	0.5504***	0.521***	0.2596*	0.3637**	0.7799***	0.3859**	0.4196**	0.6592***	0.3351**	0.3106*	0.5698***
Inland herbaceous												
Structure	0.3336***	0.352***	0.0801***	0.2912***	0.3071***	0.1677***	0.3432***	0.3075***	0.2002***	0.3083***	0.2652***	0.2107***
Composition	0.1609***	0.1974***	0.0206*	0.178***	0.1685***	0.0561***	0.2466***	0.2539***	0.1235***	0.2106***	0.2233***	0.1252***
Confounding	0.1647***	0.2331***	0.0706***	0.1463***	0.1882***	0.0441***	0.1944***	0.2242***	0.1436***	0.2124***	0.2027***	0.1478***
Landscape	0.3338***	0.2524***	0.2768***	0.215***	0.2158***	0.1911***	0.3855***	0.2294***	0.3596***	0.2259***	0.211***	0.3306***
All	0.5052***	0.5073***	0.3134***	0.4324***	0.4509***	0.2551***	0.5717***	0.4625***	0.4419***	0.4474***	0.4121***	0.4375***
Inland woody												
Structure	0.315***	0.2382***	0.2218***	0.2434***	0.2207***	0.0273*	0.2885***	0.1269***	0.2059***	0.2355***	0.1144***	0.1419***
Composition	0.1854***	0.1975***	0.1476***	0.201***	0.2126***	0.0033	0.2222***	0.1823***	0.2143***	0.1712**	0.1532***	0.1478***
Confounding	0.0711***	0.0408**	0.0061	0.0239*	0.0171*	-0.0068	0.1045***	0.0665***	0.0536***	0.0623***	0.0495***	0.0474***
Landscape	0.4211***	0.3212***	0.2451***	0.2646***	0.2686***	0.1242***	0.3674***	0.2713***	0.3903***	0.1776***	0.1876***	0.2388***
All	0.6058***	0.4789***	0.3812***	0.4436***	0.4717***	0.127***	0.5463***	0.3559***	0.4377***	0.3452***	0.2698***	0.3662***

Table S8. Adjusted R^2 for the linear relationship between different multivariate models and spectral vegetation indices, by disturbance levels.

	Year-maximum						Year-median					
Group of variables	**NDVI**	**GNDVI**	**LSWI**	**EVI**	**SAVI**	**GCC**	**NDVI**	**GNDVI**	**LSWI**	**EVI**	**SAVI**	**GCC**
Least disturbed												
Structure	0.4392***	0.4054***	0.114***	0.4071***	0.4248***	0.3427***	0.531***	0.3791***	0.2915***	0.4743***	0.3744***	0.4051***
Composition	0.4742***	0.5252***	0.1067***	0.4801***	0.5192***	0.1522***	0.5534***	0.4805***	0.2478***	0.4991***	0.4429***	0.4316***
Abiotic	0.2723***	0.2909***	0.0314*	0.293***	0.2895***	0.0900***	0.3155***	0.312***	0.0963***	0.3384***	0.3171***	0.2063***
Landscape	0.2567***	0.2682***	0.0799***	0.1874***	0.247***	0.0695**	0.1804***	0.135***	0.0945***	0.1294***	0.1075***	0.1734***
All	0.6676***	0.6682***	0.231**	0.6145***	0.6609***	0.3836***	0.7023***	0.5794***	0.3609***	0.6349***	0.5451***	0.5522***
Intermediate												
Structure	0.3882***	0.3534***	0.1623***	0.3685***	0.3658***	0.1948***	0.5514***	0.4108***	0.3689***	0.4494***	0.3661***	0.4185***
Composition	0.3635***	0.3902***	0.1455***	0.3168***	0.3138***	0.1811***	0.5061***	0.3717***	0.3308***	0.4234***	0.3479***	0.3784***

Abiotic	0.1529***	0.1531***	0.0249**	0.1198***	0.1233***	0.0310***	0.1658***	0.1586***	0.0704***	0.1623***	0.1319***	0.0708***
Landscape	0.2183***	0.2022***	0.154***	0.1162***	0.1547**	0.1537***	0.2288***	0.1341***	0.2224***	0.1194***	0.1085***	0.1995***
All	0.5667***	0.5569***	0.3094***	0.447***	0.5106***	0.2971***	0.635***	0.4952***	0.4615***	0.5242***	0.4478***	0.5139***
Most disturbed												
Structure	0.4028***	0.4106***	0.1902***	0.3918***	0.3648***	0.06339**	0.4532***	0.3503***	0.3507***	0.4062***	0.3278***	0.3121***
Composition	0.2551***	0.2925***	0.0863***	0.3375***	0.3276***	0.0174	0.3539***	0.3318***	0.1917***	0.323***	0.3017***	0.2328***
Abiotic	0.0361**	0.0549***	0.0722**	0.0333**	0.0372**	-0.0178	0.0645***	0.0716***	0.0466**	0.0589**	0.0526**	0.0276**
Landscape	0.293***	0.2148***	0.1596***	0.1807***	0.2047***	0.1309***	0.2213***	0.1456***	0.2126***	0.122***	0.1304***	0.2114***
All	0.549***	0.5242***	0.324***	0.5324***	0.5283***	0.1368***	0.5814***	0.4692***	0.4797***	0.5024***	0.4416***	0.4748***

Table S9. Multivariate models and their adjusted R^2 by spectral vegetation indices. Variables in each multivariate model are selected using a forward selection aiming to identify the most parsimonious multivariate model.

	Year-maximum		Year-median	
	Multivariate model	AdjR^2	Multivariate model	AdjR^2
NDVI	Native species richness + Tree coverage + mean precipitation + Mean precipitation + Medium vegetation coverage + bare ground coverage + Forb coverage + Litter coverage + Minimum elevation + Minimum precipitation + Average precipitation + Total diversity + Maximum precipitation + Vine richness + Graminoid coverage + Open water coverage + Shrub richness + Very small vegetation coverage + Tall vegetation coverage + Shrub coverage + Alien species coverage + Standard deviation in maximum temperature	0.6366	Tree richness + Native species diversity + Coverage Bare Ground + Coverage Tree species + Coverage Median Vegetation Layer + Standard deviation in mean temperature + Mean precipitation + Mean temperature + Minimum elevation + Maximum temperature + Coverage Open water + Graminoid coverage + Tall Vegetation Coverage + Coverage High Medium Vegetation Layer + Minimum precipitation + Maximum precipitation + Coverage small vegetation + Coverage litter + mean elevation + coverage aquatic vegetation + coverage shrubs	0.6659
GNDVI	Mean precipitation + Vine richness + Minimum elevation + Minimum precipitation + Liana coverage + Standard deviation in mean temperature + Forb coverage + Tall vegetation coverage + Small vegetation coverage + Shrub richness + Medium vegetation coverage + Standard deviation in maximum temperature + Maximum elevation + Upper tree layer coverage + soil pH	0.5703	Native species richness + Tree richness + Bare ground coverage + Open water coverage + Very small vegetation coverage + Litter coverage + Mean precipitation + Minimum temperature + Total species diversity + Forb coverage + Aquatic vegetation coverage + Shrub coverage + Minimum precipitation + Maximum precipitation + Maximum temperature + Minimum elevation + Standard deviation in species richness + Liana coverage + Water depth	0.5811
LSWI	Tree richness + Graminoid coverage + Coefficient of variation in monthly precipitation + Min	0.3726	Tree richness + Graminoid coverage + Coefficient of variation in	0.5084

	imum precipitation + Mean precipitation + Average precipitation + Minimum elevation + Minimum temperature + Medium-high vegetation coverage + Shrub richness + Vine richness + Open water vegetation coverage + Native species coverage + Alien species coverage		monthly precipitation + Minimum precipitation + Mean precipitation + Average precipitation + Minimum elevation + Medium-high vegetation coverage + Shrub richness + Vine richness + Open water coverage + Native species coverage + Alien species coverage	
EVI	Total species diversity + Tree coverage + mean precipitation + Minimum elevation + Alien species coverage + Vine richness + Mean precipitation + Graminoid coverage + Litter coverage + Native species coverage + Minimum precipitation + Maximum precipitation + Maximum temperature + Open water coverage + Standard deviation in species richness + Very small vegetation coverage + Tall vegetation coverage + Bare ground coverage + Shrub richness	0.4922	Native species richness + Tree coverage + Alien species coverage + Bare ground coverage + Species richness + Open water coverage + Very small vegetation coverage + Graminoid coverage + Native species coverage + Tree richness + Tall vegetation coverage + Standard deviation in mean temperature + Mean precipitation + Minimum precipitation + Maximum precipitation + Litter coverage + Native species richness	0.5772
SAVI	Total species richness + Tree richness + Mean precipitation + Minimum elevation + Litter coverage + Forb coverage + Mean precipitation + Vine richness + Open water coverage + Very small coverage + Minimum temperature + Tall vegetation coverage + Alien species coverage + Maximum temperature + Exposed soil coverage + Liana coverage + Medium vegetation coverage + Shrub richness + Forb richness + Native species richness + Shrub coverage + Aquatic species coverage	0.6362	Native species diversity + Tree richness + Bare ground coverage + Open water coverage + Shrub coverage + Mean precipitation + Litter coverage + Forb coverage + Graminoid coverage + Native species coverage + Total species diversity + Very small vegetation coverage + Minimum temperature + Maximum elevation + Open water coverage + Maximum temperature + Minimum precipitation + Maximum precipitation + Standard deviation in species richness	0.5802
GCC	Tree richness + TIP_PT + Maximum precipitation + Medium vegetation coverage + Minimum elevation + Native species coverage + Graminoid coverage + Minimum temperature + Shrub richness + Small vegetation coverage	0.2206	Tree richness + Maximum temperature + Mean precipitation + Native species coverage + Graminoid coverage + Minimum precipitation + Alien species coverage + Maximum precipitation + Bare ground coverage + Standard deviation in temperature + Minimum elevation + Forb coverage + Forb richness + Submerged aquatic coverage + Vine richness + pH + Exposed gravel coverage + Mean temperature + Total species diversity + Herb richness + Tall vegetation coverage	0.5524

Conclusion

Summary of findings

The earth has lost over 50% of its historical wetland extent (Davidson 2014; Kingsford et al. 2016). Remaining wetlands are subject to increasing ecosystem stress generated by droughts, biological invasions, and pathogens (Bedford 1999; Allan et al. 2013). This critical loss and degradation of wetlands has serious consequences on key ecosystem services. These beneficial services include water filtration, climate regulation, and flood protection among many others (Almeida et al. 2016; Zedler 2003; Chmura et al. 2003). The role of wetland ecosystems in sustaining human quality of life will become even more important as a growing number of cities are threatened by sea level rise or floods increasing in frequency and magnitude (Nicholls et al. 1999). Wetlands will also play a significant role in mitigating the impacts of climate changes and water pollution (Chmura et al. 2003; Zhang et al. 2016).

In response to these environmental issues, governments are dedicating substantial effort to the restoration of wetland ecosystems. However, recent local studies and global meta-analyses have revealed a high variability in restoration outcomes (Matthews et al. 2009; Meli et al. 2014; Moreno-Mateos et al. 2015). To halt the degradation of wetland resources and better target limited conservation budgets, it is necessary to maintain a long-term and consistent monitoring of wetland resources. This dissertation explored novel ways of monitoring wetland ecosystems using open source remote sensing data, which could help expand the spatiotemporal extent of current monitoring efforts for a better landscape planning and conservation of resources. Research was conducted at two different scales. At the regional scale, I used aerial images from the National Agriculture Inventory Program and satellite data from Landsat sensors to characterize the long-term trajectories of restored wetlands in the Sacramento-San Joaquin Delta of California. At the national scale, I assessed which spectral vegetation indices could best describe wetland properties across different wetland types of the conterminous United States.

In chapter 1, I surveyed 42 monitoring plans for wetland restoration projects implemented in the San Francisco estuary. This effort showed that current wetland monitoring in the San Francisco estuary is predominantly achieved through field observations of vegetation cover and composition, but that very few projects are leveraging geospatial tools to monitor the progress made towards regional or site-specific goals. In response, chapter 1 explored potential applications of geospatial tools for regional wetland monitoring through a review of recent studies conducted in the estuary and elsewhere. The literature review suggests that several geospatial tools could help measure the combined contribution of individual projects towards regional wetland conservation goals. For example, plant biomass estimation using LiDAR or multispectral data could be utilized to upscale field observations into regional estimates of ecosystem services. Additionally, ecological niche models could be implemented to help target field monitoring efforts by identifying habitats where non-native species or species with critical ecological value are likely to occur. Some wetland properties might still be best monitored in the

field due to tradeoffs among satellite datasets in resolution and extent. Such properties include species richness and the spatial distribution of individual species unless these species are dominant.

Chapter 2 and 3 sought to address some of the methodological gaps identified in the first chapter by testing novel approaches to wetland monitoring in the Sacramento-San Joaquin Delta. Chapter 2 assessed whether landscape metrics describing the shape, distribution, and heterogeneity of land cover patches could be used to characterize vegetation response to restoration treatments in wetlands. Landscape metrics were computed for 21 restored sites across an 11-year period. Changes in landscape metrics over time were linked to vegetation dynamics, via an analysis of time series of site greenness describing changes in vegetation extent and productivity over time. Results showed that fluctuations in landscape metrics followed successional patterns in restored wetlands, demonstrating a significant response of landscape metrics to time and restoration interventions. These results indicate that landscape metrics are useful in simply quantifying habitats in addition to tracking vegetation dynamics in restored wetlands.

Chapter 3 compared the phenological characteristics of 20 restored wetlands and 5 reference sites across a 17-year window. Results suggest that wetlands have a significant phenological response to restoration treatments. More recently restored sites maintained an earlier phenology than older restored wetlands or reference sites. Restored wetlands continued to observe changes in their growing season curves over time. Most sites studied in this chapter experienced an increase in mean, maximum, and integrated enhanced vegetation index, which likely result from an increase in vegetation cover reducing the background effect of water and soil. Three of the older wetlands, however, experienced a decrease in greenness over time, likely as a result of changes in land management and accumulation of litter. This chapter shows that phenological assessments in restored wetlands can highlight patterns of vegetation succession and growth in addition to serving as base data for estimating the provision of ecosystem services at a large spatial extent.

In chapter 4, I strived to advance the use of remote sensing in wetlands by measuring the sensitivity of six spectral vegetation indices to different field characteristics of wetlands including: vegetation structure, species composition, and confounding variables. Spectral vegetation indices were estimated from Landsat 5 TM and 7 ETM+ and summarized across 1,138 wetland sites of the conterminous United States using two aggregation metrics (maximum and mean). Results show that, in the global sample, NDVI is most responsive to field indicators of vegetation structure while GNDVI is most responsive to indicators of vegetation composition. However, in estuarine wetlands dominated by woody vegetation, LSWI is most responsive to vegetation structure and composition — likely because it is the only index to leverage information in the shortwave infrared band which best discriminates woody species. Aggregation metrics showed different sensitivities to multivariate models, with median greenness being more sensitive to structure and composition, but also to confounding site variables including litter, open water, and bare soil. This study highlights that the selection of a spectral vegetation index should be tailored to the type of wetland monitored and to the wetland property of interest.

Implication for wetland management

Chapter 1 suggests that remote sensing analyses and geospatial tools are sparsely used in the San Francisco estuary. This dissertation demonstrates the potential of remote sensing analyses to assist restoration and conservation efforts. Through a long-term survey of different vegetation properties including plant composition, structure, and dynamics, I showed that a significant signal of site change can be achieved using open source medium-high resolution remote sensing data. This shows the invaluable potential of remote sensing data to monitor the progress made towards regional conservation goals. It also suggests that project managers could leverage open source remote sensing dataset to track site dynamics through space and time in order to rapidly identify signs of ecosystem stress requiring adaptive management. Luckily, as discussed in Chapter 1, several platforms make the access to and analysis of satellite images more convenient and time-efficient.

The long-term analyses of vegetation dynamics conducted for this dissertation revealed a substantial variability in site properties, even among older restored sites. This result further demonstrates the importance of maintaining a consistent monitoring of restoration projects, as discussed in previous studies (Matthews et al. 2009; Berkowitz 2013; Laughlin et al. 2017). Fortunately, many of the methodological approaches developed and discussed in this dissertation are economical could be readily applied by site managers and conservation practitioners to maintain this long-term, consistent monitoring.

While remote sensing data provides an invaluable potential to assist wetland monitoring, there are limitations to the application of open source datasets, which are typically coarser, for the monitoring of certain wetland properties For example, Chapter 1 discusses challenges inherent to the mapping and monitoring of individual species using medium-high resolution remote sensing data. Chapter 3 shows that monitoring vegetation properties is also challenging during the first post-restoration year, when vegetation is still sparse. This highlights the potential to complement field observation of wetland properties with remote sensing analyses. Field observations are critical to monitoring properties that would otherwise be too challenging to track using remote sensing alone. They are also important for collecting ground-truth data that can help better interpret and validate patterns observed from remote sensing data. In turn, remote sensing analyses can assist in targeting field monitoring efforts to substantially reduce cost. These analyses can also provide continuous data in between field surveys.

Future research needs

Use landscape metrics to measure ecosystem services. Chapter 2 demonstrates the potential application of landscape metrics for the low-cost monitoring of vegetation dynamics in wetlands. Landscape metrics are already widely applied to map wildlife habitats in wetlands and other ecosystems. Few studies published to date have measured the relationships between landscape metrics and ecosystem services in wetlands, although two previous papers showed their potential to help measure water quality (Moreno-Mateos et al. 2008) and erosion control (Almeida et al. 2016). Developing a more thorough understanding of how landscape metrics modulate the provision of ecosystem services would further show their significance for wetland monitoring.

This research would also help landscape managers assess multiple wetland properties (e.g., vegetation dynamics, ecosystem services, habitat availability) using fewer, non-redundant analyses of landscape patterns.

Use near-surface remote sensing data or frequent high-resolution datasets to study the specific characteristics impacting the growing season curves of wetlands. Chapter 3 shows a significant phenological response of wetland sites to restoration treatments, however, it is difficult to identify the specific characteristics that modulate the shape of growing season curves due to the scale of Landsat data. A detailed investigation of how different growing season curves of wetlands respond to changes in species composition, proliferation of non-natives, litter accumulation, and vegetation expansion would provide critical knowledge and help future studies interpret phenological patterns observed from coarser resolution data.

References

Allan, J. D., P. B. McIntyre, S. D. P. Smith, B. S. Halpern, G. L. Boyer, A. Buchsbaum, G. A. Burton, L. M. Campbell, W. L. Chadderton, J. J. H. Ciborowski, P. J. Doran, T. Eder, D. M. Infante, L. B. Johnson, C. A. Joseph, A. L. Marino, A. Prusevich, J. G. Read, J. B. Rose, E. S. Rutherford, S. P. Sowa, and A. D. Steinman. 2013. Joint analysis of stressors and ecosystem services to enhance restoration effectiveness. Proceedings of the National Academy of Sciences of the United States of America 110:372–377.

Almeida, D., J. Rocha, C. Neto, and P. Arsénio. 2016. Landscape metrics applied to formerly reclaimed saltmarshes: A tool to evaluate ecosystem services? Estuarine, Coastal and Shelf Science 181:100–113.

Bedford, B. L. 1999. Cumulative Effects on Wetland Landscapes: Links to Wetland Restoration in the United States and Southern Canada. Wetlands 19:775–788.

Berkowitz, J. F. 2013. Development of restoration trajectory metrics in reforested bottomland hardwood forests applying a rapid assessment approach. Ecological Indicators 34:600–606.

Davidson, N. C. 2014. How much wetland has the world lost? Long-term and recent trends in global wetland area. Marine and Freshwater Research 65:934–941.

Kingsford, R. T., A. Basset, and L. Jackson. 2016. Wetlands: conservation's poor cousins. Aquatic Conservation: Marine and Freshwater Ecosystems 26:892–916.

Laughlin, D. C., R. T. Strahan, M. M. Moore, P. Z. Fulé, D. W. Huffman, and W. W. Covington. 2017. The hierarchy of predictability in ecological restoration: Are vegetation structure and functional diversity more predictable than community composition? Journal of Applied Ecology:1058–1069.

Matthews, J. W., A. L. Peralta, D. N. Flanagan, P. M. Baldwin, A. Soni, A. D. Kent, and A. G. Endress. 2009a. Relative influence of landscape vs. local factors on plant community assembly in restored wetlands. Ecological Applications 19:2108–2123.

Matthews, J. W., G. Spyreas, and A. G. Endress. 2009b. Trajectories of Vegetation-Based

Indicators Used to Assess Wetland Restoration Progress. Ecological Applications 19:2093–2107.

Meli, P., J. M. R. Benayas, P. Balvanera, and M. M. Ramos. 2014. Restoration enhances wetland biodiversity and ecosystem service supply, but results are context-dependent: A meta-analysis. PLoS ONE 9:e93507.

Moreno-Mateos, D., Ü. Mander, F. A. Comín, C. Pedrocchi, and E. Uuemaa. 2008. Relationships between Landscape Pattern, Wetland Characteristics, and Water Quality in Agricultural Catchments. Journal of Environment Quality 37:2170.

Moreno-Mateos, D., P. Meli, M. I. Vara-Rodríguez, and J. Aronson. 2015. Ecosystem response to interventions: Lessons from restored and created wetland ecosystems. Journal of Applied Ecology 52:1528–1537.